

**EVALUATION OF APPLICABILITY OF DOUBLE SHIELD
TUNNEL BORING MACHINES (DS-TBM) IN
POTENTIALLY SQUEEZING GROUNDS**

**ÇİFT KALKANLI TÜNEL AÇMA MAKİNELERİNİN
SIKIŞAN ZEMİN KOŞULLARINDA
KULLANABİLİRLİĞİNİN ARAŞTIRILMASI**

ROHOLA HASANPOUR

Prof. Dr. BAHTİYAR ÜNVER

Supervisor

Dr. JAMAL ROSTAMI

Co-Supervisor

Submitted to Hacettepe University as a partial fulfillment

to the requirements of the Postgraduate Education and

Examination Regulations for the degree of

DOCTOR OF PHILOSOPHY

in Mining Engineering

2013

This study entitled “**Evaluation of Applicability of Double Shield Tunnel Boring Machines (DS-TBM) in Potentially Squeezing Grounds**” prepared by **ROHOLA HASANPOUR** has been accepted as a **PhD THESIS** in the **DEPARTMENT OF MINING ENGINEERING** by the examination committee.

Examination Committee Chairman

(Assoc. Prof. Yasin Dursun SARI)

Member (Supervisor)

(Prof. Dr. Bahtiyar ÜNVER)

Member

(Assoc. Prof. Dr. İhsan ÖZKAN)

Member

(Prof. Dr. A. Erhan TERCAN)

Member

(Prof. Dr. Yılmaz ÖZÇELİK)

This thesis has been approved as a **PhD Thesis** by Hacettepe University, Institute for Graduate Studies in Science and Engineering.

Prof. Dr. Fatma SEVİN DÜZ
Director of the Institute for Graduate
Studies in Science and Engineering

ETHICS

I have prepared this thesis in comply with the thesis writing rules declared by Hacettepe University, Institute for Graduate Studies in Science and Engineering, I hereby declare that;

- all of the information and documents used in the thesis are obtained under the academic rules,
- all of the information and results including the visual, auditory and texts are presented according to the rules of scientific ethics,
- in the case of use of other works, they are referred to with respect to the scientific norms,
- all of the references used in the thesis are given in reference list,
- no falsification has been done on the data ,
- and any part of this thesis has not been used in any other theses submitted to this university or any other university by no means,

13/03/2013

Signature

ROHOLA HASANPOUR

ABSTRACT

EVALUATION OF APPLICABILITY OF DOUBLE SHIELD TUNNEL BORING MACHINES(DS-TBM) IN POTENTIALLY SQUEEZING GROUNDS

ROHOLA HASANPOUR

Doctor of Philosophy, Department of Mining Engineering

Supervisor: Prof. Dr. BAHTIYAR ÜNVER

Co-Supervisor: Dr. JAMAL ROSTAMI

Mach 2013, 119 pages

Despite successful use of double shield TBMs in many projects in recent years, presence of shield makes the machine susceptible to entrapment or seizure in weak rocks under high stresses experiencing high convergence. Therefore TBM may get stuck in the complicated geological structures commonly referred to as squeezing ground. This causes slow down or stoppage of machine operation, requiring manual excavation to release the machine, and sometimes even call into question the feasibility of using double shield machines. To realistically evaluate the possibility of machine seizure in such grounds, the interaction between the rock mass and shield, lining and backfilling need to be understood. This thesis explains the background theories and the application of numerical analysis for 3D modeling of mechanized tunneling by using a double shield TBM in squeezing ground. For this purpose, a comprehensive numerical simulation is developed to systematically evaluate the potential of excessive ground convergence and squeezing. Furthermore, application of double shield TBM in such grounds with the possibility of using ground improvement or lubrications to avoid shield jamming in such cases is given by using numerical analysis. This study also investigates the effects of advance rate during excavation cycle of a shielded TBM to observe the impact of tunneling advance rate on the possibility of machine jamming in the squeezing grounds. On the other hand, 3D influence of different non-uniform overcut values on deformation and contact forces developing along the tunnel were investigated. Simulation results at five reference points on the tunnel circumference along the tunnel or longitudinal displacement profile (LDP) as well as contact force profiles (LFP) on both front and rear shields have been examined. Also, maximum thrust force required to overcome friction and drive TBM forward is calculated. The results are realistic and plausible and show the potential for use of this approach to assess the risk of machine entrapment in deep tunnels within weak rocks.

Keywords: Tunnel Boring Machines, Double Shield, Squeezing Ground, Numerical Simulation, FLAC^{3D}, Time Dependent, Overcut, Ground Improvement, Lubrication.

ÖZET

ÇİFT KALKANLI TÜNEL AÇMA MAKİNELERİNİN SIKIŞAN ZEMİN KOŞULLARINDA KULLANABİLİRLİĞİNİN ARAŞTIRILMASI

ROHOLA HASANPOUR

Doktora, Maden Mühendisliği Bölümü

Tez Danışmanı: Prof. Dr. BAHTİYAR ÜNVER

İkinci Danışman: Dr. JAMAL ROSTAMI

Mart 2013, 119 sayfa

Birçok projede çift kalkanlı TBM'lerin başarılı olarak kullanılmalarına rağmen, zayıf kayalarda yüksek gerilmelerden ve yer yakınsamalardan dolayı kalkan nedeniyle makine sıkışmaya maruz kalabilmektedir. Bu yüzden karmaşık jeolojik yapıya sahip ve özellikle sıkışan ortamlarda, çift kalkanlı TBM'lerin sıkışma olasılığı vardır ve birçok projede bu sıkışma kazı işleminin durdurulması veya yavaşlamasına neden olmaktadır. Makineyi bu durumdan kurtarmak için elle kazı gerekmektedir ve bu nedenle çift kalkanlı makinelerin uygulanabilirliğinin tartışılması söz konusu olabilmektedir. Sıkışan zeminlerde makinenin sıkışarak hareket ettirilememe olasılığını gerçekçi bir şekilde değerlendirmek için, kaya kütlesi ve kalkan, segment ve dolgu aralarındaki etkileşimi iyi derecede anlamak gerekmektedir. Bu çalışmada çift kalkanlı TBM'lerin performansını sıkışan ortamlarda değerlendirmek amacıyla, gerçekçi üç boyutlu sayısal benzetimler oluşturulmuştur. Kalkan sıkışmasının önlenmesi için sıkışan ortamlarda sayısal analizlerden yararlanarak uygun iyileştirme yöntemlerinin seçilmesi önerilmiştir. Ayrıca çift kalkanlı TBM'ler ile kazılan tünellerde makinenin ilerleme hızı etkisini araştırmak için zamana bağlı sünme analizleri gerçekleştirilmiştir. Buna ek olarak tünel çevresinde kaya ve kaplama arasındaki fazla kazı etkisi sıkışmayı önlemek amacıyla incelenmiştir. Analiz sonuçları tünel çevresinde beş adet referans noktasında incelenmiş olup ve tünel boyunca deformasyonlar ve temas basınçları diyagramlar üzerinde gösterilmiştir. Sıkışmaya maruz kalan kalkan üzerinde oluşan toplam temas basınçları hesaplanmıştır. Buna dayanarak sürtünme kuvvetleri belirlenmiş ve makinenin ilerlemesini sağlamak amacıyla sürtünme direncini yenebilecek itme kuvvetleri hesaplanmıştır. Çalışma sonuçları sıkışan ortamlarda çift kalkanlı makine ile açılan tüneller için sıkışma riskini değerlendirmiş olup ve olası sıkışmalara karşı iyileştirme yöntemlerini sunmaktadır.

Anahtar Kelimeler: Tam Cepheli Tünel Açma Makinesi, Çifte Kalkanlı, Sıkışan Ortamlar; Sayısal Benzetimler; FLAC^{3B}, Zamana Bağlı Analizler, Artı Boşluk, Zemin İyileştirme, Kayganlaştırma.

ACKNOWLEDGEMENTS

I would like to give my most sincerely gratifications to all the people that with their experience, their knowledge, perseverance and professionalism, helped me in concluding this thesis.

I want to give my special thanks to my wife Aida for her understanding and her unconditional help and love. Last but not least, my love to my family who have supported me in all of my decisions and cared for me.

I would like to express my deep and sincere gratitude to Prof. Dr. Bahtiyar Ünver and Dr. Jamal Rostami whose have supervised this PhD thesis. Their personal guidance, comments and the numerous and beneficial discussions as well as the opportunity to work together with them on challenging projects made a decisive contribution to the successful accomplishment of the present research work.

Also I want to present my best thanks to the Scientific and Technological Research Council of Turkey (TÜBİTAK) for funding me during PhD period.

I am also deeply grateful to Prof. Dr. Ömer Aydan. His detailed and constructive comments were of great value.

At this point, I would like to thank to Prof. Dr. Yılmaz Özçelik and Assoc. Prof. Yasin Dursun SARI as the members of steering committee for their helpful discussions and suggestions throughout this study. Also I would like to thank to Assoc. Prof. Dr. İhsan Özkan and Prof. Dr. A. Erhan Tercan as thesis examination committee members for their invaluable criticisms and suggestions. As well, I offer my cordial thanks to all of my friends especially to Dr. Atallah Bahrami, Dr. Hojjat Hosseinzadeh and their families.

GENİŞ ÖZET

Tam cepheli tünel açma makinelerinin (TBM) dünyada ve Türkiye’de madencilik ve inşaat sektöründe kullanımını önemli ölçüde artmaktadır. TBM ile cevhere ulaşmak için ana galeri ve kuyuların açılması, kara ve demir yolu tünelleri, hidroelektrik, kanalizasyon, su ve diğer altyapı tesisleri hızlı ve emniyetli bir şekilde açılabilir. Çift kalkanlı tam cepheli tünel açma makineleri son yıllarda daha çok kullanılmaya başlanmıştır. Bu durumun temel nedeni, duraysız veya ezilmiş kaya birimlerini de içeren farklı kaya kütlelerinde, çift kalkanlı TBM’lerin daha hızlı, ekonomik ve verimli olmalarıdır.

Çift kalkanlı TBM’lerin, diğerlerinden farklı olarak, ön ve arka kısımları tamamen kalkanlar ile korunmaktadır. Ön kalkanın ileri itimi, arka kalkanı etkilemeden gerçekleşmektedir. Bu yüzden segment kaplamanın yerleştirilmesi kazı operasyonundan bağımsızdır. Bu tür TBM’lerde mükemmel ilerleme hızları elde edilebilmektedir. Çift kalkanlı TBM’lerin bir halka segment kaplama yerleştirme süresi tek kalkanlı TBM’lere göre daha azdır ve yaklaşık 10-15 dakika olarak belirlenmiştir. Bu zaman tek kalkanlı TBM’ler için 30-40 dakikadır.

Ancak çift kalkanlı TBM’ler birçok projede başarılı olarak kullanılmalarına rağmen, zayıf ve derinde yapılan kazı koşullarında karşılaşılan yüksek gerilmeler nedeniyle meydana gelen deformasyonların etkisiyle sıkışmaya maruz kalabilmektedirler. TBM sıkışmaya maruz kaldığında operasyon yavaşlamakta hatta durabilmektedir. Bu gibi durumlarda makineyi serbest bırakmak için elle kazı gerekebilir. Bu nedenle bazen çift kalkanlı makinelerin fizibilitesi dahi doğrudan sorgulanabilmektedir.

Sıkışan zeminlerde makinenin sıkışma olasılığını gerçekçi bir şekilde değerlendirmek için, kaya kütlesi ile kalkan, segment kaplama ve dolgu aralarındaki etkileşimi iyi derecede anlamak gerekmektedir. Buna ek olarak, bazı vakalar çift kalkanlı TBM’lerin sıkışan ortamlarda kazının durmasından olumsuz etkilenebileceğini göstermektedir. Hafta sonları makineyi çalıştırmamak, makinenin tamiri veya bakımı için duraklamalar ve diğer makine duruş süreleri TBM’in sıkışması açısından risk teşkil etmektedir. Bu nedenle "zaman" faktörü bu gibi koşullarda önemli bir rol oynamaktadır. Birçok durumda, TBM’in yavaşlama veya duraklama olmadığı durumlarda sıkışma problemi görülmemiştir. Bu da, ilerleme hızının kesintisizce korunması ve duraklama sürelerinin azaltılmasının sıkışmayı büyük ölçüde önleyeceğini göstermektedir.

Literatürde sıkışan zeminlerde kalkanlı TBM'lerin uygulaması hakkında pek çok çalışma bulunmaktadır. Ancak, bu çalışmalarda yeniden gözden geçirilmesi gereken bazı eksiklikler vardır. Çift kalkanlı TBM'ler ile sıkışan ortamlarda kazılan bir tünelde üç boyutlu sayısal modelleme ile makinenin sıkışma olasılığını değerlendirmek mümkündür. Sayısal modelleme, tüneli çevreleyen kaya kütleleri ile kalkan, segment kaplama ve dolgu arasındaki etkileşimi ve temas basınçlarını incelemek amacıyla kullanılmalıdır. Ancak sayısal modelleme büyük ölçüde bilgisayar hızı ve kapasitesine bağlı olduğu için geçmişte etkin ve verimli olarak kullanılamamıştır. Diğer taraftan, günümüzde tünellelikte sayısal modelleme gerçeğe en uygun şekilde yapılabilmektedir. Geçmişte yapılan çalışmalarda tüneli çevreleyen kaya kütlelerinin zamana bağlı deformasyon davranışı dikkate alınmamıştır. Ayrıca zemin iyileştirme yöntemleri de sayısal modellerde gereği kadar kullanılamamıştır. Zemin iyileştirme yöntemlerinin uygulanması ve kalkanın yüksek temas basınçlarına maruz kaldığında kayganlaştırma mekanizmasının incelenmesi ile ilgili literatürde bir çalışmaya rastlanılmamıştır.

Konu ile ilgili literatürün kısa bir incelemesi, var olan modellerde ve ilgili analizlerde bazı eksiklikler olduğunu göstermektedir. Bunlar aşağıdaki gibi sıralanmıştır:

- Kapalı-form çözümler genellikle tünel eksen yönündeki basınç dağılımı konusunda herhangi bir bilgi vermeden, sadece sıkışma potansiyeli ile ilgili kabaca bir değerlendirme sunmaktadır. Ayrıca aşırı derecede sıkışan zeminlerde büyük hatalar ortaya çıkmakta ve zemindeki gerilme dağılımı doğru bir şekilde belirlenmemektedir. Bu durum, sonuçları hem nicel hem de nitel olarak etkilemektedir. Bu sebeple aksel simetrik veya üç boyutlu sayısal modeller ile ilerleyen ayna etrafındaki gerilmelerin yeniden dağılımına dikkat edilmesi gerekmektedir. Böylece, iki boyutlu düzlemsel gerilme analizinden kaynaklanan hatalar ortadan kalkmış olacaktır. Ayrıca, tünel eksen yönünde oluşan gerilme ve deformasyonların değerlendirilmesi ile ilgili bilgi elde edilecek ve farklı sistem bileşenleri ve ara yüzlerin daha detaylı modellemesine imkân tanınacaktır.
- Literatürde verilen sayısal modelleme çalışmalarında zamana bağlı sünme ve/veya konsolidasyon özellikleri dikkate alınmamıştır. Bu sadeleştirme varsayımlarına göre, bütün plastik deformasyonlar bir anda ortaya çıkmaktadır. Ancak, zamana bağlı davranışın özellikle sıkışan zeminlerde elasto-plastik analizler ile birlikte dikkate alınması gerekmektedir.

- Eksensel simetri ve homojen varsayımlarının sonucu olarak, tünel kesitinde bırakılan artı boşluk (overcut), kalkanın çevresinde ve modelin tamamında sabit bir değer olarak alınmaktadır. Gerçekte ise tünel boyunca bu değer, tünel tavanında tabana göre daha büyüktür. Tünel etrafındaki boşluk gerçeğe uygun şekilde düzensiz olarak modellenmelidir.
- Diğer taraftan makine bileşenleri ile kayaç arasındaki en önemli sıkışma faktörü olan temas basıncı miktarı belirlenmesine yönelik çalışmalara literatürde çok az rastlanılmıştır.
- Son olarak kalkan sıkışmasını önlemek amacıyla en uygun zemin iyileştirme yönteminin seçimi yapılmalıdır. Bu durum sayısal modelleme yapılarak ayrıntılı olarak incelenmelidir. Kalkan üzerine deformasyona uğrayan kayanın yaslanması sonrasında oluşan etkileşim ve uygun kayganlaştırıcı kullanarak sürtünmenin azaltılmasına yönelik çalışmalar bulunmamaktadır.

Bu tezin genel amacı, sıkışma potansiyeli olan ortamların sayısal yöntemler ile sistematik değerlendirilmesi ve çift kalkanlı TBM'lerin karşılaştığı bu tür ortamlarda zemin iyileştirme veya kayganlaştırma yöntemleri ile sıkışmasının önlenmesidir. Tez çalışmasının hedefleri aşağıdaki gibi özetlenmiştir:

- Sayısal benzetimler ile sıkışma ortamlarını sistematik olarak değerlendirmek ve görgül ve yarı görgül yaklaşımlardan yararlanarak bu benzetimlerden elde edilen sonuçların doğrulamasını yapmak.
- Sıkışan ortamlarda çift kalkanlı TBM'ler ile açılan tüneller için üç boyutlu gerçekçi sayısal benzetimler oluşturmak ve makinenin bu tür ortamlarda kullanılabilirliğini elasto-plastik ve zamana bağlı sayısal analizler ile değerlendirmek.
- Sıkışan kaya koşulları dikkate alınarak kaya kütlesi, kalkan, kaplama ve dolgu arasındaki etkileşimin en gerçekçi üç boyutlu sayısal benzetimini yapmak.
- Sayısal analizler ile sıkışmaya maruz kalan kalkanın üzerine gelen toplam basınçları hesaplamak ve makinenin ilerlemesini sağlamak amacıyla itme gücünün tahmininde bulunmak.
- Sıkışan zeminlerde çift kalkanlı TBM'lerin en önemli parametresi olan artı boşluk (overcut) etkisini duyarlılık sayısal analizleri ile muhtemel sıkışmayı belirlemek amacıyla incelenmek.

- Çift kalkanlı TBM'lerin sıkışmasının önlenmesi için tünel çevresinde oluşan plastik bölgeye göre uygun iyileştirme yöntemlerinin seçilmesini araştırmak.
- Sıkışmış ve kaya kütlesi tarafından temas basıncına maruz kalan kalkana hareket sağlanması için kalkan ile kaya arasındaki uygulanan kayganlaştırma mekanizmasını incelemek.

Bu tezin amaçları çerçevesinde, sıkışan ortamlarda kalkanlı TBM'lerin uygulanabilirliğinin değerlendirilmesi için kapsamlı bir sayısal benzetim geliştirmiştir. Sayısal analizler için sonlu farklar yöntemi ile çalışan FLAC^{3D} programı kullanılmıştır. Bu çalışmada geliştirilen model bir çift kalkanlı TBM uygulamasında kullanılan her türlü işlem aşaması ve geometrisini en gerçekçi şekilde içermektedir.

Bu çalışmadan elde edilen sonuçlar aşağıda verilmektedir:

- a) Tünel açma makineleri (TBM), TBM işletim parametreleri ve aksama süresini meydana getiren unsurlar özellikle çift kalkanlı makineler için kısaca gözden geçirilmiştir. Şimdiye kadar sıkışan ortamların sınıflandırılması için önerilen görgül ve yarı görgül yaklaşımlar ve teorilere değinilmiştir. Daha sonra bu yaklaşımlardan hesaplanan değerler, ilk sayısal benzetim sonuçlarının doğrulaması için kullanılmıştır.
- b) Üç boyutlu sayısal modelleme ve benzetim işlemleri sıkışan zeminlerde çift kalkanlı TBM ile açılan bir mekanize tünel için gerçekleştirilmiştir. Bu modelleme makine bileşenlerini dikkate alarak geliştirilmiştir. Böylece bu modeller çift kalkanlı TBM ile açılan bir tüneldeki tüm değişkenleri göz önüne alarak kaya kütlesi, kalkan, kaplama ve dolgu arasındaki etkileşimin sıkışan koşullarda en gerçekçi üç boyutlu sayısal benzetimini sunmaktadır.
- c) Tünel çevresinde beş adet referans noktası analiz sonuçlarını değerlendirmek amacıyla seçilmiştir. Bu noktalarda, tünel boyunca deformasyonlar ve temas basınçları diyagramlar üzerinde gösterilmiştir. Sıkışmaya maruz kalan kalkan üzerinde oluşan toplam temas basınçları hesaplanmıştır ve böylece sürtünme kuvvetleri belirlenmiş ve makinenin ilerlemesini sağlamak amacıyla sürtünme direncini yenebilecek itme kuvvetleri hesaplanmıştır.
- d) Ayrıca, kalkan ve kaplama üzerinde etkili olan zemin basıncı, P , ve plastik bölge, R_p miktarları ile makina itme kuvveti tarafından üstesinden gelinmesi gereken sürtünme kuvvetleri de hesaplanmıştır. Buna ek olarak modelleme, tünel sınırı

boyunca yatay σ_{xx} , düşey σ_{zz} , aksenal σ_{yy} , ve makaslama σ_{xy} , σ_{yz} , σ_{xz} , gerilmelerinin çıkartılmasını sağlamaktadır.

- e) Zamana bağlı sayısal analizler makine ilerleme hızını incelemek için gerçekleştirilmiştir. Bu amaçla, Burger sünme viskoplastik modeli (Model CVISC) ve güç-kuralı viskoplastik modeli (Model CPOW), seçilen çalışma örnekleri üzerinde uygulanmıştır. Bu modelleme ile tünel boyunca zamana karşı kalkan ve kaya arasındaki temas basıncı ve segmentler üzerine gelen basınç miktarının tahmini mümkün olmaktadır.
- f) Sayısal analizler 4 farklı makine ilerleme hızı için yapılmıştır. Böylece kalkan üzerinde oluşan temas basıncı grafikleri çizilerek makine ilerleme hızının etkisi gösterilmiştir. Daha sonra ilerleme hızına bağlı olarak gereken itme kuvvetleri hesaplanmıştır ve grafiksel olarak farklı ilerleme hızlarında sunulmuştur.
- g) Sıkışma riskinin tahmini için belirlenen farklı artı boşluk (overcut) değerlerine göre sayısal elasto-plastik analizler yapılmıştır. Böylece tünel sınırında ve aynasındaki zeminin ışınal yer değiştirmesi ve sıkışma koşulları incelenmiştir. Tünel etrafında oluşan yenilme bölgeleri 4 farklı artı boşluk koşulu için verilmiştir olup farklı artı boşluklarında oluşan yenilme bölgeleri için yorumlar yapılmıştır.
- h) Sıkışan zemin koşullarında aşırı deformasyonu önlemek veya yavaşlatmak amacıyla sayısal benzetimler kullanılarak uygun zemin iyileştirme yöntemleri modellenmiştir. Sayısal ve teorik analizlerden yararlanarak plastik bölgenin çapına göre ayna üstü delik yöntemi (probe drilling) ve kaya saplama iyileştirme yöntemleri değerlendirilmiştir. Elde edilen sonuçlara göre, probe drilling yöntemi sıkışan zeminlerde makine sıkışmasını önlemek için çok etkili bir seçim olabilmektedir. Kaya saplaması ise sadece segment kaplama etrafındaki oluşan basınçları düşürmektedir.
- i) Tünel içine doğru ilerleyen kaya kütlesi, kalkana karşı yüksek sürtünme kuvvetleri oluşturmakta olup ve bunun sonucunda kalkanın ileriye doğru hareketini engellenmektedir. Bu sorun kısmen, kaya içerisinde artı boşluk uygulaması ile çözüle bilirse de ancak bazı durumlarda oluşturulan boşluk çok hızlı bir şekilde zemin deformasyonu nedeniyle dengelenmiştir. Kalkan ile zemin teması nedeniyle yüksek sürtünme kuvvetleri oluşmaktadır. Bu durumlarda, bentonit gibi kayganlaştırıcı uygulaması ile sürtünme azaltılarak kalkanın ileriye doğru hareketi

sağlanabilmektedir. Kayganlaştırma mekanizmasını arařtırmak amacıyla duran bir TBM'in kayganlařtırıcı uygulaması ile ve kayganlařtırıcı olmadan yeniden hareket ettirilmesi kořulları farklı sũrtũnme katsayıları iin grafiksel olarak incelenmiřtir.

ift kalkanlı TBM'lerin zellikle sıkıřan, derin ve uzun tũnellerde uygulanması sırasında sıkıřma olasılıđının nceden tahmini nemlidir. Bu alıřmadan elde edilen sonuların sıkıřan ortamlarda aılacak olan tũneller iin TBM seiminin dođru yapılmasına olanak sađlayacađı dũřũnũlmektedir. TBM'in sıkıřması sorunu ile karřılařıldıđında bu durumun nlenebilmesi ve alınması gereken nlemlerin neler olduđu da alıřma sonularından elde edilebilmektedir. Bu alıřma, tek kalkanlı TBM'lerden daha karmařık olan ift kalkanlı TBM'lerin 3B gereki modellemesinin ilk defa ve tũm ayrıntıları ierecek biimde yapılmıř olması dolayısıyla nemlidir.

Anahtar Kelimeler: ifte Kalkanlı Tũnel Ama Makinesi; Sıkıřan Ortamlar;  Boyutlu Sayısal Analizler; Zamana bađlı Analizler; Zemin İyileřtirme Yntemleri; Kayganlařtırma Mekanizması.

TABLE OF CONTENTS

RECOGNITION AND CONFIRMATION	ii
ETHICS	iii
ABSTRACT	iv
ÖZET	v
AKNOWLEDGEMENT	vi
GENİŞ ÖZET	vii
TABLE OF CONTENTS	xiii
LIST OF NOTATION	xvi
1. INTRODUCTION	1
1.1. General	1
1.2. Research Objectives	3
1.3. Methodology	3
1.4. Scope of Work	4
2. LITERATURE REVIEW	8
3. DS-TBM TUNNELING IN SQUEEZING GROUND	14
3.1. Introduction to Shielded TBM	14
3.1.1. Single Shield TBM	14
3.1.2. Double Shield TBM	14
3.2. Application of Double Shield TBMs in Long Deep Tunnels	16
3.3. Squeezing Ground	18
3.3.1. Empirical Approaches	18
3.3.2. Semi-Empirical Approaches	20
3.4. Analysis of Rock Mass Response in Squeezing Conditions	24
3.4.1. Closed Form Solutions	25
3.4.1.1. Elasto-Plastic Solutions	25
3.4.2 Numerical Analyses	28
3.4.2.1. Continuum Approach	28
3.4.2.2. Discontinuum Approach	29
4. NUMERICAL STUDY FOR EVALUATION OF HOEK AND MARINOS APPROACH	30

4.1. Numerical Approach.....	30
4.1.1. Numerical Model	30
4.1.2. Numerical Results	32
5. NUMERICAL MODELING OF A TUNNELING WITH A DOUBLE SHIELD TBM	37
5.1. Introduction	37
5.2. Modeling of TBM–Rock Mass Interaction in Squeezing Conditions	37
5.3. Three Dimensional Numerical Modeling	38
5.3.1. Assumptions and Considerations for Modeling	38
5.3.2. Numerical Modeling Method.....	39
5.3.3. Numerical Modeling of Rock Mass	40
5.3.4. Numerical Modeling of the Main TBM Components	41
5.3.5. Modeling the Interaction between the Machine Components and Ground	44
5.4. Simulation Procedure and TBM Advance Rate	45
5.5. Numerical Modeling of the Excavation Process	47
5.6. Verification of Numerical Simulation	49
5.6.1. Verification of Numerical Modeling by Using Ground Reaction Curve (GRC)	50
5.6.2. Verification of Numerical Modeling by Using Hoek and Marinos Approach for Squeezing Grounds	51
5.7. DS-TBM Excavation Results	51
5.7.1. Result of Analysis for Cutter-head and Front Shield	52
5.7.2. Result of Analysis for Rear shield	56
5.7.3. Result of Analysis for Total Tunnel Excavation with DS-TBM	60
5.7.4. Thrust Force Calculations.....	62
5.8. Stress History of the Ground.....	64
6. TIME DEPENDENT ANALYSIS	68
6.1. Introduction	68
6.2. Creep Behavior of Material.....	69
6.3. Time Dependent Response.....	70
6.4. Time Dependent Numerical Modeling	74
6.4.1 Assumptions for Numerical Model.....	74
6.4.2 Creep Model of the Analysis	74
6.4.2.1. CVISC model	75
6.4.2.2. Power Law Creep Model (CPOW Model).....	75
6.5. Results of Numerical Analysis	76

6.5.1. DS-TBM Time Dependent Excavation Results for CVISC Model	76
6.5.2. Effect of Advance Rate	79
6.5.3. Evaluation of TBM Entrapment Risks	80
6.5.4. Effect of Advance Rate on Loading of Segmental Lining	82
6.6. Results of Numerical Analysis for CPOW Model	83
7. IMPACT OF OVERCUT ON INTERACTION BETWEEN SHIELD, GROUND AND SUPPORT	84
7.1. Introduction	84
7.2. Shield–Ground Interaction	84
7.2.1. Shield-Ground Interaction at the Tunnel Crown	85
7.2.2. Shield-Ground Interaction at the Tunnel Wall	88
7.3. Comparison of the Extent of the Plastic Zone.....	89
7.4. Thrust Force Calculations	91
7.5. Interaction between Ground and Segmental Lining	92
8. APPLYING IMPROVEMENT METHODS FOR PREVENTING TBM ENTRAPMENTS	94
8.1. Introduction	94
8.2. Ground Improvement Methods	95
8.2.1. Grouting from Probe Drilling Holes	95
8.2.1.1. Probe Drilling Method: Numerical Simulation	97
8.2.2. Ground Reinforcement	101
8.2.2.1. Applying Rock Bolt: Numerical Simulation.....	102
8.2.3. Forepoling	103
8.2.4. Lowering of the Groundwater Table	104
8.3. Application of Lubricants Such as Bentonit	104
9. CONCLUSIONS AND RECOMMENDATIONS	106
REFERENCES	110
APPENDIX A.....	115
APPENDIX B.....	118

LIST OF NOTATION

A	power-law constant
B	tunnel span or diameter
c	cohesion of the ground
c_p	peak cohesion
c_r	residual cohesion
D	tunnel diameter
D_h	Hoek disturbance factor
d_p	plastic zone diameter
E	Young's modulus of the ground
E_i	Young's modulus of intact rock
f	increasing function of time
f_c	uniaxial compressive strength
F	thrust force
F_N	thrust force of auxiliary system
F_f	thrust force needed for overcoming friction
F_i	installed thrust force
F_r	required thrust force
G	shear modulus
G_0	shear modulus at spring no.0
G_1	shear modulus at spring no.1
G_f	creep modulus
G^K	Kelvin shear modulus
G^M	Maxwell shear modulus
GSI	Geological Strength Index
H	depth of cover
K_0	ratio between the horizontal and vertical stress components
K_l	stiffness of the lining
K_s	stiffness of the shield
L	length of the shield
m_i	Hoek material constant
m_p	Hoek-Brown constant
m_r	Hoek-Brown constant
n	power-law exponent

N	rock mass number
p	ground pressure
p_o	in situ stress
p_i	support pressure
p_c	pressure on lining
p_{cr}	critical pressure
Q	rock mass quality
r	real shield radius
R	tunnel radius
R_p	radius of the plastic zone
s_p	Hoek-Brown constant
s_r	Hoek-Brown constant
t	time
t_s	lining installed time
T	torque or relaxation time
u_r	radial displacement of the ground (at the tunnel boundary)
UCS	Uniaxial Compressive Strength
AR	advance rate
x	radial co-ordinate (distance from the tunnel axis)
y	axial co-ordinate fixed to the advancing tunnel face (distance behind the tunnel face)
z	elevation
β	reduction coefficient
ε	percentage strain defined by tunnel closure to tunnel diameter
$\dot{\varepsilon}$	strain rate versus time
ε^c	creep strain
ε_r^c	radial strain
ε_θ^c	tangential strain
ε_f	failure strain limit
ε_f	tunnel face strain
ε_e	elastic strain limit
ε_θ^e	elastic strain limit for the rock mass
$\varepsilon_\theta^\alpha$	tangential strain around a circular tunnel
ε^{ne}	time-dependent inelastic strain
ε^p	plastic strain

ε_p	peak strain limit
ε_s	softening strain limit
ε_t	tunnel strain
ε_θ^a	strain level around a circular tunnel
ϕ_p	peak friction angle
ϕ_r	residual friction angle
ΔR	size of the radial gap between shield and bored profile
ΔR_c	size of the radial gap between cutter-head and bored profile
ΔR_f	radial gap size of the front shield (double shielded TBM)
ΔR_l	size of the radial gap between lining and bored profile
ΔR_r	radial gap size of the rear shield (double shielded TBM)
γ	unit weight of the ground
η_l	viscosity
η^K	Kelvin viscosity
η^M	Maxwell viscosity
η_p	normalized strain level
η_s	normalized strain level
η_f	normalized strain level
φ	internal friction angle of the ground
μ	shield skin friction coefficient
ν	Poisson's ratio of the ground
W	weight of TBM
σ	the deviator stress
σ_0	initial stress
σ_1	maximum principal stress
σ_3	minimum principal stress
σ_{ci}	uniaxial compressive strength of intact rock
σ_{cm}	uniaxial compressive strength of rock mass
σ_h	horizontal stress of ground
σ_t	Tensile strength
σ_v	vertical stress of ground
σ_{xx}	axial stress at x direction
σ_{yy}	axial stress at y direction
σ_{zz}	axial stress at z direction
σ_{xy}	shear stress

σ_{zy}	shear stress
σ_{xz}	shear stress
σ_r^c	radial stress
σ_θ^c	tangential stress
ψ	dilatancy angle of the ground

1. INTRODUCTION

1.1. General

Applications of shielded Tunnel Boring Machines (TBM) in mechanized tunneling have become popular in recent years. Need for new infrastructure including road, rail, water, waste water, and utility tunnels have increased significantly. Speed of excavation and flexibility of these machines in coping with various ground conditions is superior to conventional tunneling. Today, almost all rock mass conditions can be bored by modern TBMs with tunnel diameter varying from less than 2 m to 15 m.

Alternatively Double Shields TBMs are amongst the most technically sophisticated excavation machines in use by tunneling industry. Combining the Gripper principle and the installation of the segments in a perfectly coordinated process, Double Shields can easily be adapted to the particular geological conditions of any tunnel alignment. Recent development and use of versatile machines have opened new horizons for the use of DS-TBMs in unknown and adverse ground conditions. The use of shield around the TBM allows the machine to pass through weak grounds and adverse geological conditions. Successful use of double shields in many projects clearly indicates the capability of this concept in providing an efficient performance in various ground conditions.

However, using the shielded machine limits access to the walls for observation of ground conditions and presence of shield makes the machine susceptible to entrapment or seizure in weak rocks under high stresses which results in high convergence. This is even more so in the case of the double shield TBMs, which is indeed a more complex machine than the gripper or the single shield TBM. Also double shield machines are longer than their single shield peers and thus more likely to get trapped as the ground gradually deforms behind the tunnel face. Therefore TBM may get stuck (including shield jamming and cutter-head blocking) in the complicated geological structures commonly referred to as squeezing ground, which requires manual excavation to release the machine. This is a time consuming, costly, unsafe, slow, and labor intensive work that should be avoided as much as possible. Thus, the main question in selection of shielded TBMs for many tunneling projects in squeezing ground remains the possibility of machine seizure in the ground. Stoppage of a machine in squeezing ground is bad news in many respects. First of all, the time after stoppage has a negative impact lead to machine seizure. Also, the process of releasing the machine is very labor intensive since it can only be done by manual labor and thus is very slow and dangerous. Therefore, examining the possibility of machine stoppage

due to excessive ground convergence is an important step in tunnel design involving the use of double shield TBMs. In addition, some of the case histories indicate that interruptions of the double shield TBM drive may be unfavorable in squeezing ground; this includes weekends, stoppages for machine repair or maintenance, or other machine downtimes. Therefore the "time" factor plays an important role in such conditions that should be considered in analyses. In several cases, the TBM did not become jammed until there was a slowdown or standstill in the TBM drive, which suggests that maintaining a high gross advance rate and reducing standstill times may have a positive effect in avoiding entrapment.

There are many studies about the application of shielded TBMs in squeezing ground in the literature. However, these studies seem to have some shortcomings that must be reevaluated. Some shortcomings are as follows:

- There are empirical and semi empirical approaches for identification and quantification of squeezing behavior, which need to be reevaluated based on numerical analysis.
- In numerical simulation of tunnels that are excavated by using the double shield TBMs, the exact 3D numerical simulations for evaluation of machines in squeezing grounds to evaluate ground convergence, contact pressure between shield and ground, and also interaction between segmental lining and backfilling are scarce. This refers to the need for more extensive application of the 3D numerical simulations of squeezing grounds for identification and quantification of squeezing behavior for a given geological setting and ground conditions.
- While the squeezing process is a time dependent phenomenon, lack of related analyses for evaluation of applicability of double shield TBMs concerning time dependent ground convergence is evident in many studies. This is also true with respect to interaction between shield, ground, and ground support where design of supports, either using numerical or empirical analysis, was done without such considerations.
- Numerical simulation for design and selection of the appropriate ground improvement methods for preventing jamming of the shield and study of the lubrication mechanism when shield is subjected to ground convergence pressure are not provided in the literature.

1.2. Research Objectives

This thesis aims to develop a comprehensive numerical simulation for evaluation of applicability of shielded TBMs in squeezing grounds. Moreover, the overall objective of the study is the systematic evaluation of potential of excessive ground convergence and of encountering ground squeezing and application of shielded TBMs in such grounds with the possibility of using ground improvement or lubrications to avoid shield jamming in such cases. In particular the goals of the thesis work can be summarized as follows:

- Evaluating of the empirical and semi empirical approaches for identification and quantification of squeezing behavior of the ground based numerical analysis results
- Creating a comprehensive realistic 3D numerical simulations for performance evaluation of double shield TBMs in squeezing grounds in order to calculate the ground convergence, contact forces and assess the possibility of entrapment for given machine and cutter-head configuration
- Study of elasto-plastic and time dependent behavior of tunnels that have been excavated by double shield TBMs
- Evaluation of overcut relative to interaction between shield, ground and support on the basis of numerical analyses in squeezing grounds
- Selecting the appropriate ground improvements methods in squeezing grounds to control the amount of ground convergence for preventing the TBM or shield jamming
- Evaluation of lubrication mechanism between shield and rock when shield is subjected to ground convergence pressure

The study also allow for a more objective evaluation of machine selection for specific ground conditions to quantify the risks of machine entrapment and allow for selection of double shield for use in various grounds, especially deep rock tunnels, with calculated risks of machine's working conditions and possibility of encountering ground squeezing and possible mitigation plans.

1.3. Methodology

Methodology used for this study is to collect field information from published literature and empirical and semi empirical results to allow for better understanding of the ground

behavior in potentially squeezing grounds. This information is used for validation of the numerical modeling that is the main emphasis of the current study. Finite Difference method, and in particular FLAC^{3D} program is used to simulate the behavior of the ground and to calculate the amount of ground convergence and interaction between the ground and main TBM components. A parametric study is performed to develop a realistic assessment of overcut and machine entrapment. The parametric study also takes into account the time dependent behavior of the ground and the impact of daily advance rate. This has been followed by examination of the possibility to mitigate potential problems using overcut, ground improvement measures and finally application of various shield lubrication systems.

1.4. Scope of Work

Scope of works for this thesis is selected with respect to the goals and to achieve the objectives of the study. Since the main emphasis of this thesis is on numerical analysis, a comprehensive numerical simulation of tunnel convergence is performed by FLAC^{3D} numerical modeling software. The models include a cylindrical tunnel, much like what is mined by a double shield TBM. The model is set up to account for the cutter-head and shield geometries and allow the interaction between the ground and the shield and cutter-head to evaluate the contact forces. Scopes of works applied in the thesis are as follows:

- First, sensitivity analyses have been performed on initial model for determination of the effects of boundary conditions, size of mesh near tunnel, total number of zones, running time and unbalanced forces.
- The next step involved quantification of ground convergence by referring to some hypothetical material properties to allow for better understanding of the ground behavior and identification of potentially squeezing grounds. This information was used for validation of the numerical modeling that is the main emphasis of the current study. In this regard a semi empirical approach was used to determine the potential for ground squeezing conditions and for calculation of the amount of convergence in various ground conditions. Also numerical simulation for identification of potential of squeezing is applied on the related data to the same cases. The results of modeling using numerical analysis are compared to semi empirical approach.
- The required parameters for simulation of tunneling with double shield TBMs divide into three groups that are as follows: a) Machine data include the required

thrust force F_r , weight of the machine W , shield length L , shield stiffness K_s , the skin friction coefficient μ , and the stiffness of the lining K_l , b) Ground and geological data including the Young's modulus E , Poisson's ratio ν , uniaxial compressive strength f_c , internal friction angle ϕ , dilatancy angle ψ and the initial stress σ_0 , and c) Performance and speed variables such as the tunnel radius R , tunnel advance rate, radial gap size or overcut ΔR . Considering these parameters, numerical analysis for evaluation of the most critical variable including overcut has been performed. Also a sensitivity analysis of tunnel advance rate was performed, which allows to determine the impact of time dependent behavior of the ground depending based on given material properties.

- For evaluation of the risks for machine entrapment with respect to potentially squeezing conditions and estimated ground convergence some simulation were performed by using numerical viscoelastic analysis for determination of radial displacement u_r of the ground at the tunnel boundary and tunnel face for given shield length L and overcut ΔR . Also, the amount of ground pressure p and plastic zone R_p acting upon the shield and the lining, and the amount of frictional forces that need to be overcome by machine thrust were calculated. In addition, the modeling allows for extracting the history of the axial stresses (σ_{xx} , σ_{yy} , σ_{zz}) and shear stresses (σ_{xy} , σ_{xz} , σ_{yz}) and principal stress paths along the tunnel boundary.
- The time dependent analysis was performed for assessment of effects of creep and time on tunnel convergence. For this purpose, power law creep model, and Burger-creep visco-plastic model were applied on selected case studies. This allows for prediction of tunnel closure u_r and contact pressure p on the lining along the tunnel versus time. Also, an extensive time dependent analyses were performed by considering the amount of overcut, shield length, and excavation speed for evaluation of the potential for jamming. This analysis has made the determination of the speed of cutting for avoiding of shield jamming.
- Appropriate ground improvement methods to strengthen the ground and prevent or slow down ground convergence in squeezing ground conditions have been studied by numerical simulations as well. Various ground improvement methods have been evaluated for control of the plastic zone through the use of numerical and theoretical analysis. The objective was to evaluate and select the appropriate

ground improvement for different ground conditions to avoid or minimize the risk of TBM entrapment.

- High frictional forces against the shield formed due to rock mass movement into the tunnel could prevent the advancing of the TBM forward. This issue can be partially addressed by implementing an overcut into the rock, but in some cases the ground convergence is so fast that it compensates the overcut and the walls come to contact with shield before it could pass through. This contact produces high frictional forces against the shield that needs to be overcome by machine thrust. Applying a pressurized lubricant such as bentonite, when shield is subjected to ground convergence pressure can reduce the friction and allow the shield to move forward. Numerical sensitivity analysis has been carried out for determination of required thrust force F_r as a function of skin friction coefficient μ during ongoing excavation and for restarting TBM after a standstill.

This thesis is organized in 9 Chapters. In Chapter 2, a comprehensive literature survey on tunneling experience involving double shield TBMs in squeezing ground conditions is summarized.

In Chapter 3, a brief review about the shielded TBM and operational parameters with emphasis on double shield TBMs is offered. The empirical and semi empirical solutions for determination of potential squeezing problems in tunnels have been extensively covered in rest of the chapter.

In Chapter 4, a numerical model has been developed based on Hoek and Brown yield criterion model. Using the model, parametric studies were performed for evaluation and verifying of Hoek and Marinos semi empirical approach in squeezing ground.

In Chapter 5, 3D modeling of mechanized tunneling by using a double shield TBM in squeezing ground is developed for elasto-plastic numerical analysis. 3D finite difference numerical simulation program, FLAC^{3D}, is used for modeling of the double shield and universal double shield TBMs for excavation of long deep tunnels through various rock masses that exhibit squeezing behavior.

In Chapter 6, time dependent behavior of rock masses around tunnel is investigated to observe the impact of advance rate on the possibility of machine entrapment and evaluation of machine entrapment risks in the squeezing grounds. For this purpose, time-dependence modeling with respect to creep material properties of rock mass in severe

squeezing conditions is considered on some case studies. Two time dependent constitutive models including a Burger-creep visco-plastic model combining the Burger's model and the Mohr-Coulomb model (CVISC) and a power-law visco-plastic model combining the two-component power law and the Mohr-Coulomb model (CPOW) are applied to the numerical model for describing the tunnel time dependent response associated with severely squeezing conditions.

In Chapter 7, numerical analysis is continued to evaluate the impact of the over-boring (overcut), one of the main effective factors at DS-TBM tunneling, on the possibility of machine jamming.

In Chapter 8, a review of ground improvement methods and numerical analysis of ground deformation with additional support measures are provided. The impact of ground improvement methods is studied by using numerical analysis to see if such measures can reduce the magnitude of the ground convergence and reduce the risks of using double shield TBMs in potentially squeezing grounds. The interaction between ground and shield when shield is subjected to ground convergence pressure and application of pressurized lubricant is studied by sensitivity analysis using numerical simulations.

Finally in Chapter 9, conclusions and recommendations of the study for future follow up studies are summarized.

2. LITERATURE REVIEW

The study of squeezing behavior of the ground during tunnel excavation has been of interest to experts for years. This is due to great difficulties in completion of underground operation along with major delays in construction schedules and cost overruns. One of the case histories of interruptions in the shield TBM tunneling in squeezing ground is Nuevo Canale Val Viola in Italy. In this project a 3.60 m diameter double shield TBM was used for excavation when the TBM got trapped because of squeezing ground conditions in the pelitic and phyletic rock during a one-week holiday stoppage. In the Tunnel 38 of the Yindaruqin Irrigation Project in China, a 5.54 m diameter double shielded TBM was trapped in clayey sandstone during a maintenance stop [1]. Table 2.1 is a list of the case histories where squeezing ground problems were reported to be the cause of jamming of the shield, excessive convergences and jamming of the back-up equipment. These incidents show that the ground behavior is the most important parameter in tunneling process. This is especially true for complex ground conditions such as rock tunnels in heavily folded and metamorphosed areas, in highly variable formations, with frequent faults along the tunnel alignment, at great depths, and finally, in mixed face situations.

There are several methods for design and analysis of tunnels that have been used by various researchers and engineers. The method of characteristic lines is a closed form solution that is the simplest and widely used analysis method in tunneling. It has also been used by Kovari [2] with respect to some of the issues of TBM tunneling in squeezing ground. Vogelhuber later applied the convergence-confinement method for investigating the crossing of a shear zone at great depth with a double shielded TBM of 10 m diameter [1]. He was thereby able to differentiate between the short-term and long-term behavior of the ground. The method of characteristic lines is still used today for analyzing the interaction between ground and support also with regard to deformable segmental linings of shield-driven tunnels through squeezing rock [3, 4].

The main disadvantage of the method of characteristic lines is that it does not provide the longitudinal distribution of the ground pressure acting upon the shield and the lining. For this purpose, additional assumptions must be introduced. Therefore, for example, Hisatake and Iai [5] proposed a time dependent (creep) non-dimensional displacement function for the longitudinal distribution of the radial ground displacements, while Moulton et al. [6] and Feknous et al. [7] introduced three-dimensional diagrams that show support pressure as a function of convergence and distance from the tunnel face. But making an assumption

about the distribution and magnitude of the ground pressure is an even stronger simplification in the analysis methods.

Table 2.1. DS-TBM entrapment experiences in squeezing condition [1]

Project (country), Tunnel length	TBM type, Manufacturer, Boring diameter	TBM operation year
Stillwater Tunnel (USA), 12.9 km	Double shielded TBM, Robbins, 2.91 m	1978-1979
Los Rosales Tunnel (Colombia), 9.1 km	Double shielded TBM, Robbins, 3.54 m	1987-1990
Yindaruqin Irrigation Project, Tunnel 38 (China), 5.1 km	Double shielded TBM, Robbins, 5.54 m	1990-1992
Evinos – Mornos Tunnel (Greece), 29.4 km	Double shielded TBM, Robbins, 4.04 m	1993-1994
Guadiaro – Majaceite Tunnel (Spain), 12.2 km	Double shielded TBM, NFM-Boretec-Mitsubishi, 4.88 m	1995-1997
Umiray – Angat Tunnel (Philippines), 13.2 km	Double shielded TBM, Robbins, 4.88 m	1998-2000
Fujikawa Transport and Pilot Tunnels (Japan), 4.5 and 3.7 km	Double shielded TBM, (unknown), 3.50 m Double shielded TBM, (unknown), 5.00 m	1999-1999 2000-2001
Nuovo Canale Val Viola Tunnel (Italy), 18.8 km	Double shielded TBM, Wirth, 3.60 m	1999-2004
Salazie Aval Tunnel (France), 9.4 km	Double shielded TBM, Herrenknecht, 3.85 m	1999-2005
Shanxi Wanjiashai Yellow River Diversion Project, Connection Works Tunnel Nr. 7 (China), 13.5 km	Double shielded TBM, Robbins, 4.82 m	2000-2001
Shanggongshan Tunnel (China), 13.8 km	Double shielded TBM, Robbins, 3.65 m	2003-2005
Ghomroud Tunnel, Sections 3 and 4 (Iran), 16.5 km	Double shielded TBM, Wirth, 4.50 m	2004-2008
Gilgel Gibe II Tunnel (Ethiopia), 25.8 km	Double shielded TBM, Seli, 6.98 m	2005-2009

This approach was followed by Eisenstein and Rossler who developed design charts for the operability of double shielded TBMs in gripper mode [1], as well as by Vigl and Jager [8] in their discussion of the latest developments in double shielded TBMs. On the basis of numerical calculations, Garber [9] improved the convergence-confinement method, provided charts for the design of deep tunnels in low permeability saturated porous media and applied the proposed semi-analytical solution method to the back-analysis of the segmental lining for the Nuclear Research Centre Connecting Gallery (Belgium), which was excavated by a single shielded TBM ($D = 4.81$ m).

Other investigators have attempted to get around the drawbacks of analytical solutions by introducing empirical functions based on field measurements, which describe the longitudinal distribution of the radial displacement of the tunnel boundary. Schubert [10] showed the effect of the advance rate on tunnel closure in a specific case using the relationships proposed by Sulem et al. [11]. Farrokh et al. [12], Jafari et al. [13] and Khademi Hamidi et al. [14] evaluated ground pressure and thrust force requirement in their

empirical investigation into the double shielded TBMs of the Ghomroud Tunnel (Iran, $D = 4.50$ m) and the Nosoud Tunnel (Iran, $D = 6.73$ m).

The performance of TBMs in squeezing ground can also be assessed by evaluating and correlating the operational parameters of the TBM. This was done, e.g., by Kawatani et al. [15] for the Takisato Tunnel (Japan, double shielded TBM, $D = 8.30$ m) and by Farrokh and Rostami [16] and [17] for the Ghomroud Tunnel (Iran).

In spite of the applications mentioned above, one should bear in mind that the reliability of empirical methods is in general limited, as they are based upon correlations of field data obtained in specific projects with potentially different conditions. Axially symmetric or three-dimensional numerical models pay due attention to the spatial stress redistribution in the vicinity of the advancing face, thus eliminating the errors introduced by the assumption of plane strain conditions and providing information on the evolution of stresses and deformations in the longitudinal direction as well as allowing a more detailed modeling of the different system components (i.e., ground, TBM, tunnel support) and their interfaces [18].

The initial results of spatial numerical analyses have already been presented by Lombardi, who discussed the influence of the advance rate on the lining loading for the simplified case of a lining that starts to become loaded 40 m behind the face [1]. Lombardi's work dealt with aspects of tunneling in overstressed rocks from a fundamental point of view. In the majority of cases reported in the literature, however, the numerical investigations have been carried out in the framework of specific TBM projects. So, for example, Lombardi and Panciera [19] analyzed the feasibility of a double shield TBM drive for the Guadiaro–Majaceite Tunnel (Spain, $D = 4.88$ m) taking account of the effects of advance rate and of time-dependent ground behavior.

Fully three-dimensional computational models have been applied by Cobreros et al. and by Simic a study which considers creep effects as well for the Guadarrama Tunnel (Spain, double shielded TBM, $D = 9.51$ m) [1]. Also Graziani et al. [20] have a same study for the planned Brenner Base Tunnel (Austria, double shielded TBM, $D = 11.00$ m). Other project related investigations include those of Wittke et al. [21], who evaluated the stresses and deformations of the shield structure of the single shielded TBM of the Hallandsas Tunnel (Sweden, $D = 10.70$ m) taking account of seepage flow and dealing with the structural

detailing of the shield by making a simplifying a priori assumption that the ground closes the steering gap at a distance of 4 m behind the working face.

Another group of papers involves numerical investigations, which do not take specific account of the shield in the computational model. For example, Shalabi [22] carried out a back analysis of the creep deformations and pressures of the Stillwater Tunnel (USA, $D = 3.06$ m) by assuming that the tunnel is lined up to the face. Amberg [23] and Lombardi et al. [24] investigated the effect of advance drainage on ground response for the excavation of the service tunnel of the planned Gibraltar Strait Tunnel between Morocco and Spain ($D = 6.50$ m). Amberg [23] and Lombardi et al. [24] simulated the shield by applying a support pressure of 1 MPa at the face and at the excavation boundary around the shield. All of these works assessed the feasibility of the TBM drive by comparing the computed radial displacements in the machine area with the size of the radial gap between shield and ground.

Schmitt investigated the behavior of single shielded TBMs by means of fully three-dimensional, step-by-step simulations of tunnel excavation, thus gaining a valuable insight into the effects of non-uniform convergence and of non-hydrostatic shield and lining loading [1], while Ramoni and Anagnostou [25] employed axisymmetric numerical models in order to investigate the effects of thrust force, over boring, shield length and skin friction coefficient between the shield and the ground with respect to the problem of shield jamming.

Ramoni and Anagnostou [26] and [27] created the model by implementing the stress-point algorithm in accordance with the so-called “steady state method”, a numerical procedure for solving problems with constant conditions in the tunneling direction by considering a reference frame, which is fixed to the advancing tunnel face. A recent description of the computational method (including its further development for poro-elastoplastic materials) and numerical comparisons with the step-by-step simulation of an advancing tunnel can be found in Cantieni and Anagnostou [28], respectively.

The steady state method makes it possible to solve the advancing tunnel heading problem in one single computational step, i.e., without the need to simulate several sequences of excavation and support installation. The computational economy and numerical stability of the steady state method made it possible to carry out a comprehensive parametric study and, based upon the numerical results of the study, to work out design nomograms

concerning shield loading and the thrust force required to overcome friction in respect of the different TBM types [29].

Time effects were taken into account by Sterpi and Gioda [30], who highlighted the fundamental effect of creep, as well as by Einstein and Bobet [31] and Ramoni and Anagnostou [32], who studied the consolidation processes associated with the development and subsequent dissipation of excess pore pressures around the tunnel in a low-permeability water-bearing ground.

A quick review of the literature published on this topic shows some shortcomings in the available models and related analysis as follows:

- The simplified closed-form solutions are widely used in studies that provide only a rough assessment of the squeezing potential without providing any information concerning rock pressure distribution in the longitudinal direction.
- The assumption of plane strain conditions, which underlies the closed-form solutions, introduces large errors in the case of heavily squeezing ground and do not correctly reproduce the actual stress history of the ground, and this may influence the results not only quantitatively, but also qualitatively. For this reason, axially symmetric or three-dimensional numerical models pay due attention to the spatial stress redistribution in the vicinity of the advancing face, thus eliminating the errors introduced by the assumption of plane strain conditions and providing information on the evolution of stresses and deformations in the longitudinal direction as well as allowing a more detailed modeling of the different system components and their interfaces.
- The reliability of empirical methods, in general, is limited as they are based on correlations of field data obtained in specific projects with potentially different conditions and need to evaluate with respect to sufficient number of numerical analysis to produce reliable results.
- The keyword “simplification” can be observed almost in most of spatial analysis. For instance, for simplification, the time-dependent ground response due to creep or consolidation is not taken into account in most of these analyses. According to this simplifying assumption, all plastic deformations occur instantaneously. However, time dependent behavior must be considered especially in squeezing ground with elasto-plastic analysis.

- In some of studies, the assumption of homogeneity presupposes that uniform ground conditions persist along the alignment and may be conservative if the TBM crosses a single short geological fault zone.
- As a consequence of the assumption of axial symmetry, the pressure obtained is “homogenized” over the tunnel cross-section due to the fact that the model assumes an overcut that is constant around the circumference of the shield, while in reality the shield slides along the tunnel floor, which means that the overcut is bigger above the crown than in the lower portion of the tunnel cross-section.
- Finally, the evaluation of overcut by using numerical and theoretical analyses, selecting the appropriate ground improvement methods for preventing the shield jamming, and lubrication mechanism between shield and rock when shield is subjected to ground convergence pressure to allow machine move forward has not been studied properly.

3. DS-TBM TUNNELING IN SQUEEZING GROUND

3.1. Introduction to Shielded TBM

There are two types of shielded TBMs used for tunneling in hard deep rocks:

- a) Single shield TBMs: are primarily for use in soft ground or in rock masses with short stand-up time and in fractured rock. These types of machines are sensitive to squeezing ground and face instabilities. In many cases where the ground is unstable and there is need for face pressure, alternatively, where there is no possibility of using grippers to propel the machine forward, single shield is the primary choice.
- b) Double shield TBMs: are for driving in fractured rock with low stand-up time, where the ground allows for use of grippers in significant portion of the tunnel alignment. They can achieve very good performance in good to fair rock and are even more sensitive to squeezing ground and to face instabilities.

3.1.1. Single Shield TBM

To support the tunnel temporarily and to protect the machine and the crew, this type of TBM is equipped with a shield (Figure 3.1). The shield extends from the cutter head over the entire machine. The tunnel lining is installed under the protection of the rear shield, or so called tail shield. Support with reinforced concrete segments has become the most commonly used system, while there are precedents of use of steel rib and wood logs where the final lining of the tunnel is cast in place or casting pipes. The segments are either installed as final lining (single pass construction) or as temporary lining with later addition of an in-situ concrete inner skin (known as Cast in Place 'CIP' or two pass lining) dictated by the geology and the application of the tunnel. The machine is moved forward by using thrust jacks directly against the existing tunnel support [33].

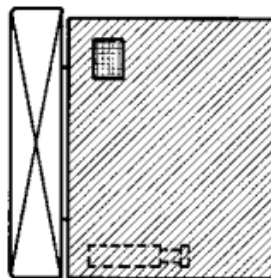


Figure 3.1. Single shield TBM [33]

3.1.2. Double Shield TBM

The double shield or telescopic shield TBMs consist of main components, the front shield and the gripper or main shield, and tail or rear shield. Various shield sections are connected

to each other with telescopic jacks and an articulation joint allows for steering of the front shield relative to gripper /tail shield. The machine can either adequately clamp itself radially in the tunnel using the gripper units of the gripper shield; or where the geology is bad and gripping is not possible, can push off the segmental lining in the direction of the drive. The front shield can thus be thrust forward without influencing the gripper shield, so that in general continuous operation is possible, nearly independent of the installation of the lining (Figure 3.2) [33].

The double shield TBM has disadvantages compared to the single shield TBM. When used in fractured rock with high strength, the rear shield can block due to the material getting into the telescopic joint. This is falsely described as the shield jamming, and in practice can be mitigated by cutting windows in the telescoping section to allow for discharging the debris. Blocking and jamming are however caused differently and should therefore be clearly differentiated.

The apparent advantages of the rapid advance of a double shield TBM is apparent when considering advance cycle per ring of about 30-40 minutes. With a double shell lining with installation time and advance cycle per ring of about 10-15 minutes, the higher purchase price and the greater need for repairs are no longer an issue, thus making the double shield economical [33]. Obviously, in bad ground conditions when the front and rear shields are locked and the machine moves forward by pushing against the installed segments, the advance cycle of both machines are the same, which is the sum of excavation and segment installation times.

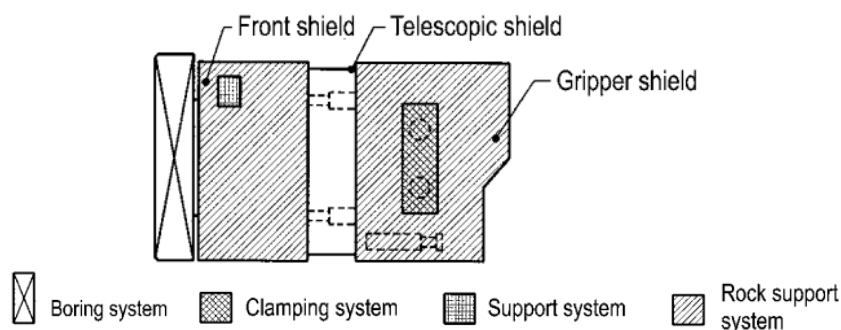


Figure 3.2. Double shield TBM [33]

The development of special segment systems such as the hexagonal or honeycomb segment, for the excavation of tunnels with double shield machines has been used successfully. These segments theoretically allow for continuous advance of the machine, with no delays for segment installation, since it is done during the excavation cycle.

Shorter construction periods with fully lined, long pressure tunnels can only be built by double shield machines. Even with rock characteristics ideal for gripper or open TBMs, the need for two distinct operations, including excavation and lining, the total tunnel completion time could be longer than using one pass method by using a double shield machine.

Under ideal conditions, double shields in the diameter range 5 to 12m can reach average advances of 25 to over 70 m/day. The cycle time for boring and installation of a segment ring (hexagonal segment, 1.3 m long) for 5 m excavation diameter is typically 15 min. The TBM is re-gripped time is 1.5 min and the assembly of a segment ring is performed in approximately 5-10 min [33].

3.2. Application of Double Shield TBMs in Long Deep Tunnels

Double shield TBMs have become a machine of choice in many cases due to their ability to cope with hard rocks as well as weak and unstable rocks [34]. As shown in Figure 3.3, these machines consist of the front shield with a cutter-head, main bearing and drive, a gripper shield with clamping unit (gripper plates), and tail shield and auxiliary thrust cylinders. Front and gripper shields are connected by a section (the telescopic shield) with telescopic thrust cylinders, which operate as the main thrust cylinders during normal operations. Where the rock is weak and it is not possible to grip, the necessary thrust forces can be provided by auxiliary thrust cylinders pushing off the segmental lining.

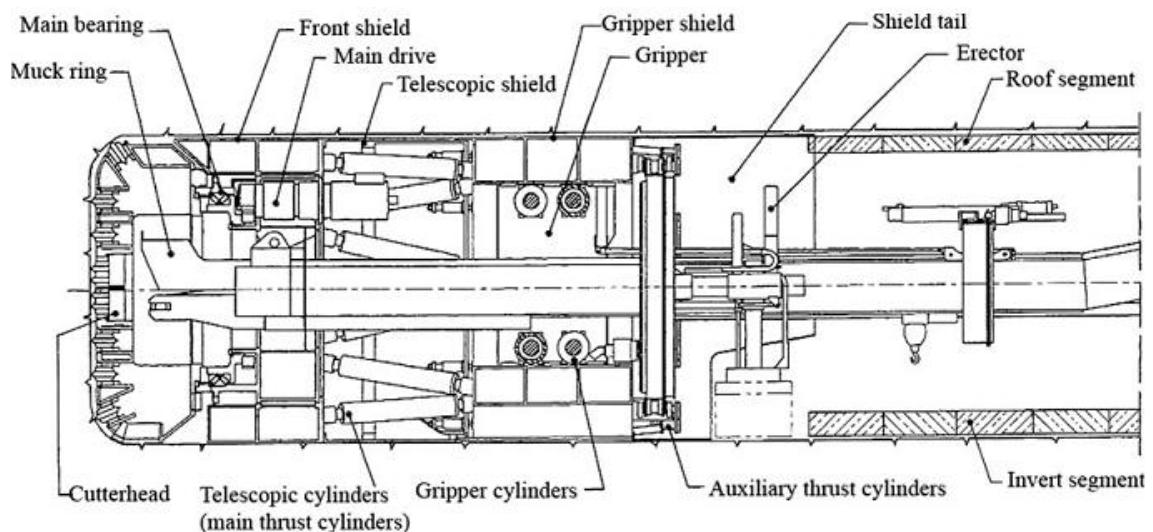


Figure 3.3. Longitudinal section of a double shield TBM [33]

In the first mode of operation using the telescopic cylinders to propel the machine, the auxiliary thrust cylinders only hold the segmental lining and the tail shield is stationary while the segment is erected during the stroke. In the second mode, which is also called

single shield mode, the front and gripper shield are locked to form a stiff unit and the auxiliary cylinders produce the necessary forward thrust [33].

Furthermore, the design of double shield TBM was improved with the introduction of the universal double shield TBM. Compared to the traditional double shield TBM, DS-TBMs have a shorter shield length and incorporate the conical shape in the shield structure by stepwise reduction of the shield diameters towards the back of the machine (Figure 3.4) [1].

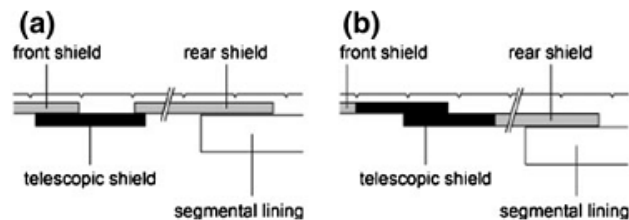


Figure 3.4. Construction schemes for the telescopic shield of double shield TBMs: a) classic design and b) modified design [1]

Shorter shield length means that the redistribution of the stresses in the ground and the displacement of the walls are not fully developed and consequently the possible squeezing forces on the shield (and the risk of getting trapped) will be lower. The conical arrangement of the shields provides more space for ground deformations, reducing the risk of shield jamming, eliminating the problem of packing the joint in loose ground, and preventing interlocking of squeezing rock resulting in a hindrance of the advance [34].

On the other hand, total shield length in DS-TBMs is ideally equal to the length of a single shield TBM of similar diameter. High main and auxiliary thrust force has been developed in DS-TBMs to move the shields even in very rapidly squeezing ground. Also since in large diameter tunnels the instability phenomena occur more rapidly, this feature allows the DS TBM to advance with maximum productivity in a wider range of ground conditions [34].

However, severe squeezing conditions may lead to deformations that are much greater than the gap or annular space between the ground and the shield which is created by the overcut and the conical shape of the shields. In extreme cases the totality of the shield surface would be in contact with the rock mass that has rapidly converged to embrace the shield. Countermeasures such as ground pre-treatment by grouting or drainage, pre-support of the ground by pipe umbrella, overcuts (maximum up to 30 cm), installation of higher thrust force (maximum up to 150 MN) and torque (maximum up to 30 MNm) and reduction of

the shield skin friction by lubrication of the interfaces are possible to allow the technical feasibility of the TBM drive in such conditions [1].

3.3. Squeezing Ground

The discussion of squeezing ground covered in this section, with some minor changes and summarizing, are taken from study by Barla on the subject [35]. The reader can refer to the reference citation for more detailed information.

As stated by the International Society of Rock Mechanics (ISRM), squeezing is the time dependent large deformation of the rock structures, which occurs around the tunnel and is essentially associated with creep, caused by exceeding a threshold shear stress. Deformation may terminate during construction or continue over a long period of time. The squeezing behavior is usually associated with poor rock mass, deformable with low strength properties such as micaschists, calcschists, graphiticschists, claystones, clay-shales, marly-clays, and etc. [35].

There are series of empirical and semi empirical solutions for determination of potential squeezing problems in tunnels. The empirical approaches are essentially based on classification schemes and in terms of the tunnel depth and rock mass quality. Two of these approaches include Singh et al. [36] and Goel et al. [37]. The empirical relationships are intended to identify potential squeezing problems in tunnels, in terms of the tunnel depth and rock mass quality.

The semi-empirical approaches also provide indications of potential for ground squeezing. However, they provide some tools for estimating the expected deformation around the tunnel and/or the support pressure required, by using closed form analytical solutions for a circular tunnel in a hydrostatic stress field. The common starting point of all these methods for quantifying the squeezing potential of rock is the use of the “competency factor”. Two main examples of such methods are Aydan et al. approach [38], based on the experience with tunnels in Japan, and Hoek and Marinos approach [39].

3.3.1. Empirical Approaches

The empirical approaches are essentially based on classification schemes. Two of these approaches are mentioned in the following.

a) Singh et al. (1992) approach

Based on 39 case histories, by collecting data on rock mass quality Q [40] and overburden H , Singh et al. [36] plotted a clear cut demarcation line to differentiate squeezing cases from non-squeezing cases (Figure 3.5).

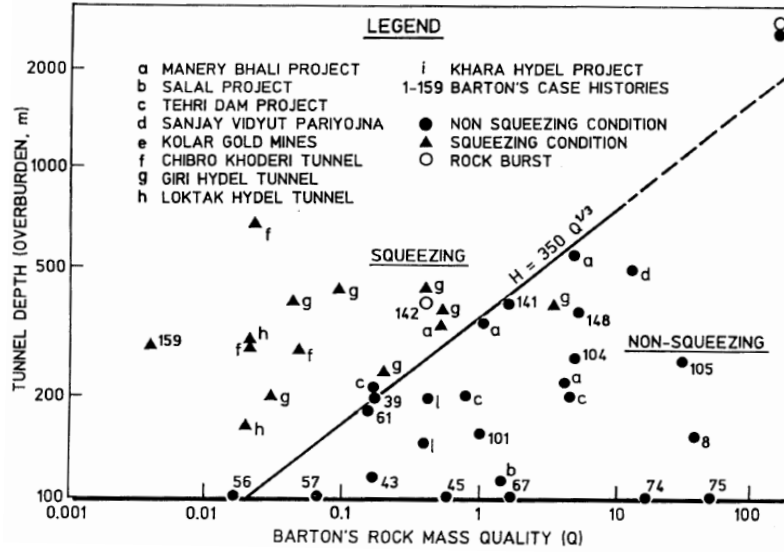


Figure 3.5. Singh et al. [36] approach for predicting squeezing conditions

For squeezing conditions:

$$H \gg 350 Q^{1/3} [m] \quad (3.1)$$

For non-squeezing conditions:

$$H \ll 350 Q^{1/3} [m] \quad (3.2)$$

With the rock mass uniaxial compressive strength σ_{cm} estimated as

$$\sigma_{cm} = 0.7 \gamma Q^{1/3} [MPa] \quad (3.3)$$

γ = rock mass unit weight.

b) Goel et al. (1995) approach

A simple empirical approach developed by Goel et al. [37] is based on the rock mass number N , defined as stress-free Q as follows:

$$N = (Q)_{SRF=1} \quad (3.4)$$

which is used to avoid the problems and uncertainties in obtaining the correct rating of parameter SRF in Barton et al. [40] Q . Considering the tunnel depth H , the tunnel span or diameter B , and the rock mass number N from 99 tunnel sections, Goel et al. [37] have plotted the available data on a log-log diagram between N and $H \times B^{0.1}$ (Figure 3.6).

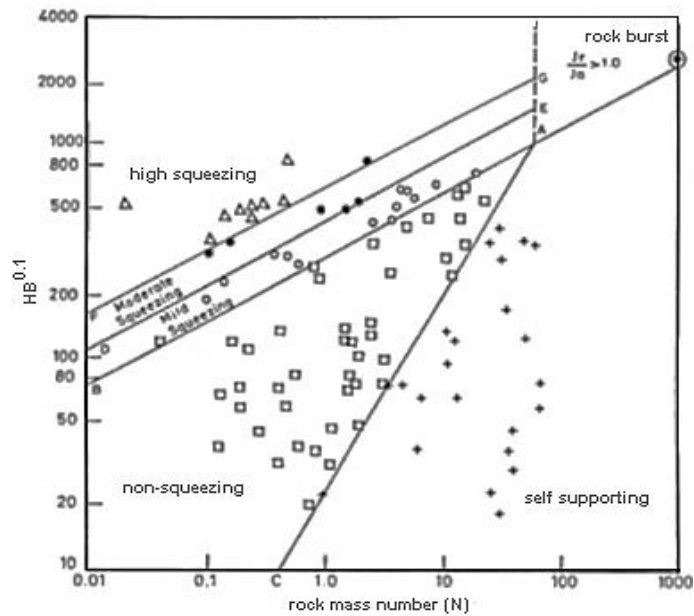


Figure 3.6. Goel et al. [37] approach for predicting squeezing conditions

For squeezing conditions:

$$H \gg (275 N^{0.33}) B^{-1} [m] \quad (3.5)$$

For non-squeezing conditions:

$$H \ll (275 N^{0.33}) B^{-1} [m] \quad (3.6)$$

- Degree of squeezing

Degree of squeezing has been represented by tunnel convergence as follows according to Singh et al. [36] and Goel et al. [37] approaches:

- (i) Mild squeezing convergence 1-3% tunnel diameter
- (ii) Moderate squeezing convergence 3-5% tunnel diameter
- (iii) High squeezing convergence >5% tunnel diameter

3.3.2. Semi-Empirical Approaches

The empirical relationships are intended to identify potential squeezing problems in tunnels, essentially in terms of the tunnel depth and rock mass quality (the Q or $(Q)_{SFR=1}$ index is used). The semi-empirical approaches are giving indicators for predicting squeezing. However, they also provide some tools for estimating the expected deformation around the tunnel and/or the support pressure required by using closed form analytical solutions for a circular tunnel in a hydrostatic stress field. The common starting point of all these methods for quantifying the squeezing potential of rock is the use of the “competency

factor”, which is defined as the ratio of uniaxial compressive strength σ_c/σ_{cm} of rock/rock mass to overburden stress γH . Two of such methods are discussed in the following [35].

a) Aydan et al. (1993) approach

Aydan et al. [38], based on the experience with tunnels in Japan, proposed to relate the strength of the intact rock σ_{ci} to the overburden pressure γH , by implying that the uniaxial compressive strength of the intact rock σ_{ci} and of the rock mass σ_{cm} are the same. As shown in Figure 3.7, which gives a plot of data of surveyed tunnels in squeezing rocks in Japan, squeezing conditions will occur if the ratio $\sigma_c/\gamma H$ is less than 2.0.

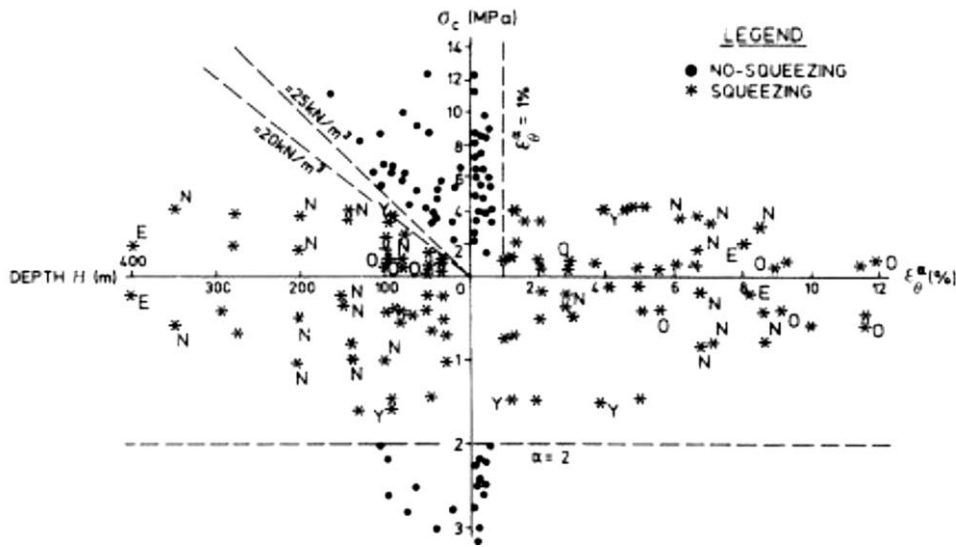


Figure 3.7. Aydan et al. [38] approach for predicting squeezing conditions

The fundamental concept of the method is based on the analogy between the stress-strain response of rock in laboratory testing and tangential stress-strain response around tunnels.

As illustrated in Figure 3.8, five distinct states of the specimen during loading are experienced, at low confining stress σ_3 (i.e. $\sigma_3 \leq 0.1\sigma_{ci}$). The following relations are defined which give the normalized strain levels η_p , η_s and η_f .

$$\eta_p = \frac{\varepsilon_p}{\varepsilon_e} = 2\sigma_{ci}^{-0.17} \quad (3.7)$$

$$\eta_s = \frac{\varepsilon_s}{\varepsilon_e} = 3\sigma_{ci}^{-0.25} \quad (3.8)$$

$$\eta_f = \frac{\varepsilon_f}{\varepsilon_e} = 5\sigma_{ci}^{-0.32} \quad (3.9)$$

where ε_p , ε_s and ε_f are the strain values shown in Figure 3.8, as ε_e is the elastic strain limit.

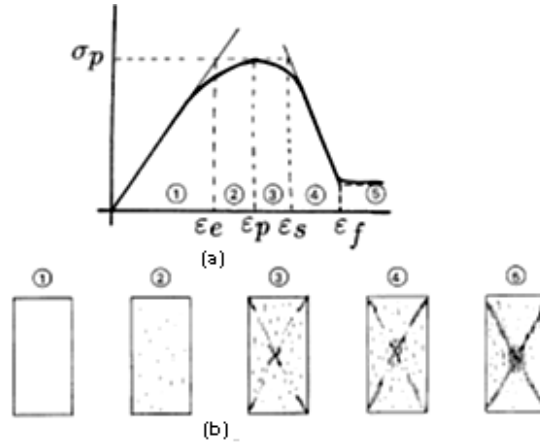


Figure 3.8. Idealized stress-strain curve and associated states for squeezing rocks [38]

Based on a closed form analytical solution, which has been developed for computing the strain level ε_{θ}^a around a circular tunnel in a hydrostatic stress field, the five different degree of squeezing are defined as shown in Table 3.1, where are also given some comments on the expected tunnel behavior [38].

Table 3.1. Classification of squeezing behavior according to Aydan et al. [38] approach

class no.	squeezing degree	symbol	theoretical expression	comments on tunnel behavior
1	non-squeezing	NS	$\varepsilon_{\theta}^a / \varepsilon_{\theta}^e \leq 1$	The rock behaves elastically and the tunnel will be stable as the face effect ceases
2	light-squeezing	LS	$1 \leq \varepsilon_{\theta}^a / \varepsilon_{\theta}^e \leq \eta_p$	The rock exhibits a strain-hardening behavior. As a result, the tunnel will be stable and the displacement will converge as the face effect ceases
3	fair-squeezing	FS	$\eta_p \leq \varepsilon_{\theta}^a / \varepsilon_{\theta}^e \leq \eta_s$	The rock exhibits a strain-softening behavior and the displacement will be larger. However, it will converge as the face effect ceases
4	heavy-squeezing	HS	$\eta_s \leq \varepsilon_{\theta}^a / \varepsilon_{\theta}^e \leq \eta_f$	The rock exhibits a strain-softening at much higher rate. Subsequently, displacement will be larger and it will not tend to converge as the face effect ceases
5	very heavy-squeezing	VHS	$\eta_f \leq \varepsilon_{\theta}^a / \varepsilon_{\theta}^e$	The rock flows, which will result in the collapse of the medium and the displacement will be very large and it will be necessary to excavate the opening and install heavy supports

Note: for η_p , η_s and η_f see above equation; ε_{θ}^a is the tangential strain around a circular tunnel in a hydrostatic stress field whereas ε_{θ}^e is the elastic strain limit for the rock mass.

b) Hoek and Marinos (2000) Approach

Hoek [41] used the ratio of the rock mass uniaxial compressive strength σ_{cm} to the in situ stress p_0 as an indicator of potential tunnel squeezing problems. In particular, Hoek and Marinos [39] showed that a plot of tunnel strain ε_t (defined as the percentage ratio of radial tunnel wall displacement to tunnel radius) against the ratio σ_{cm}/p_0 can be used effectively to assess tunneling problems under squeezing conditions.

Hoek and Marinos [39] found that the percentage strain in the rock mass surrounding a tunnel in weak overstressed rock is defined by the equation:

$$\varepsilon_t = 0.2 \left(\frac{\sigma_{cm}}{p_0} \right)^{-2} \quad (3.10)$$

where ε is the percentage strain defined by (tunnel closure/tunnel diameter $\times 100$). σ_{cm} is the uniaxial compressive strength of the rock mass. p_0 is the in situ stress defined by the product of the depth below surface and the unit weight of the rock mass.

Similarly, by recognizing the importance of controlling the behavior of the advancing tunnel face in squeezing rock conditions, Hoek [42] gave the following approximate relationship for the strain of the face ε_f (defined as the percentage ratio of axial face displacement to tunnel radius)

$$\varepsilon_f = 0.15 \left(\frac{\sigma_{cm}}{p_0} \right)^{-2} \quad (3.11)$$

The ratio of plastic zone diameter d_p to tunnel diameter d is given by the equation 3.12. Note that this analysis is based on the assumption that the horizontal and vertical in situ stresses are equal. This assumption is reasonable for very weak rock which cannot sustain high shear stresses such that, over geological time, anisotropic in situ stresses will tend to equalize.

$$\frac{d_p}{d} = 1.25 \left(\frac{\sigma_{cm}}{p_0} \right)^{-0.57} \quad (3.12)$$

On the basis of the above and consideration of case histories for a number of tunnels in Venezuela, Taiwan and India, Hoek [41] gave the curve of Figure 3.9 to be used as a first estimate of tunnel squeezing problems.

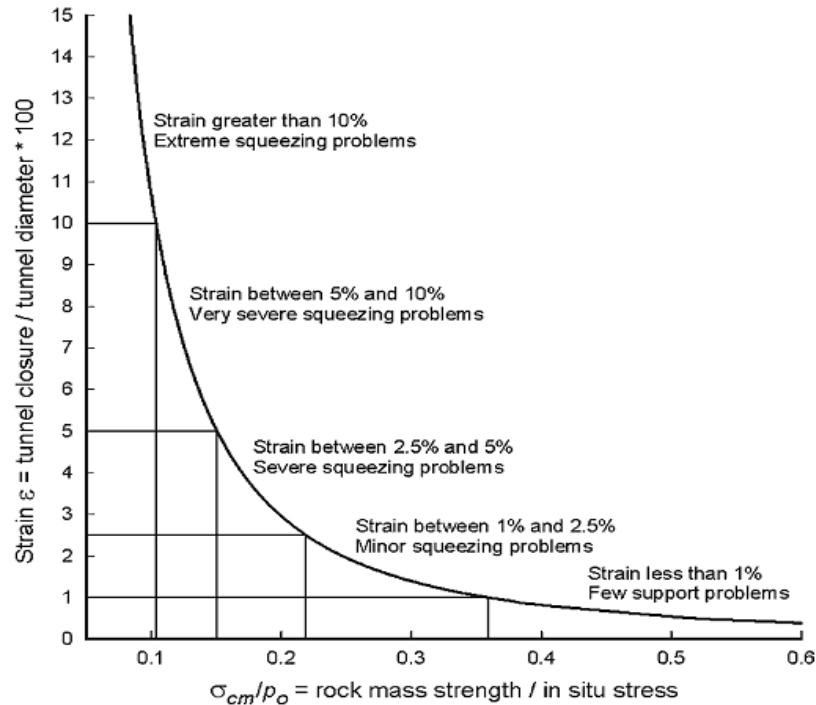


Figure 3.9. Approximate relationships between strain and the degree of difficulty associated with tunneling through squeezing rock for tunnels with no support [41]

3.4. Analysis of Rock Mass Response in Squeezing Conditions

Squeezing condition stands for large time-dependent convergence during tunnel excavation. It takes place when a particular combination of induced stresses and material properties pushes some zones around the tunnel beyond the limiting shear stress at which creep starts. Deformation may terminate during construction or continue over a long period of time [35].

The magnitude of tunnel convergence, the rate of deformation and the extent of the yielding zone around the tunnel depend on the geological and geotechnical conditions, the in-situ state of stress relative to rock mass strength, the groundwater flow and pore pressure and the rock mass properties. Squeezing is therefore synonymous with yielding and time-dependence; it is closely related to the excavation and support techniques which are adopted. If the support installation is delayed, the rock mass moves into the tunnel and stress redistribution take place around it. On the contrary, if deformation is restrained, squeezing will lead to long-term load build-up of rock support [35].

Methods for analysis of tunnels in squeezing rock conditions need to consider:

- The onset of yielding within the rock mass, as determined by the shear strength parameters relative to the induced stress

- The time dependent behavior.

An additional requirement is the estimation of the support pressure which is able to control the extent of the yielding zone around the tunnel and the resulting deformations. This poses considerable difficulties when the rock mass strength σ_{cm} relative to the in situ stress p_0 is low and complex support/excavation sequences are envisaged in order to stabilize the tunnel during construction [35].

3.4.1. Closed Form Solutions

The usual approach is to assume the tunnel to be circular and to consider the rock mass subjected to a hydrostatic in situ state of stress, in which the horizontal and vertical stresses are equal. If the attention is paid to the rock mass response to excavation, which is described by the “ground reaction curve” or “rock characteristic line”, one can plot the relationship between the support pressure p_i and the displacement u_r of the tunnel perimeter as shown in the Figure 3.10.

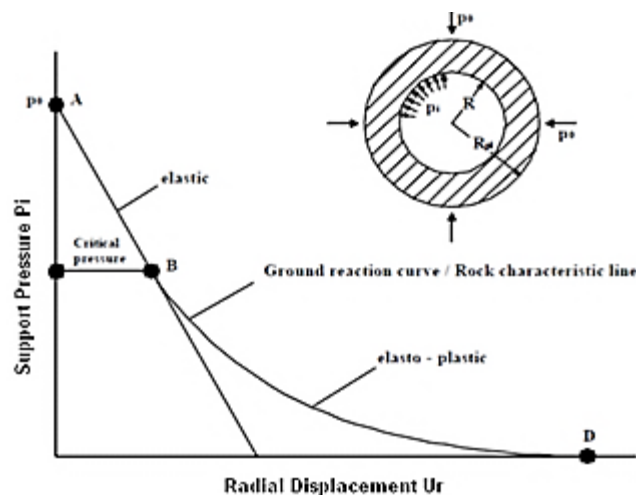


Figure 3.10. Axisymmetric tunnel problem: development of plastic zone around the tunnel and ground reaction curve/rock characteristic line [35]

3.4.1.1. Elasto-Plastic Solutions

If the rock mass is assumed to behave as an elasto-plastic-isotropic medium, the following models can be used (Figure 3.11):

- (1) Elastic perfectly plastic
- (2) Elasto-plastic, with brittle behavior
- (3) Elasto-plastic, with strain softening behavior

(a) The rock mass behave Mohr-Coulomb yield criterion. The rock mass strength and deformation characteristics are defined in terms of:

c_p, c_r = Cohesion (p and r stand for peak and residual values respectively)

ϕ_p, ϕ_r = Friction angle (p and r stand for peak and residual values respectively)

E = Young's modulus

ν = Poisson's ratio

ψ = Dilation angle

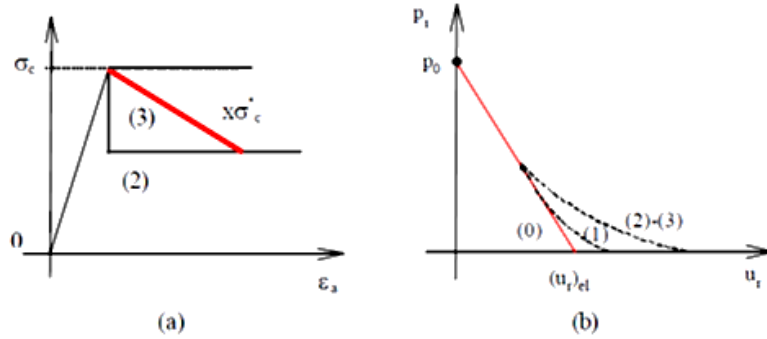


Figure 3.11. Elasto-plastic stress-strain models generally used to derive the ground reaction curve: (a) stress strain laws; (b) ground reaction curves [35]

Based on the available solutions from Ribacchi and Riccioni [35]:

- For the radius of the plastic zone:

$$R_{pl} = R \cdot \left\{ \frac{(p_0 + c_r \cdot \cotg\phi_r) - (p_0 + c_p \cdot \cotg\phi_p) \cdot \sin\phi_p}{p_i + c_r \cdot \cotg\phi_r} \right\}^{\frac{1}{N_\phi^{(r)} - 1}} \quad (3.13)$$

With:

$$N_\phi^{(r)} = \frac{1 + \sin\phi_r}{1 - \sin\phi_r} \quad (3.14)$$

- For the critical pressure p_{cr} , defined by the initiation of plastic failure of the rock surrounding the tunnel:

$$p_{cr} = p_0 \cdot (1 - \sin\phi_p) - c_p \cdot \cos\phi_p \quad (3.15)$$

- For the radial displacement u_r in the elastic zone ($r \geq R_p$):

$$u_r = \frac{1 + \nu}{E} \cdot (p_0 - p_{cr}) \cdot \frac{R_{pl}^2}{r} \quad (3.16)$$

- For the radial displacement u_r in the plastic zone ($R < r < R_p$):

$$u_r = \frac{1 + \nu}{E} \cdot \left\{ \frac{R_{pl}^{K'+1}}{r^{K'}} \cdot (p_0 + c_p \cdot \cot g \phi_p) \cdot \sin \phi_p + (p_0 + c_r \cdot \cot g \phi_r) \cdot (1 - 2\nu) \cdot \left(\frac{R_{pl}^{K'+1}}{r^{K'}} - r \right) \right. \\ \left. - \frac{\left[1 + N_\phi^{(r)} \cdot K' - i \cdot (K' + 1) \cdot (N_\phi^{(r)} + 1) \right] \cdot (p_i + c_r \cdot \cot g \phi_r)}{(N_\phi^{(r)} + K') \cdot R_\phi^{N_\phi^{(r)} - 1}} \cdot \left(\frac{R_{pl}^{N_\phi^{(r)} + K'}}{r^{K'}} - r^{N_\phi^{(r)}} \right) \right\} \quad (3.17)$$

with

$$K' = \frac{1 + \sin \psi}{1 - \sin \psi} \quad (3.18)$$

(b) The rock mass behave according to Hoek-Brown yield criterion. The rock mass strength and deformation characteristics are defined in terms of:

σ_{ci} = uniaxial compressive strength of the intact rock;

m_p, m_r, s_p, s_r = Hoek-Brown constants;

According to Brown et al. [43], the computations can be performed by the following equations:

- For the radius of the plastic zone:

$$R_p = R \cdot \exp \left[N - \frac{2}{m_r \cdot \sigma_{ci}} \cdot \sqrt{m_r \cdot \sigma_c \cdot p_i + s_r \cdot \sigma_c^2} \right] \quad (3.19)$$

$$M = \frac{1}{2} \cdot \sqrt{\left(\frac{m_p}{4} \right)^2 + \frac{m_p \cdot p_0}{\sigma_{ci}} + s_p} - \frac{m_p}{8} \quad (3.20)$$

$$N = \frac{2}{m_r \cdot \sigma_{ci}} \cdot \sqrt{m_r \cdot \sigma_{ci} \cdot p_0 + s_r \cdot \sigma_{ci}^2 - m_r \cdot \sigma_{ci}^2 \cdot M} \quad (3.21)$$

- For the critical pressure p_{cr} , defined by the initiation of plastic failure of the rock surrounding the tunnel:

$$p_{cr} = p_0 - M \sigma_c \quad (3.22)$$

- For the radial displacement u_r in the elastic zone ($r \geq R_p$):

$$u_r = \frac{1 + \nu}{E} \cdot (p_0 - p_{cr}) \cdot \frac{R_p^2}{r} \quad (3.23)$$

- For the radial displacement u_r in the plastic zone ($R < r < R_p$):

$$u_r = \frac{M \cdot \sigma_{ci} \cdot 2 \cdot (1 + \nu)}{E \cdot (f + 1)} \cdot \left[\frac{(f - 1)}{2} + \left(\frac{R_p}{r} \right)^{f+1} \right] \cdot r \quad (3.24)$$

where f is:

$$f = 1 + \frac{m_p}{2 \cdot \sqrt{\frac{m_p p_{cr}}{\sigma_{ci}}} + s_p} \quad (3.25)$$

3.4.2 Numerical Analyses

The use of numerical analyses is advisable in cases where the σ_{cm}/p_0 ratio is below 0.3, and it is highly recommended if this ratio falls below about 0.15, when the stability of the tunnel may become a critical issue. Significant advantages are envisaged by using numerical analyses at the design stage, when very complex support/excavation sequences, including pre-support/stabilization measures are to be adopted, in order to stabilize the tunnel during construction.

On the other hand, the most important disadvantage of the empirical and semi empirical approaches for use in the tunneling by a double shield TBM is that the calculated squeezing levels by using these approaches along the tunnel is not taking to account the TBM advance rate and face effect. Therefore to account for the impact of TBM advance rate and the ground behavior relative to the distance from the face, numerical simulations can be used to allow for modeling of the relevant geological, geometrical, and time related parameters.

Very powerful computer codes have been developed and are now available for the stress and deformation analysis of tunnels. It is therefore possible to develop reliable predictions of tunnel behavior, provided a proper understanding of the real phenomena as observed in practice is available. With respect to closed-form solutions, anisotropic in situ stress fields can now be considered, together with multiple excavation stages, the influence of face advance, and the important three-dimensional conditions which occur in the immediate vicinity of the face, the consequence of liner placement delay, etc.

3.4.2.1. Continuum Approach

If the equivalent continuum approach is used, with the assumption that the rock mass is a continuum with homogenous properties in all directions for the strength and deformability, a given constitutive equation for the rock mass is defined as; elastic, elasto-plastic, visco-elastic, elastic-visco-plastic the domain methods. With this setting, various numerical solutions including the finite element (FEM such as Plaxis2D or 3D), and the finite difference (FDM) methods (such as FLAC2D or 3D), can be used.

One of the obvious advantages of numerical methods in the analysis and design of tunnels in squeezing rock conditions is the use of more complex stress-strain models for the rock

mass such as the strain softening behavior and time dependent behavior, which can be implemented with both FEM and FDM. Another advantage of the numerical modeling is the ability to incorporate more complex geometries of the tunnel (i.e. non circular), or various tunnel-lining arrangements.

3.4.2.2. Discontinuum Approach

In weak rock masses which exhibit a squeezing behavior, the use of continuum representations of the medium subjected to excavation is reasonable. In general, the results obtained are applicable with success in practical tunnel design, provided that engineering judgment and precedent experience are used. However, there are cases where discontinuum modeling could be the most appropriate approach in order to analyze a given problem. For example, the rock mass is argillite, intersected by beddings which strike nearly parallel to the tunnel axis. A nearly vertical discontinuity system is as well present. Both the bedding and the jointing are very closely spaced and persistent so that the rock mass is subdivided into very small blocks. The DFN (Discrete Feature Network) model will be created in order to simulate the rock mass behavior by using the Distinct Element Method (DEM) and the UDEC code.

4. NUMERICAL STUDY FOR EVALUATION OF HOEK AND MARINOS APPROACH

In this Chapter, Hoek and Marinos semi empirical approach [39] is used for determination of squeezing levels at 12 hypothetical intrinsic tunnel excavations with different material properties. Furthermore, relating numerical analyses were performed by using the finite difference method, FLAC^{3D}, for evaluation of semi empirical approach. Plastic radius for each model were calculated for both of approaches and compared with each other.

4.1. Numerical Approach

For performing three dimensional numerical analysis, FLAC^{3D} program (Fast Lagrange Analysis of Continua in three dimensions), which is based on the finite difference method, was used. The program was developed by Peter Cundhall, and was subsequently distributed as commercial software by the Itasca Consulting Group company. Moreover, due to the large displacements occurring at tunnel around in the soft rock mass, the explicit finite difference method or the FLAC^{3D} program was used for the numerical analysis in order to avoid the problem of numerical instabilities in physical processes.

4.1.1. Numerical Model

A hypothetical three dimensional model was developed for parametric study. This model is used by considering isotropic material properties of the rock mass and the model was divided to half system generates. The 3D block model and relevant dimensions were presented in the Figure 4.1a that shows a isometric view of the model; the horizontal (x), longitudinal (y) and vertical (z) directions are 75, 60 and 150 m, respectively. For simplicity and accuracy of plastic zone radii calculation, the model is subjected to some changes with respect to conventional FLAC^{3D} models, so that the meshes around tunnel were altered to circular meshes. These changes are also shown in Figure 4.1b.

Preliminary investigations were carried out to determine the required distance from the tunnel face to edge of model to prevent the edge effect on displacements and stresses magnitudes of the numerical model in the advancing direction of the tunnel. It was found that a distance larger than 5 times the diameter of tunnel to the face is necessary to prevent the edge effect.

The rock mass is assumed to follow a linear elastic and perfectly plastic model according to Mohr-Coulomb failure criterion. But as input data using in the numerical model, the rock mass parameters according to Hoek Brown were used. For this purpose, a FISH code

was developed in FLAC^{3D} that considers Hoek–Brown criterion parameters and compiles them to Mohr-Coulomb parameters with respect to study from Hoek and Brown.

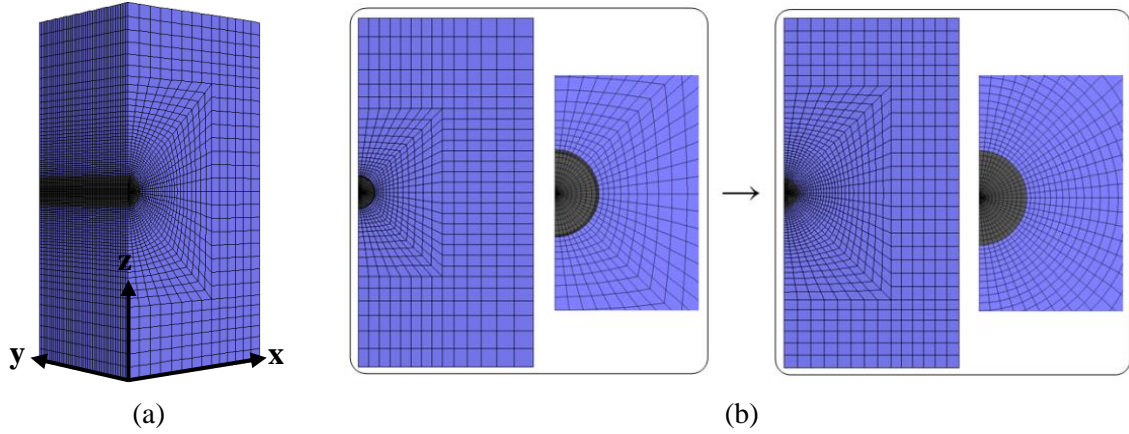


Figure 4.1. a) A half three-dimensional isometric view of the model b) Apply changing to mesh around tunnel to circular mesh

The initial field stress due to overburden forces was applied through the depth of the tunnel. It is assumed that this stress varies linearly with depth. Therefore, in situ state of stress is assumed to be isotropic and equal to γH . On the other hand, the ratio between the horizontal and vertical stress components is assumed to be 1 (Hydrostatic condition). Table 4.1 shows the tunnel and rock mass material properties according to Hoek-Brown criteria. These parameters are supposed to be constant for all of 12 models.

Table 4.1. Tunnel and rock mass parameters

Parameters	Unit	Value
Overburden, H	[m]	500
Unit weight of rock mass, γ	[kg/m ³]	2650
Elastic Modulus of intact rock, E_i	[GPa]	8
Poisson ratio, ν	-	0.25
Hoek Disturbance factor, D_h	-	0
Tunnel Diameter, D	[m]	6

For parametric studies, the rock mass parameters including GSI (Geological Strength Index), UCS (Uniaxial Compressive Strength) and m_i were considered as main variables. In Table 4.2, the individual parameters with range of their variation are summarized. In

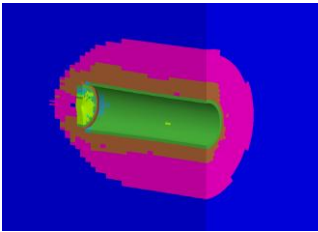
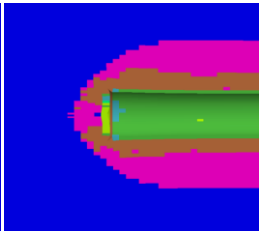
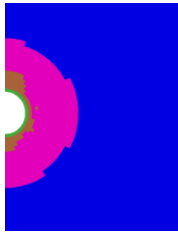
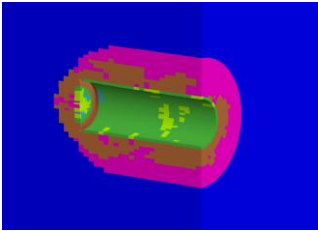
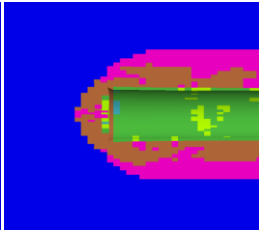
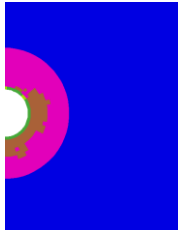
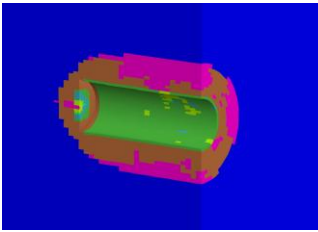
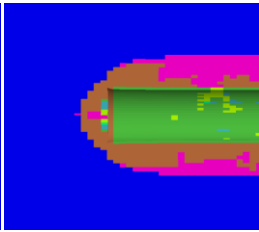
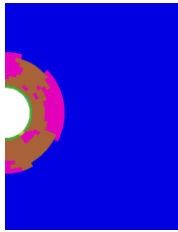
numerical simulation, it was assumed that the tunnel was excavated in dry rock mass. Therefore the effective stress from water pressure was not taken into account.

Table 4.2. Range of values of variable parameters of rock mass

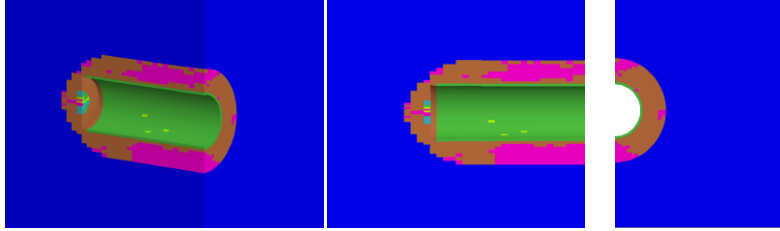
Parameter	Unit	Range of Value
Geological Strength Index, <i>GSI</i>	-	20 / 25 / 30 / 35
Uniaxial compressive strength of intact rock, <i>UCS</i>	[MPa]	10/ 20 / 30 / 40
Hoek material constant for intact rock, m_i	-	6 / 12 / 16 / 22

4.1.2. Numerical Results

Results of numerical analysis for different rock mass parameters are given for 12 models in Figure 4.2. Additionally, the calculated plastic radiuses from both semi-empirical and numerical approaches are given in Table 4.3. These magnitudes are extracted for different material properties and normalized and compared in Figure 4.3.

a) GSI Variations				
Model No.	3D view of plastic zones	Longitudinal view	Sectional view	Rock mass parameters
1				H = 500 m $\gamma = 26 \text{ kN/m}^3$ $E_i = 8 \text{ GPa}$ $\nu = 0.25$ GSI = 20 UCS = 35 MPa $m_i = 10$
2				H = 500 m $\gamma = 26 \text{ kN/m}^3$ $E_i = 8 \text{ GPa}$ $\nu = 0.25$ GSI = 25 UCS = 35 MPa $m_i = 10$
3				H = 500 m $\gamma = 26 \text{ kN/m}^3$ $E_i = 8 \text{ GPa}$ $\nu = 0.25$ GSI = 30 UCS = 35 MPa $m_i = 10$

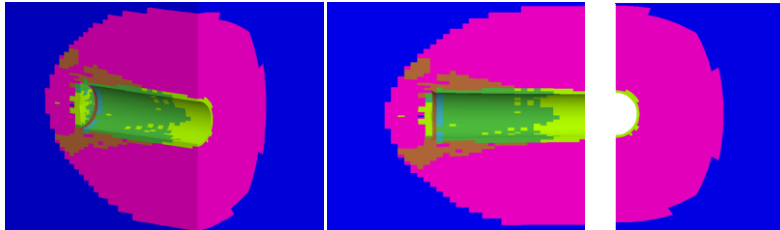
4



H = 500 m
 $\gamma = 26 \text{ kN/m}^3$
 $E_r = 8 \text{ GPa}$
 $\nu = 0.25$
GSI = 35
 UCS = 35 MPa
 $m_i = 10$

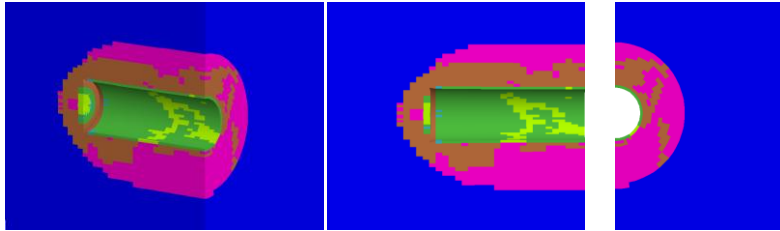
b) UCS Variations

5



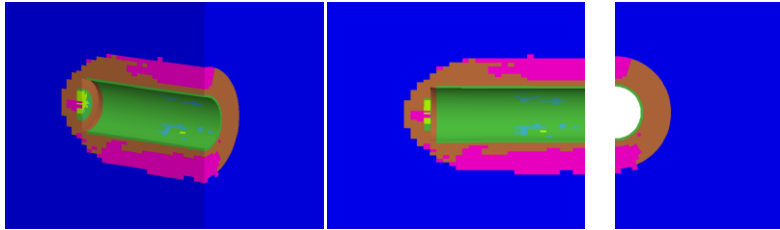
H = 500 m
 $\gamma = 26 \text{ kN/m}^3$
 $E_r = 8 \text{ GPa}$
 $\nu = 0.25$
 GSI = 35
UCS = 10 MPa
 $m_i = 10$

6



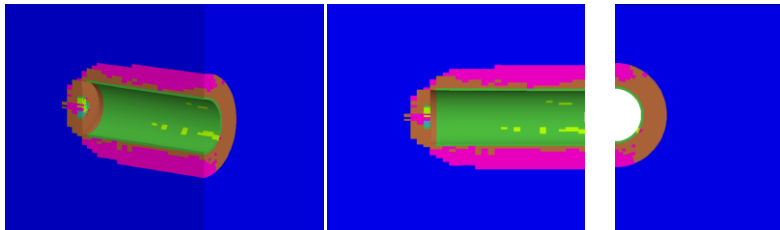
H = 500 m
 $\gamma = 26 \text{ kN/m}^3$
 $E_r = 8 \text{ GPa}$
 $\nu = 0.25$
 GSI = 35
UCS = 20 MPa
 $m_i = 10$

7



H = 500 m
 $\gamma = 26 \text{ kN/m}^3$
 $E_r = 8 \text{ GPa}$
 $\nu = 0.25$
 GSI = 35
UCS = 30 MPa
 $m_i = 10$

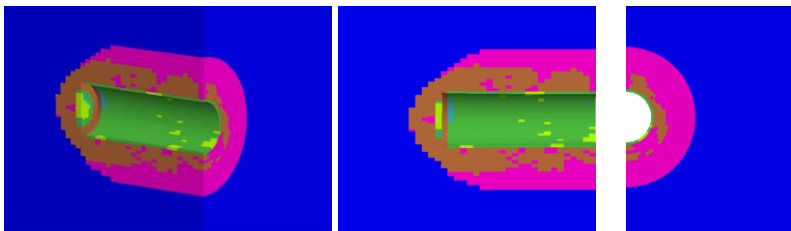
8



H = 500 m
 $\gamma = 26 \text{ kN/m}^3$
 $E_r = 8 \text{ GPa}$
 $\nu = 0.25$
 GSI = 35
UCS = 40 MPa
 $m_i = 10$

c) m_i Variations

9



H = 500 m
 $\gamma = 26 \text{ kN/m}^3$
 $E_r = 8 \text{ GPa}$
 $\nu = 0.25$
 GSI = 35
 UCS = 35 MPa
 $m_i = 6$

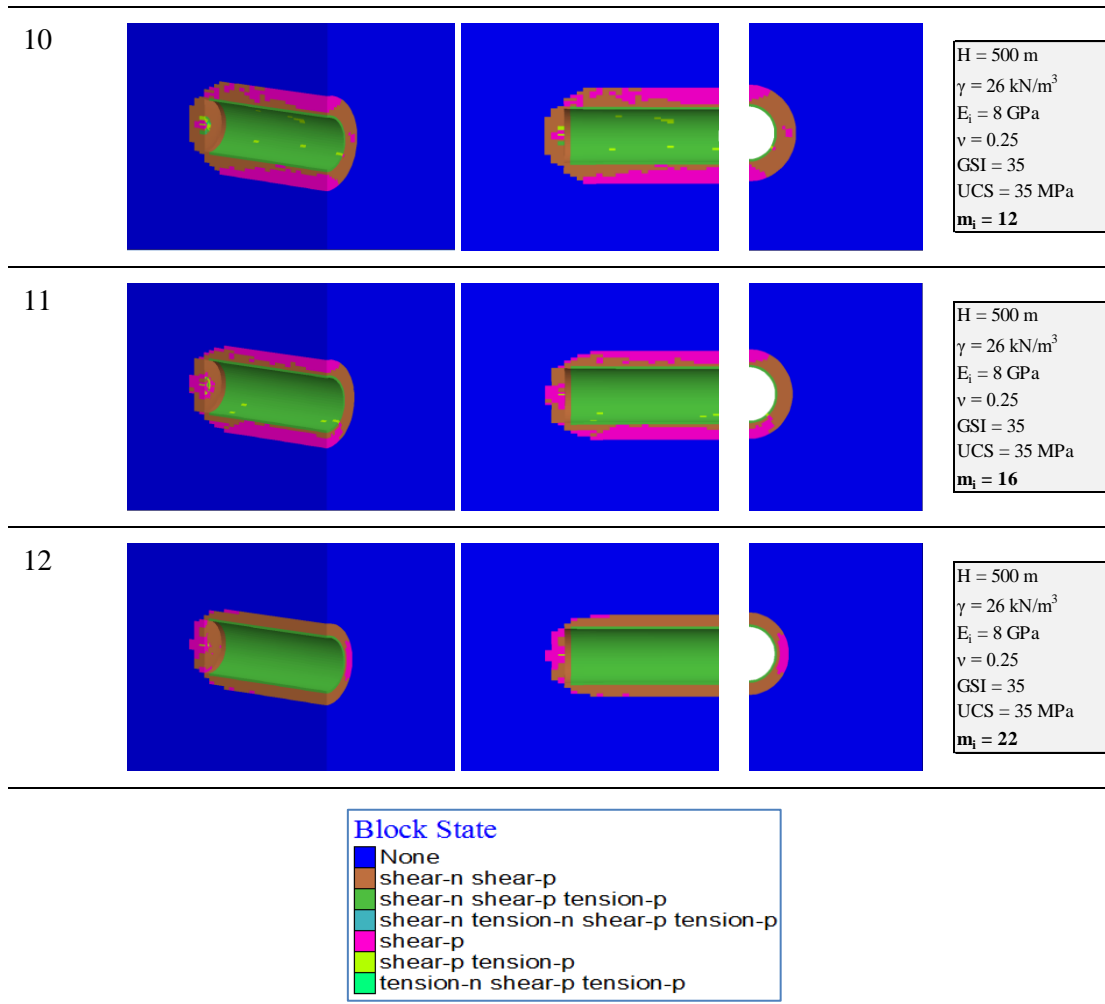
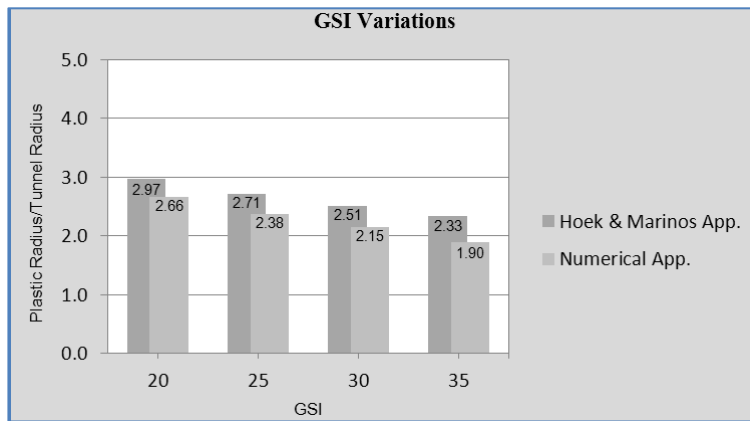


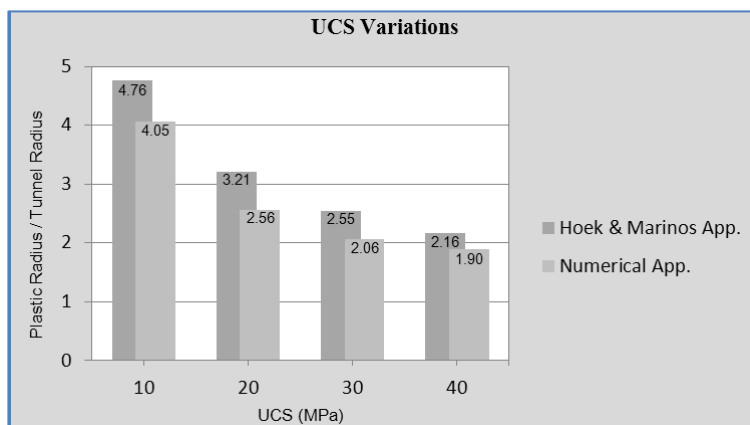
Figure 4.2. Twelve hypothetical models and relating plastic zone views for a) GSI variations b) UCS variations c) m_i variations

Table 4.3. Calculated plastic radius from numerical and semi empirical approaches

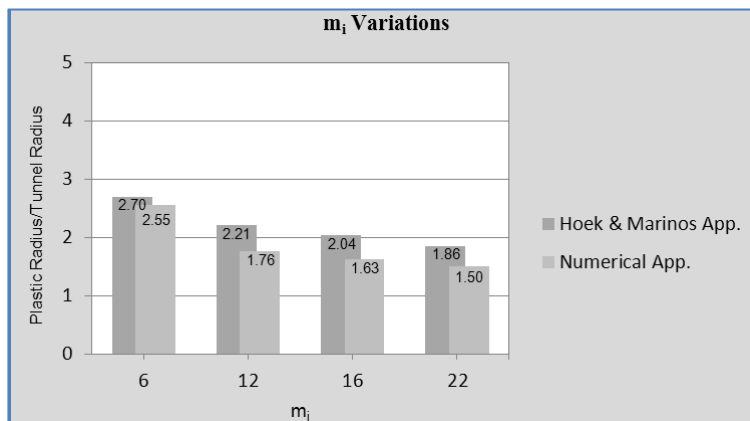
Model No.	R_p (semi-empirical)	R_p (numerical)	ΔR_p
1	8.92	7.98	0.94
2	8.14	7.13	1.01
3	7.52	6.46	1.06
4	7.00	5.70	1.30
5	14.29	12.16	2.13
6	9.63	7.68	1.95
7	7.64	6.18	1.46
8	6.49	5.70	0.79
9	8.10	7.65	0.45
10	6.64	5.28	1.36
11	6.11	4.88	1.23
12	5.57	4.50	1.07



$H = 500 \text{ m}$
 $\gamma = 26 \text{ kN/m}^3$
 $E_i = 8 \text{ GPa}$
 $\nu = 0.25$
 $GSI = 20, 25, 30, 35$
 $UCS = 35 \text{ MPa}$
 $m_i = 10$



$H = 500 \text{ m}$
 $\gamma = 26 \text{ kN/m}^3$
 $E_i = 8 \text{ GPa}$
 $\nu = 0.25$
 $GSI = 35$
 $UCS = 10, 20, 30, 40 \text{ MPa}$
 $m_i = 10$



$H = 500 \text{ m}$
 $\gamma = 26 \text{ kN/m}^3$
 $E_i = 8 \text{ GPa}$
 $\nu = 0.25$
 $GSI = 35$
 $UCS = 35 \text{ MPa}$
 $m_i = 6, 12, 16, 22$

Figure 4.3. Comparing plastic radiuses resulted from the numerical and Hoek semi empirical approaches

The results show an approximate conformity between semi empirical approach and numerical calculation results, but values from numerical results are always slightly less than values from the semi empirical results. This is due to fact that the numerical analysis considers 3D effects on deformation values. Hereinafter the Hoek and Marinos semi

empirical method has been used for verification of numerical simulations that were developed for analysis of tunnel excavation with a DS-TBM.

5. NUMERICAL MODELING OF A TUNNELING WITH A DOUBLE SHIELD TBM

5.1. Introduction

Double Shield TBMs are amongst the most technically sophisticated excavation machines in use by tunneling industry. However, using the shielded machine limits access to the walls for observation of ground conditions and presence of shield makes the machine susceptible to entrapment or seizure in weak rocks under high stresses which results in high convergence. Therefore TBM may get stuck (including shield jamming and cutter-head blocking) in the complicated geological structures, which requires manual excavation to release the machine. This is a time consuming, costly, unsafe, slow, and labor intensive work that should be avoided as much as possible. Thus, the main question in selection of shielded TBMs for many tunneling projects remains the possibility of machine seizure in the ground [17]. Also use of TBMs in very severe ground conditions is yet under discussion due to some negative experiences which resulted in very low rates of advancement and even in standstill [34].

For design of mechanized tunneling in such conditions, the complex interaction between the rock mass, the tunnel machine, its system components, and the tunnel support has to be analyzed in detail and three dimensional models including all these components are better suited to correctly simulate this interplay and avoid the errors introduced by assumption of plane strain conditions [28]. This is even truer in the case of the double shield TBM (DS-TBM), which is indeed a more complex machine than the gripper or the single shield TBM. Also double shield machines are longer than their single shield peers and thus more likely to get trapped as the ground gradually deforms behind the tunnel face.

In this Chapter, 3D finite difference numerical simulation program, FLAC^{3D}, has been used for modeling and evaluation of the feasibility of utilizing double shield TBMs in long deep tunnels in potentially squeezing ground. This section also describes comprehensive 3D modeling that may be used for simulation of the single shield, double shield and universal double shield TBMs for excavation of deep tunnels through various rock masses that exhibit squeezing behavior.

5.2. Modeling of TBM–Rock Mass Interaction in Squeezing Conditions

Three dimensional numerical models pay due attention to the spatial stress redistribution in the vicinity of the advancing face, thus eliminating the errors introduced by the assumption of plane strain conditions and providing information on the evolution of stresses and

deformations in the longitudinal direction as well as allowing a more detailed modeling of the different system components and their interfaces.

For modeling the TBM excavation in squeezing rock masses, including the analysis of TBM–rock mass interaction, two main methods have been offered in the literature: the axisymmetric models and the fully 3D modeling. The axisymmetric simulations in the case of squeezing ground have been proposed by Ramoni and Anagnostou [25], [29], and [44]. 3D models of deep tunnel excavation in rock masses have been developed by Cobrerros et al. and Simic [1] for the Guadarrama Tunnel (Spain), and by Graziani et al. [20] for the Brenner Base Tunnel.

A quick review of the literature mentioned above shows some shortcomings in the available 2D models and related analysis so that few exact 3D numerical studies have been carried out where the connection between squeezing phenomena and double shield TBM excavation has been simulated. Also as a consequence of the assumption of axial symmetry in numerical simulations, the pressure obtained is “homogenized” over the tunnel cross-section due to the fact that the model assumes an overcut that is constant around the circumference of the shield, while in reality the shield slides along the tunnel floor, which means that the overcut is bigger above the crown than in the lower portion of the tunnel cross-section.

5.3. Three Dimensional Numerical Modeling

5.3.1. Assumptions and Considerations for Modeling

The required parameters for 3D modeling of tunneling by a DS-TBM are based on data from excavation of the Lyon–Turin Base Tunnel, [34] and [45]. This is due to presence of rock mass and TBM parameters of the case for using in the numerical modeling.

For numerical modeling of a mechanized tunneling by a double shield TBM, the presence of water pressure and consolidation problems is not taken into account in this study. It is noted that the impact of water pressure and consolidation can be conventionally applied in the numerical calculations.

As the model refers to deep tunnels, the in situ state of stress is applied as a uniform initial stress without consideration of the free ground surface and of the stress gradient due to the gravity. It is assumed that this stress varies linearly with depth and is isotropic, equal to γH . This assumption is reasonable since at higher depth coefficient of horizontal stress or K_0 approaches “1”, indicating a uniform litho-static stress condition. It should be noted that

differential stresses can also be modeled by the numerical simulations if needed and as applicable in given project conditions, especially if in-situ stress measurements are available.

5.3.2. Numerical Modeling Method

For the three dimensional numerical analysis, FLAC^{3D} program (Fast Lagrange Analysis of Continua in three dimensions) was used. Due to the large deformations occurring in the simulated area of the tunnel around in the weak rock mass and in squeezing ground, this method was deemed suitable to avoid the problem of numerical instabilities during the analysis.

The required parameters for simulation of tunneling with double shield TBMs divide into three groups that are as follows: a) Machine data include the required thrust force F_r , weight of the machine W , shield length L , shield stiffness K_s , the skin friction coefficient μ , and the stiffness of the lining K_l , b) Ground and geological data including the Young's modulus E , Poisson's ratio ν , uniaxial compressive strength f_c , internal friction angle ϕ , dilatancy angle ψ and the initial stress σ_0 , and c) Performance and speed variables that involves the tunnel radius R , tunnel advance rate, radial gap size or overcut ΔR . Considering these parameters, numerical analysis for identifying the impact of overcut affecting ground behavior has been studied in Chapter 7.

In order to model a mechanized tunneling process by a universal double shield TBM, various three dimensional models were developed in FLAC^{3D}. A parametric study was carried out to determine the required distance from the tunnel face to the edge of the final segmental ring to prevent the edge effect on displacements and stress magnitudes of the numerical model in the advancing direction of the tunnel. The initial results indicated that a distance larger than 2.5 times the diameter of tunnel to the face (in hard rock) and larger than 4 times tunnel diameter (in weak rock) is necessary to prevent the edge effect. Also by consideration of the modeling rules discussed earlier, the 3D block model and relevant dimensions were selected and implemented, as shown in Figure 5.1. The screen shots show the cross section of the model where the horizontal (x), longitudinal (y) and vertical (z) directions are 75, 100 and 150 m, respectively. The tunnel radius is 4.72 m taken as given in studies from Zhao et al. [34].

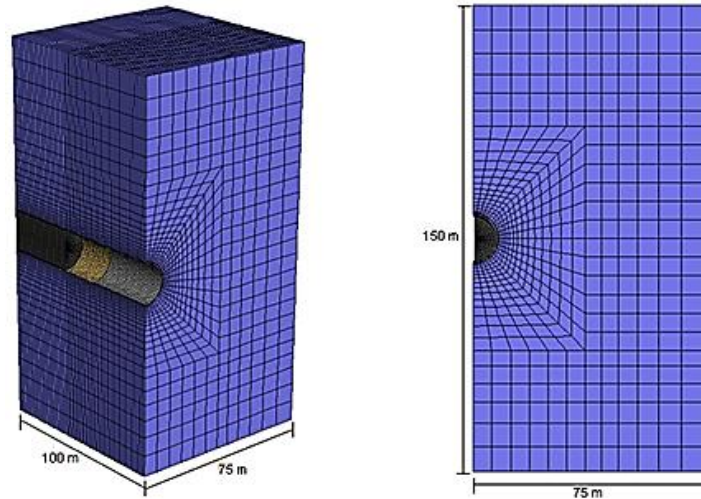


Figure 5.1. Geometric dimensions of the numerical model of tunneling by a DS-TBM

5.3.3. Numerical Modeling of Rock Mass

The rock mass is assumed to follow a linear elastic and perfectly plastic behavior according to Mohr-Coulomb failure criterion. Any constitutive law based on these assumptions for rock masses can be implemented in the model.

The assumed rock mass parameters are shown in Table 5.1 and are based on the information obtained from the back analysis of data from excavation of the Lyon–Turin Base Tunnel [34]. These parameters are selected in order to verify and compare the numerical analysis results with measured data from that case study. The dilatancy angle ψ was not treated as an independent parameter but was taken as a function of the angle of internal friction ϕ as follows: [1].

$$\psi = \begin{cases} 1 & \text{for } \phi \leq 20^\circ \\ \phi - 20 & \text{for } \phi > 20^\circ \end{cases} \quad (5.1)$$

Table 5.1. Rock mass parameters: Lyon–Turin Base Tunnel [34]

Parameter	Unit	Value
Elastic modulus, E	GPa	2.0
Poisson's ratio, ν	-	0.25
Cohesion, c	MPa	2.0
Friction angle, ϕ	°	24
Dilatancy angle, ψ	°	4
Unit weight, γ	kg/m ³	2650

The in-situ state of stress is assumed to be isotropic and equal to 26 MPa, to represent the conditions to be met along the Base Tunnel at depth of nearly 1000 m.

5.3.4. Numerical Modeling of the Main TBM Components

A comprehensive 3D model of a shield TBM has been developed in FLAC^{3D} so that all properties of the main TBM components can be used as variables at each step of analyses. The model can be applied in various rock mass conditions including hard, weak and intermediate rock masses.

The cutter-head, different shield types and their main components can be modeled easily by small changes in input data for shield and backfilling materials. Other TBM components are updated with respect to type of TBM only by changing of values assigned to each component. For example, a single shield TBM is modeled by removing the rear shield elements and changing the cement grouting material properties to pea gravel material for annular gap backfilling. Same procedure could be used to simulate machine advance in the tunnel and extrusion of the segments from the tail shield.

The result of analysis includes the deformation and stresses related to all of the monitoring points in the tunnel and on the shield and cutter-head, also deformations and failure stresses relating to the interaction between the rock mass and cutter-head and between the rock mass and shields as well between backfilling and support can be monitored or observed in each step of analyses. This is in the form of longitudinal and sectional profiles and as the contours in desired cross sections within the model. Data from each step and for all the points is saved as a text file, so it can be transferred to excel file for evaluation of all deformation and stress behaviors along the tunnel walls and on various cutter-head and shield components. An excel spreadsheet has been prepared for evaluation of analysis results of various TBM types and configurations in case of changing machine specifications to evaluate their impact on the system behavior. The model can also be modified to implement some ground improvement measures such as injection of grout or lubricants between the ground and shield in the 3D numerical model. The more explanations about ground improvement methods and effect of lubrication on shield jamming will be covered in Chapter 8.

Figure 5.2 shows the schematic view of the assumed DS-TBM arrangement in the case of squeezing rocks. Also Table 5.2 shows the main features of the TBM to be considered in the modeling. The cutter-head, shield, segmental lining, and annular gap backfill were considered to behave as linear elastic material, with pertinent properties listed in Table 5.3.

Table 5.2. Geometric dimensions for DS-TBM components [45]

Parameter	Unit	Value
Cutter-head diameter	[m]	9.37
Shield diameter	[m]	9.23
Cutter-head length	[m]	0.75
Front shield length	[m]	5
Rear shield length	[m]	6
Shield thickness	[cm]	3
Outer lining diameter	[m]	9
Segment width	[m]	1.5
Segment thickness	[cm]	45

Table 5.3. Mechanical properties of DS-TBM components [45]

Material Properties	Unit	Shield and cutter-head	Segmental lining	Backfilling Soft phase	Backfilling Hard phase
Elastic Modulus	[GPa]	200	36	0.5	1.0
Poisson's ratio	-	0.3	0.2	0.3	0.3
Unit weight	[kN/m ³]	76	30	24	24

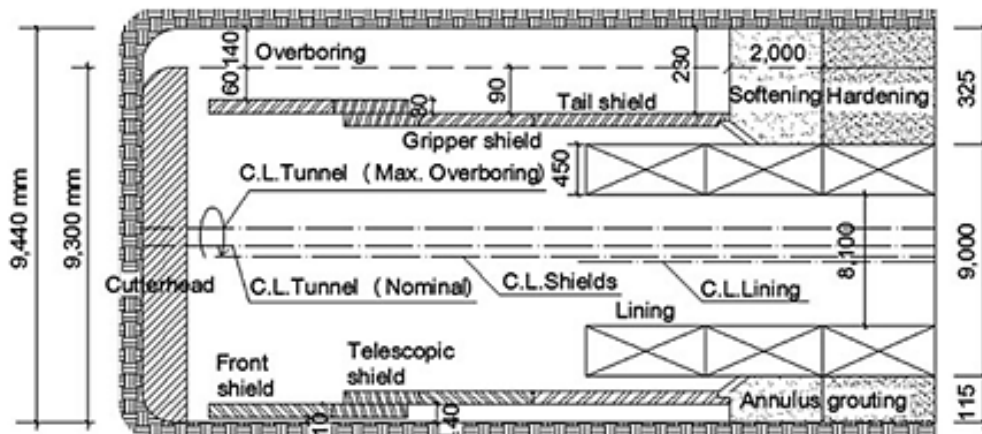


Figure 5.2. Schematic DS-TBM arrangements in squeezing rock used in the numerical modeling [45]

In the initial simulations the TBM is modeled as a cylinder with variable thickness and diameter. Front and rear shields are modeled with the thickness and material properties of steel that is typically used to manufacture TBM shields. Thrust force of cutter on the cutter-head is applied to the excavation face.

Annular gap backfill was assumed to be cement grout and a variable modulus of elasticity was assumed for the backfill to represent different states of the cement grout. The soft phase was used for first 2 m of backfill and hard phase for the rest of longitudinal profile of backfill. In hard rock excavations, the material properties of the backfill were changed to represent pea gravel properties. Similarly, segmental lining was modeled relating to lining geometry with the stiffness and material properties of concrete. No joints were introduced and the lining was considered to be continuous and the load on the lining was assumed to be applied only by the rock mass. Discretization of numerical model of DS-TBM is illustrated in Figure 5.3 a. Also the cutter-head, the front and rear shields, segmental lining, overcut and the annular gap backfilling were shown in the discrete numerical model in Figure 5.3 b.

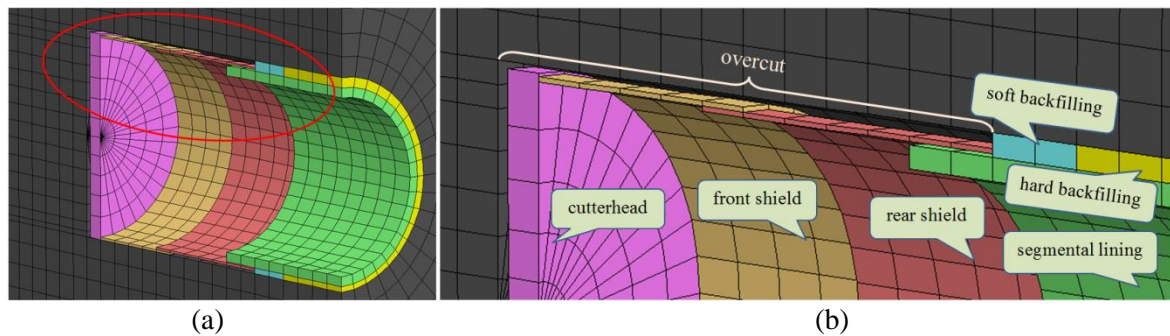


Figure 5.3. Numerical model of tunneling with DS-TBM a) Complete model b)

Discretization of model

In modeling of the shield skin, the total weight of the TBM was applied by normal stress to elastic area of invert which was in contact with tunnel invert. The bedrock for the applying of the TBM weight effect and lying of shield skin was adopted according to the recommendations from Ramoni and Anagnostou [1]. This area was considered to be lower $\alpha=45^\circ$ of the tunnel invert. Accordingly, the recommendation is reflected in the numerical model by normal stress loading to bottom and laid the bottom section of the shield skin (Figure 5.4).

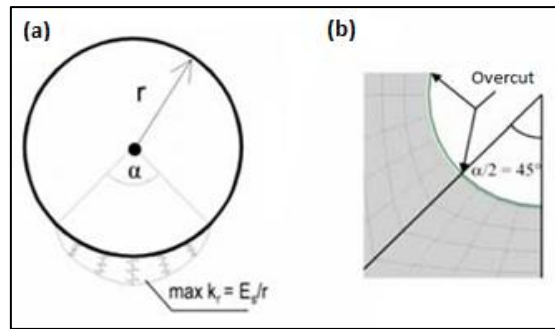


Figure 5.4. (a) Approach the elastic bedding in hard rock tunneling (b) Detailed discretization bearing shield skin area for numerical simulation of shield TBM model [1]

5.3.5. Modeling the Interaction between the Machine Components and Ground

In this study, the contact between cutter-head and rock mass as well between shields and rock mass has been modeled by using the interface elements on both tunnel and shield boundaries by considering the gap between them according to non-uniform undercut in the shielded TBM. Cross section of a front shield and the rear shield are illustrated in Figure 5.5. The numerical formulation used in this study is based on the large strain assumption, but sometimes unforeseen errors such as penetration of rock mass into shield elements occur within numerical calculations. Therefore for avoiding the problems due to large displacements in squeezing grounds, the method of displacement control has been applied to contact surfaces. For this purpose, a FISH code was developed in FLAC^{3D} that controls all displacements with respect to non-uniform undercut at each solving step of numerical analysis. Increasing of gap due to conical shape of the shield is considered in the code. This property of model distinguishes the modeling in this study from other 3D models that have been developed for numerical simulation of shield TBMs in the past.

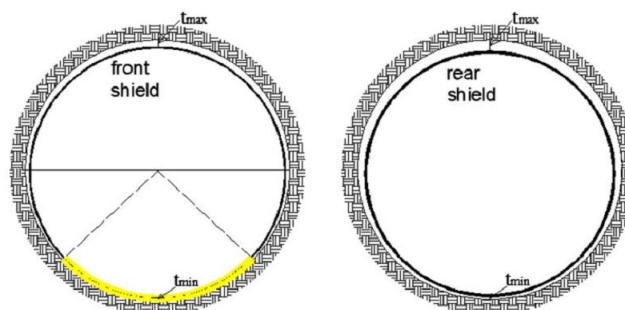


Figure 5.5. Cross section of a DS-TBM at the front shield and the rear shield [34]

Another advantages of model developed for this study is using Mohr-Coulomb or Hoek-Brown failure criterion as input data depending on the field measurements and ground conditions. In order to perform numerical analysis of tunnel excavation in the rock mass, a

series of FLAC^{3D} models have been developed which uses the Mohr-Coulomb failure criterion. However, to use Hoek–Brown failure criterion in the model, a FISH code was written in FLAC^{3D} to implement Hoek–Brown parameters as constitutive model and map the anticipated rock behavior into Mohr-Columb parameters. Hence, in addition to the uniaxial compressive strength, σ_{ci} and Elastic modulus of intact rock, the rock mass parameters including Geological Strength Index, GSI, material constant, m_i and Disturbance factor, D_h , are used for modeling of rock mass.

5.4. Simulation Procedure and TBM Advance Rate

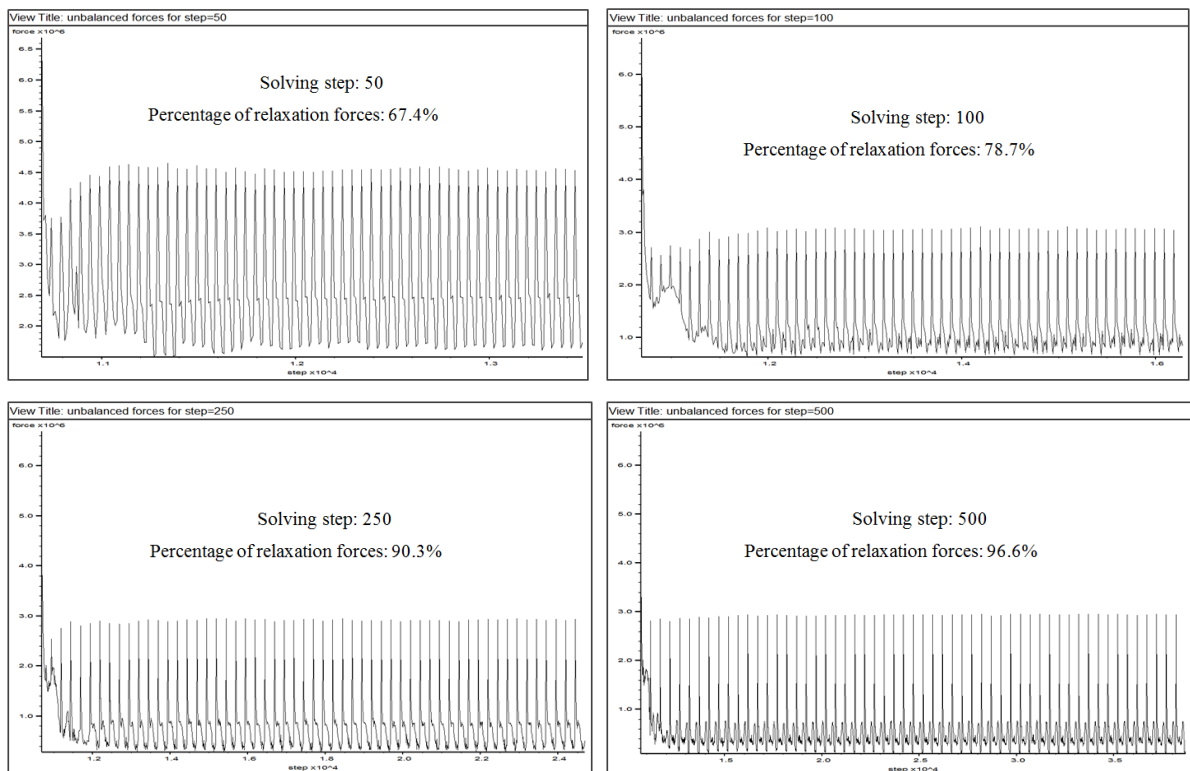
Because of large deformations occurring at tunnel excavation in squeezing grounds, the large displacement setting approach in the finite difference method was applied to the simulated model. The ongoing TBM excavation was simulated by a step-by-step method depending on the excavation length and construction stages. Assessment effect of step-by-step analysis method on the numerical results is studied in this section. It is noted that the adopted step-by-step method leads to simulate a succession of standstills and not a continuous process. Therefore for reproducing the continuous process of TBM excavation, the excavation length for each solving step is made with fine mesh equal to 1 m in order to reproduce the continuous process of TBM excavation [46].

Excavation of a tunnel is accomplished by applying forces that are required to maintain equilibrium with the initial stress state in the surrounding material as loads on the perimeter of the tunnel. These loads are then reduced to zero to simulate the excavation (steady-state condition). But the tunnel excavation by a TBM is a continuous process and the unbalance forces don't drop to zero because of machine advance rate except when machine stops due to maintenance or other long delays. Therefore the effect of TBM advance rate (subsequently the time factor) on the results should be considered in the numerical calculations.

Although time-dependent stress-strain behavior of the rock mass was not included in the step-by-step analysis conducted, but the time effect during advance of excavation is taken into account by relaxing of unbalance forces gradually over some steps. The cutter-head, shield skin, segmental lining and backfilling were installed after the specified value of relaxation of the loads in the numerical simulation of double shield TBM. This means that after the indicated value of relaxation of the unbalance forces, the tunnel convergence has been allowed to continue, meaning controlled ground movement into tunnel.

For accurate numerical simulation of tunnel excavation by a shield TBM, it is necessary to include TBM advance rate effect by considering the overcut and shield length for evaluation of the potential of machine entrapment. Also it may be required to assess TBM entrapment risks for critical status in which machine are subjected to slowdown or standstill for an extended time.

In this section, relaxation of the unbalance forces for each solving step of numerical analysis is presented by the percentage value of relaxation. This value depends on the material properties surrounding the tunnel, shield length, annular gap between the ground and shield (overcut), and speed of machine movement in the tunneling. To obtain the appropriate percentage of relaxation for numerical analysis, the simulated initial model was subjected to unbalanced forces by different step-by-step excavation of tunnel. Unbalanced forces along the tunnel are monitored at each solving step and results are illustrated in Figure 5.6. In the steady state condition, the solving step of 1000 offered the best results and the percentage of relaxation was close to 100% where the balance of forces are reached and the maximum displacement was recorded. In this excavation case, for correct representation of continuous excavation by a shielded TBM and accounting for the time factor in step-by-step analysis, an 87% relaxation of the unbalance loads for each step of analysis was used [45].



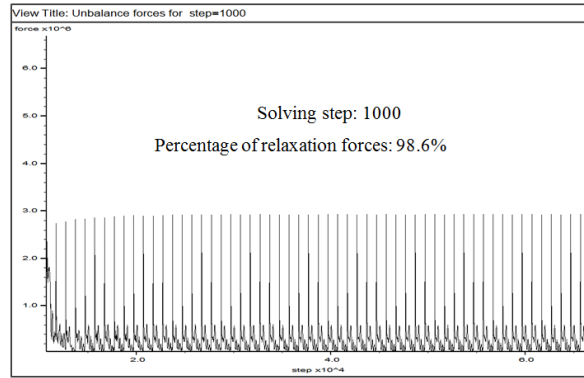


Figure 5.6. Percentage values of unbalanced forces for different solving steps

For other tunneling methods including NATM tunneling depending on the rock mass properties, this value may be within the range of 95% to 100% in a case where the support is installed 4 m behind the face (fully steady state condition).

5.5. Numerical Modeling of the Excavation Process

The excavation stages and the total number of steps for the numerical model were simulated based on the construction design of cutter-head, front and rear shields for a double shield TBM. The total number of the solving steps depends on operation modes of the TBM in squeezing ground and advance rate. In this study, a total of 41 excavation steps were simulated consisting of the 1 initial undisturbed ground and 40 excavation steps. Furthermore, the excavation stages for simulated model are defined as follows and illustrated in Figure 5.7:

- a) In the first stage, initial in-situ stresses are implemented and correct distribution of stresses is applied to the rock mass model.
- b) In the second stage, tunnel boring starts, solving time set up with respect to advance rates, cutter-head is activated, the thrust force and TBM weight are applied to face and invert of tunnel respectively and are maintained for all stages of excavation. The contact analysis between the cutter-head and rock mass is performed in this stage. The maximum cutter-head thrust force has been set to 17 MN for the given machine size [45].
- c) In the third stage, front shield moves forward and is considered in the model. Numerical results are examined for evaluation of probable contact between the rock mass and front shield. Also, the entrapment risks are analyzed when contact occurs between the walls and shield.

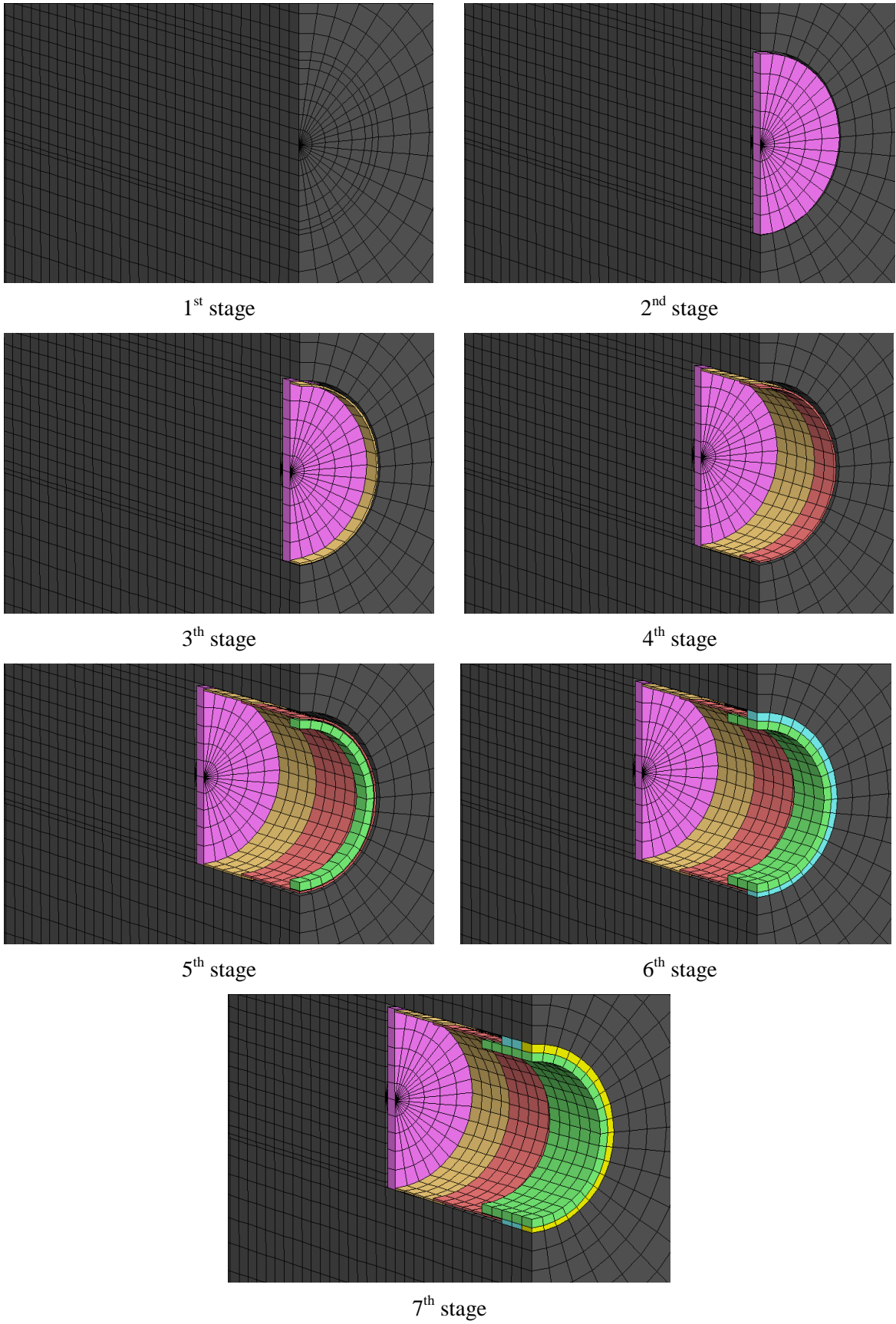


Figure 5.7. DS-TBM tunneling construction stages of numerical simulation

- d) In the fourth stage, rear shield with reduced diameter (compared to front shield by considering the conical shape of rear shield) is activated by considering the length of rear shield. Analysis of numerical results for this stage is the same as third stage.
- e) In the fifth stage, installation of the segmental linings is implemented inside the rear shield.
- f) In the sixth stage, the segmental ring is subjected to ground loading on the segments is assumed to start from the third segment behind the machine. Moreover, the injection of backfill into the annular space between rock mass and lining by using the soft grout is started. This also allows for simulation of pea gravel in other types of machine.
- g) In the seventh stage, backfilling the annular space by hard grout is implemented.

The model is set up such that when a segment ring is extruded from the tail shield, the material property of the rear shield is replaced by the material property of soft filling for the annular space in the area of the first two segmental rings. It should be noted that in modeling of the lining, the joints between segments and adjacent rings are not considered.

5.6. Verification of Numerical Simulation

Numerical analysis has been performed for examination of the longitudinal displacement profile (LDP) for the intrinsic excavation condition as shows in Figure 5.8. Rock mass properties are applied to model accordance to material properties from Table 5.1. Relaxation of redistributed stresses due to tunnel boring occurs when distance to face is 32 m and displacement magnitude after that is calculated about 34.6 cm. Furthermore, according to Figure 5.9, plastic radius is estimated to be 12.60 m.

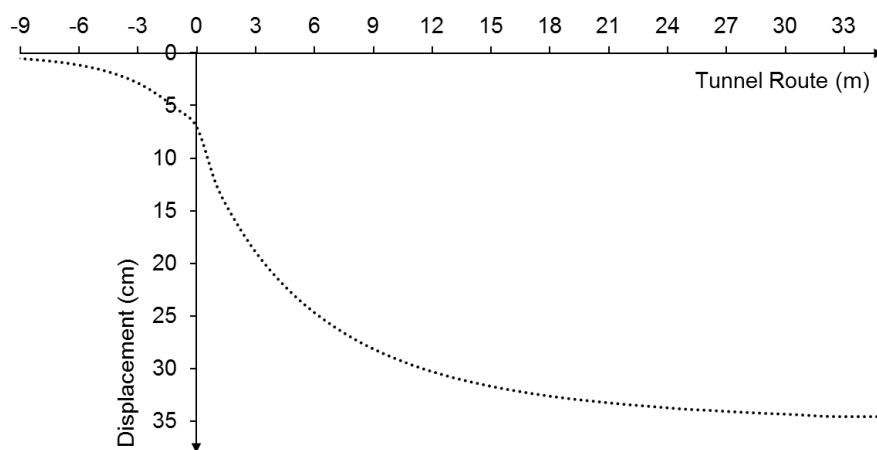


Figure 5.8. LDP for intrinsic excavation conditions

In order to verify and assess the accuracy and applicability of numerical simulation results, two methods including ground reaction curve (GRC) and Hoek and Marinos approach are used for verification of numerical results. The results from both methods are compared with the results of numerical analysis for intrinsic excavation condition.

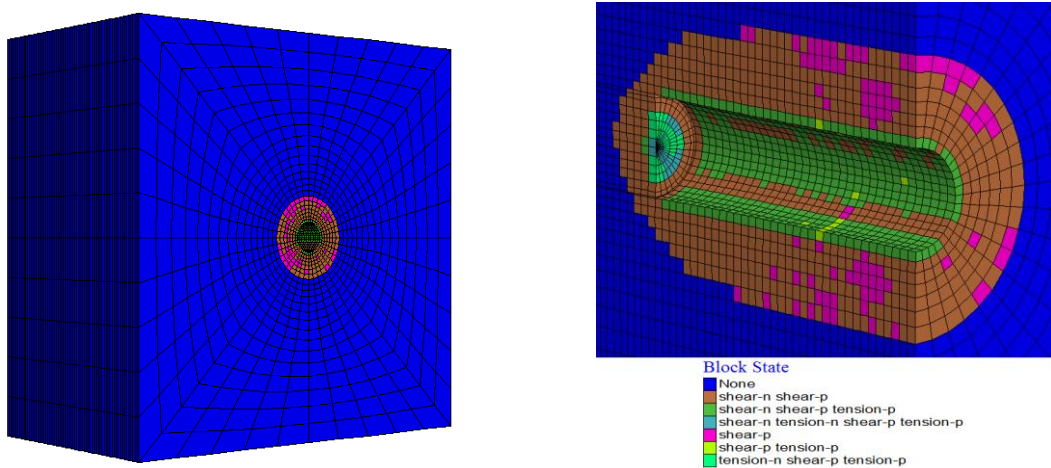


Figure 5.9. Plastic zone radius $R_p = 12.60$ m calculated from numerical results

5.6.1. Verification of Numerical Modeling by Using Ground Reaction Curve (GRC)

The main assumptions in the analysis by GRC method are as follows:

- Tunnel is circular.
- In-situ stress field is hydrostatic.
- Rock mass is isotropic and homogeneous. Failure is not controlled by major structural discontinuities

By considering the assumptions mentioned above, the GRC for given rock mass material properties (Table 5.1) and tunnel parameters is illustrated in Figure 5.10.

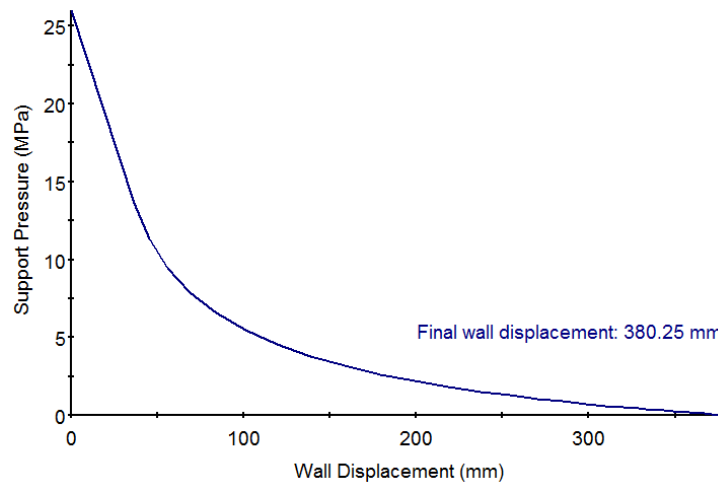


Figure 5.10. Ground Reaction Curve (GRC) for the given rock mass properties and tunnel parameters with respect to Hoek-Brown yield criterion

As shown in the Figure 5.10, the final wall displacement without any support system (intrinsic excavation) is calculated as 38 cm. This value is measured about 34.6 cm for numerical investigation. The smaller value for numerical calculation is due to 3D effect of simulated model. Also plastic zone radius from Hoek-Brown yield criterion is calculated about 13.04 m (Figure 5.11). This value is 12.60 m for numerical analysis. It means that FLAC^{3D} numerical model generates a significantly close result to GRC solution. So FLAC^{3D} can be reliably used for the computations throughout numerical analysis.

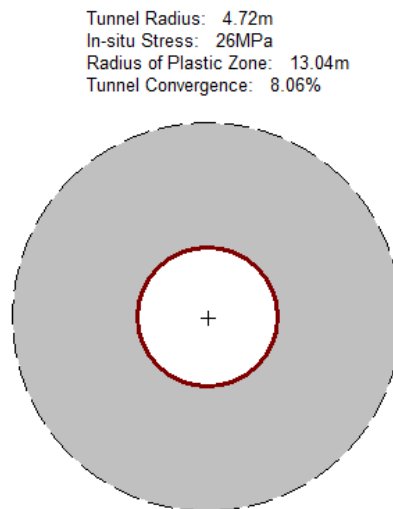


Figure 5.11. Plastic zone radius for the given rock mass properties and tunnel parameters

5.6.2. Verification of Numerical Modeling by Using Hoek and Marinos Approach for Squeezing Grounds

The calculated plastic radius and percentage strain in the rock mass surrounding the tunnel for intrinsic excavation by using the Hoek and Marinos approach are calculated 13.40 m and 3.56% respectively. The percentage strain is defined by ratio of tunnel closure to tunnel diameter. Therefore with respect to tunnel diameter ($d = 9.44$ m) the tunnel closure is determined 33.6 cm. The comparison with numerical results shows that there is a good conformity between semi empirical approach and numerical calculation results.

5.7. DS-TBM Excavation Results

In this section, the analysis is carried out in terms of longitudinal displacement profile (LDP) on the tunnel circumference to detect the probable contact forces between rock and cutter-head and both front shield and rear shield after each step. Furthermore, the stress history of the ground as well as the thrust force required in order to overcome friction are evaluated for 40 m excavation of tunnel.

Five reference points are selected on tunnel circumference as well as on shield boundaries for extracting the results of numerical analysis. Over boring (overcut) amounts relating to each reference point are calculated and considered in the analysis. The schematic drawing of the reference points and relevant overcut amounts are shown in Figure 5.12. The relevant overcut for rear shield is different than front shield and increases with respect to outside diameter (OD) of the shield at any given point towards the tail shield. LDP and contact forces are investigated for transient conditions and also for the complete model by considering the gap between the shields and the rock mass that is not uniform.

For the specified solving step with advancing of tunnel, the shape of longitudinal displacement and force profile (LDP and LFP) changes relative to the previous solving step. Therefore LDPs and LFPs are controlled at each solving steps to find out where the shields and cutter-head get in contact with the rock mass. Also amount of forces in the contact points evaluated at every step for assessment of entrapment risk. In this study, the shields are assumed to be rigid and are not subjected to any failure due to bending and buckling.

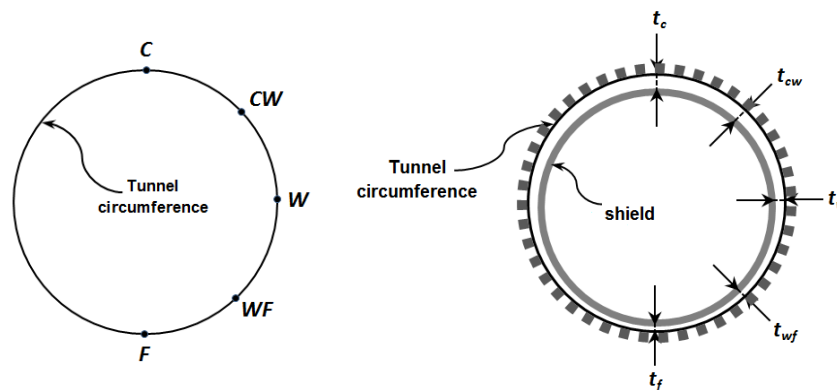


Figure 5.12. Monitoring points on tunnel and shield circumference and relevant overcut

5.7.1. Result of Analysis for Cutter-head and Front Shield

Displacement contours for the first 6 m of excavation for entrance of the cutter-head and front shield length is illustrated in Figure 5.13. The displacements predicted by the model shows that the closure of the non-uniform overcut between tunnel and front shield in the crown will not occur, But for other reference points contact will take place towards the end of the front shield and the shield starts to support the excavation walls. The contact of the shield invert (in this case, both front and rear shield) is due to the weight of the machine and it provides additional confinement to the excavation surface near the tunnel face.

Figures 5.14 to 5.18 show the simulation results along five reference points in terms of longitudinal displacement profile (LDP) at tunnel circumference and contact force profiles (LFP) on the cutter-head and front shield.

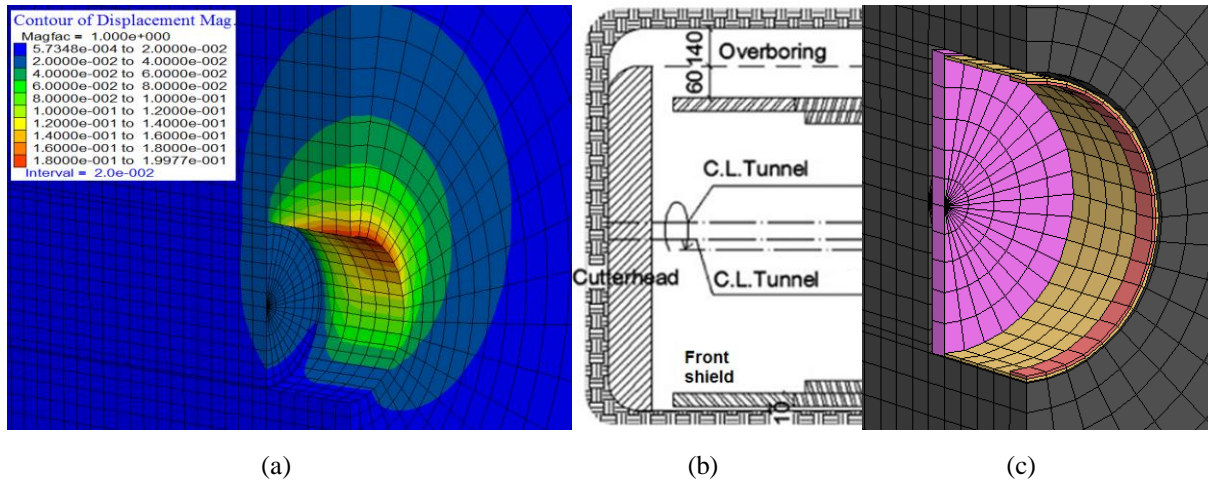


Figure 5.13. Numerical results for front shield a) Displacement contours b) Overcut dimensions and c) Numerical model

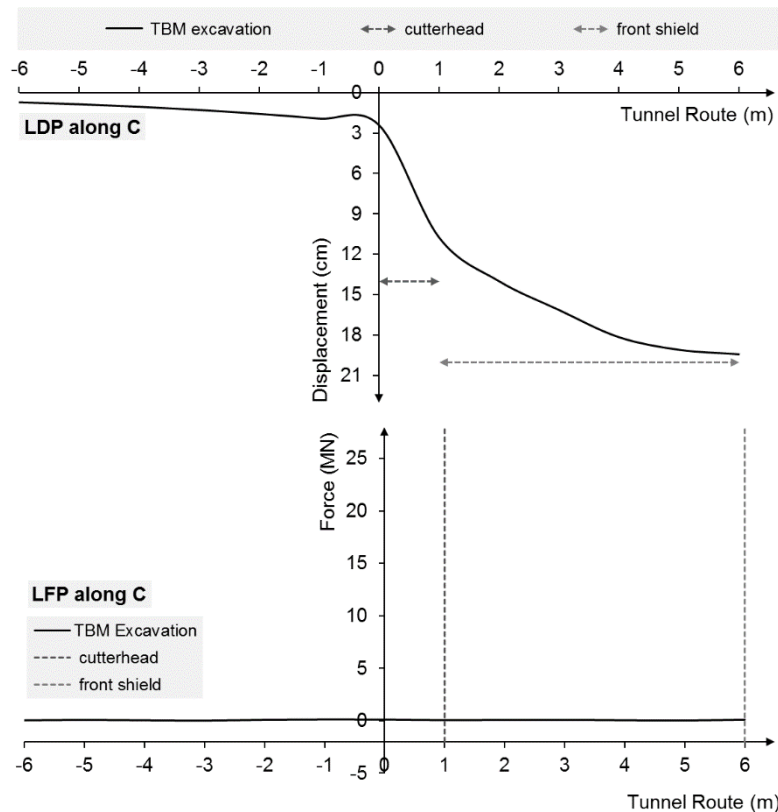


Figure 5.14. LDP and LFP along point C on the front shield (tunnel crown)

Figure 5.14 depicts the LDP at the crown (point C) and LFP on the cutter-head and on the front shield in the contact and non-contact points between rock mass and machine

components. As displayed in the Figure, there is no contact between rock mass and cutter-head also between rock mass and front shield. Therefore the contact forces on the both cutter-head and shield are nearly zero. However, a slowdown or standstill in TBM advance may cause extended area of contact between rock and shield in the crown, and hence higher frictional forces.

The conditions for point CW are same as point C (Figure 5.15), but the closure of gap between the front shield and the ground occurs at end of the front shield. This means that the contact between shield and ground started in last solving step, and minimal forces from rock about 1.75 MN is applied to the shield. This due to non-uniform overcut that is smaller than in the point CW cause to closure of gap and support the shield.

Figure 5.16 shows the LDP and LFP at tunnel wall or spring-line level (point W) on the cutter-head and on the front shield. As can be observed in this Figure, the closure of overcut between the cutter-head and the tunnel wall occurs right after excavation and ground exerts 5.60 MN force to cutter-head. Because of larger overcut around the front shield than cutter-head, contact forces decrease for front portion of front shield. At about 2 m distance to face where the shield starts to support the forces from excavation walls, contact forces increase on front shield and the maximum force is about 15.3 MN.

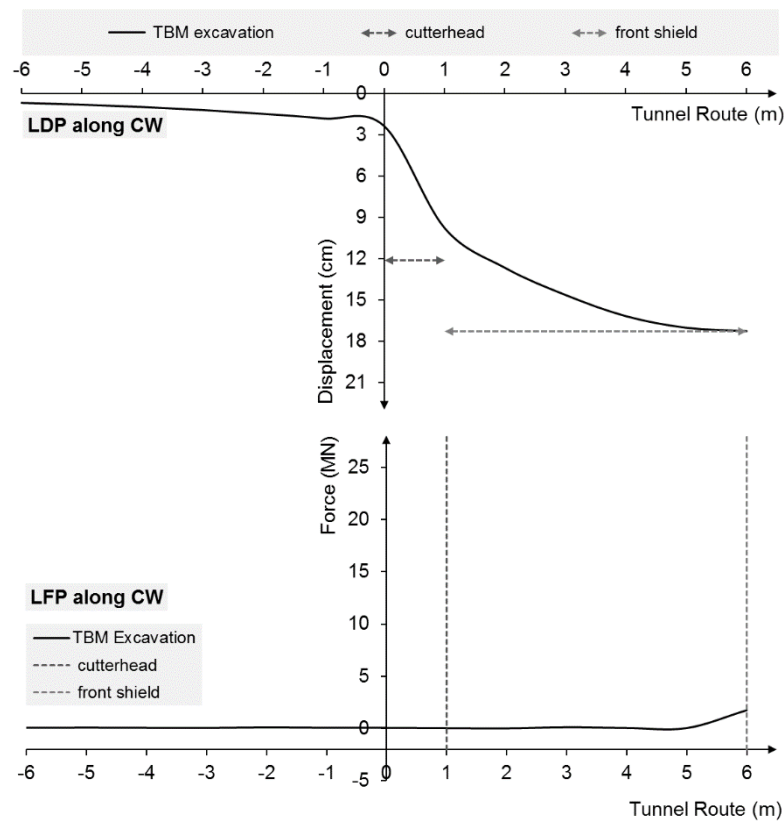


Figure 5.15. LDP and LFP along point CW on the front shield

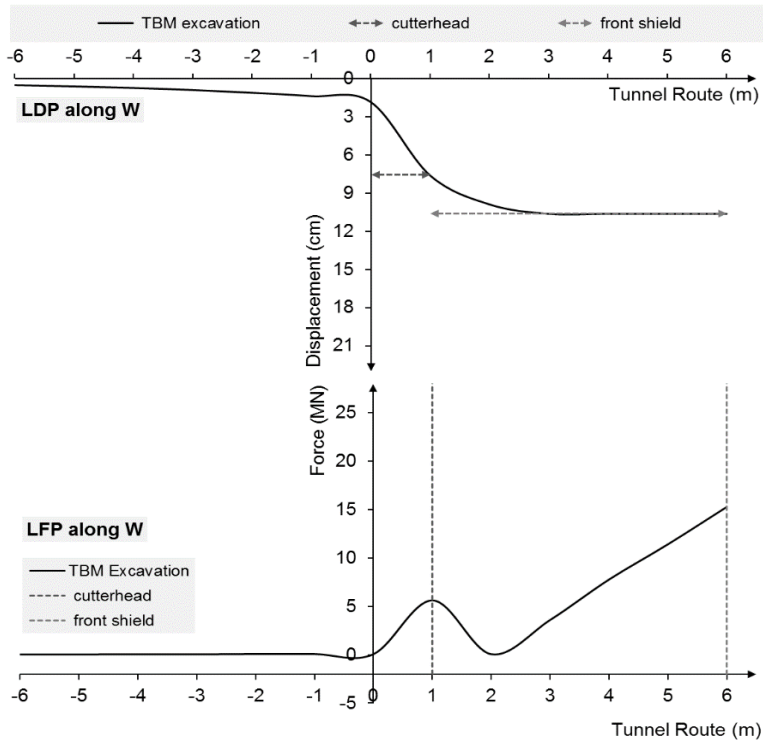


Figure 5.16. LDP and LFP along point W on the front shield (tunnel wall)

Figure 5.17 shows the LDP and LFP at point WF. The overcut between the cutter-head and the ground is closed instantly after excavation and ground applies 9.70 MN to cutter-head. The closure of gap between the front shield and the tunnel wall occurs at 2 m distance to face. Maximum contact force in this point is about 18.1 MN.

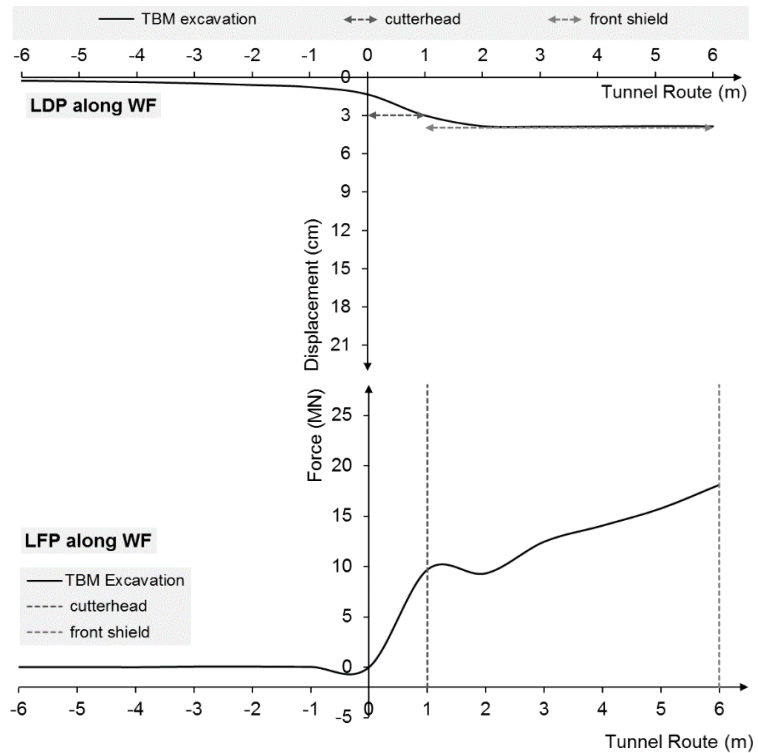


Figure 5.17. LDP and LFP along point WF on the front shield

Contact between front shield and cutter-head with invert starts right after excavation (Figure 5.18). At this point uplift of the machine may occur which may lead to a reduction of the free gap at the crown. Maximum contact forces on cutter-head and front shield are calculated to be 16.6 MN and 22.5 MN respectively.

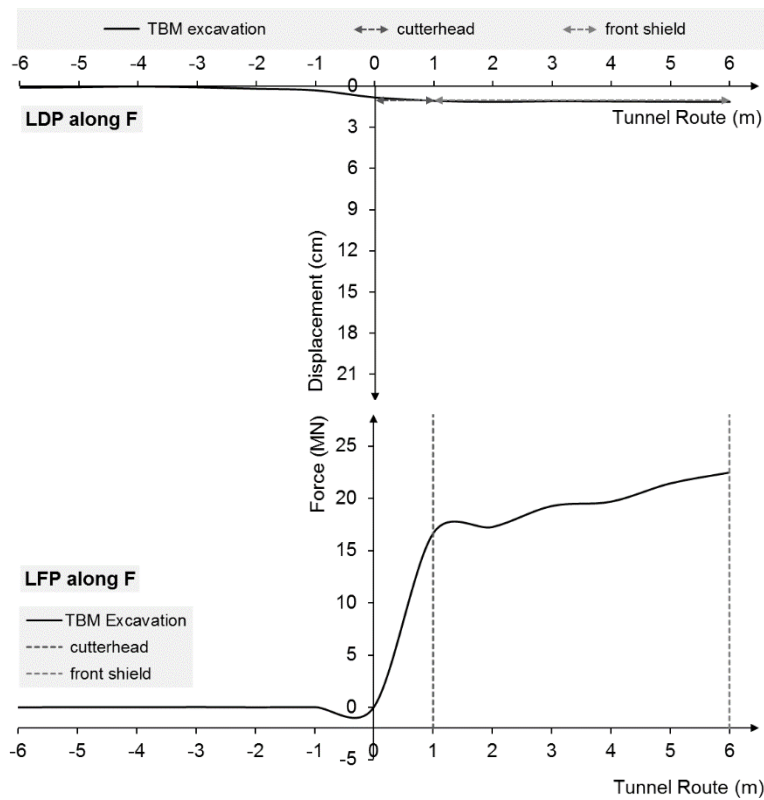
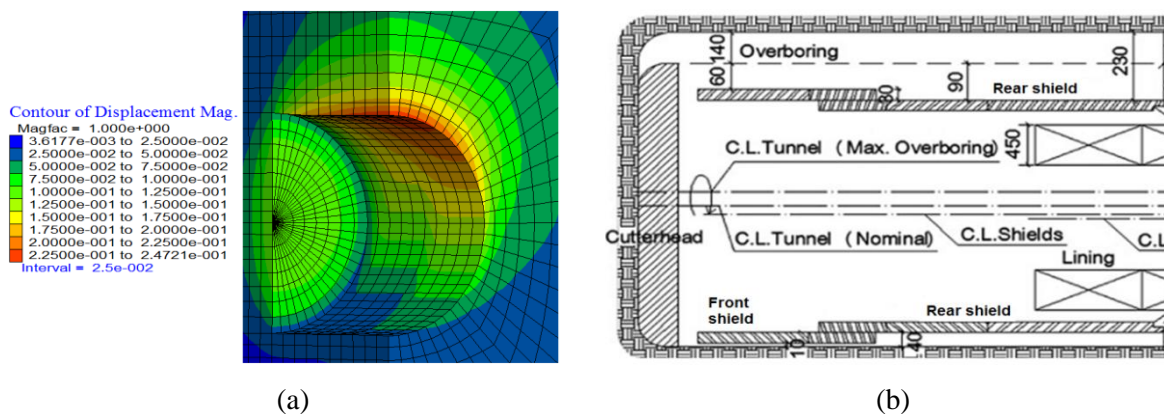
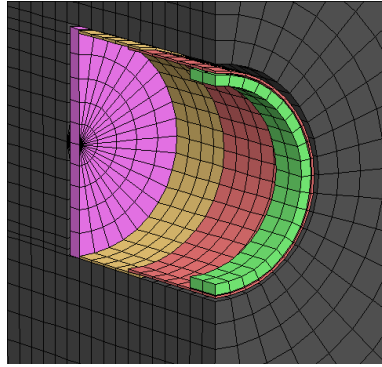


Figure 5.18. LDP and LFP along point F on the front shield (tunnel invert)

5.7.2. Result of Analysis for Rear shield

Displacement contours for 12 m excavation according to total length for cutter-head, front and rear shields are shown in Figure 5.19. Considering the displacement magnitudes it is predicted that the closure of the non-uniform overcut between tunnel and rear shield will occur.





(c)

Figure 5.19. Front and rear shield a) Displacement contours b) Overcut dimensions (c) Numerical model

Figure 5.20 shows the LDP and LFP at the crown (point C) on the shield. In this stage similar to Figure 5.14, the closure of overcut between the front shield and the ground occurs at end of the front shield, but rock mass starts to load on the front shield with respect to previous step. This demonstrates that with advancing of tunnel, contact force has been applied on the front shield. Due to conical shape of the shield, the contact forces between ground and rear shield is initially reduced to zero. It is interesting that despite the presence of contacts between rear shield and ground, amount of forces put on the shield by rock mass is minimal. A slowdown or standstill in TBM advancing may cause the contact force to rise rapidly. The maximum contact force on front shield TBM is about 5.9 MN.

The contact forces applied to the both shields at point CW are 7.5 MN and 4.20 MN for front shield and rear shield, respectively (Figure 5.21).

Furthermore, the simulation results are observed at points W, WF, and F in terms of LDP on tunnel circumference and LFP on the shields (Figures 5.22 to 5.24). As can be observed in these Figures, the closure of gap between ground and TBM components occurs right after excavation and ground loads imposes contact forces to the shield surface. Due to conical shape of the shields, the contact forces between ground and rear shield are reduced, but with advancing of tunnel the forces are increased again. Contact force, where size of overcut is less, is bigger than other places. This means that due to closure of gap in these points instantly after boring, contact between ground and shields occurs. Therefore with advancing of tunnel, applied forces from ground to shield increases.

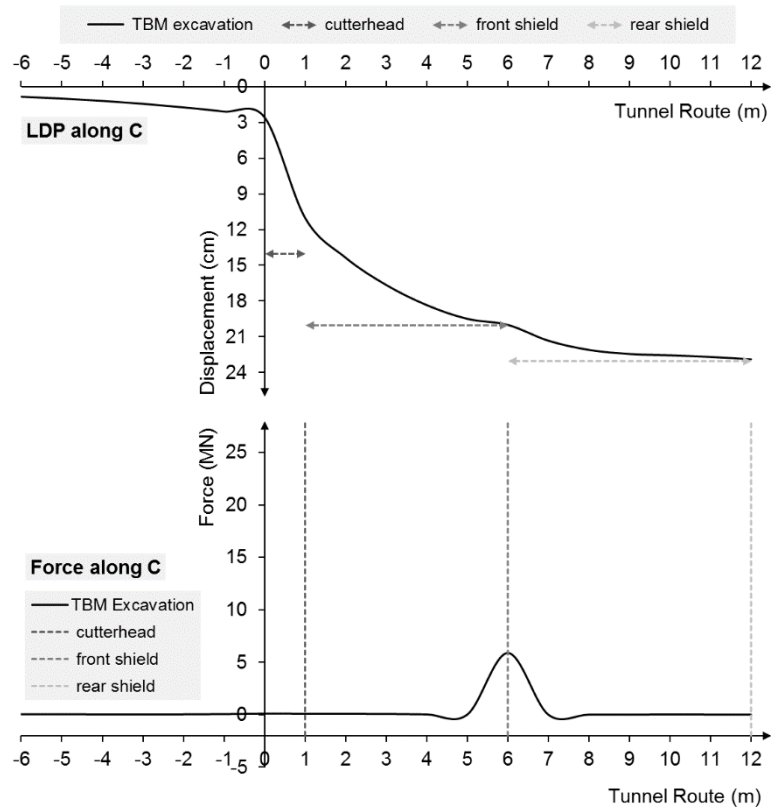


Figure 5.20. LDP and LFP along point C on the shields (tunnel crown)

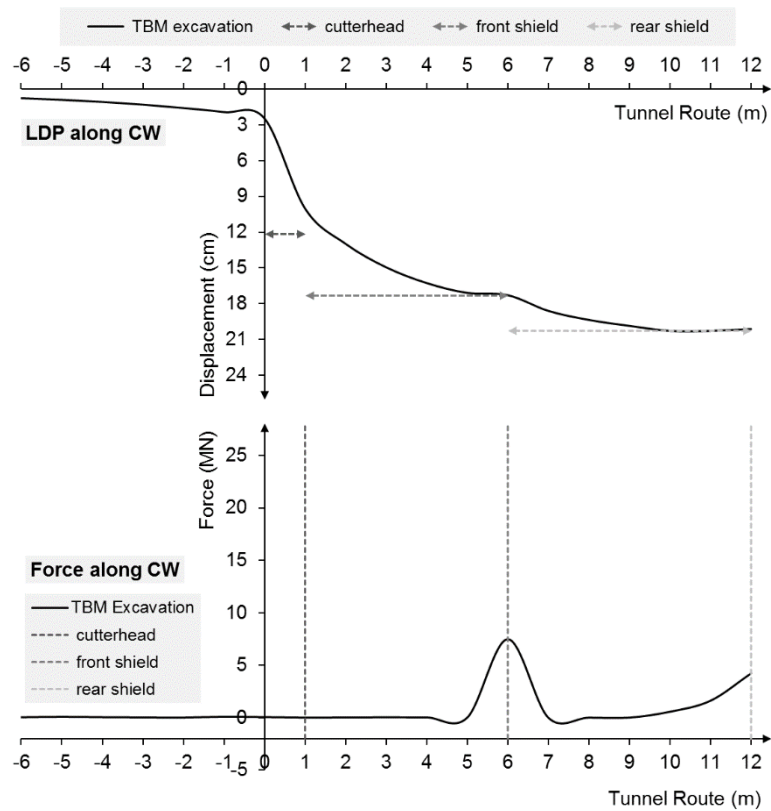


Figure 5.21. LDP and LFP along point CW on the shields

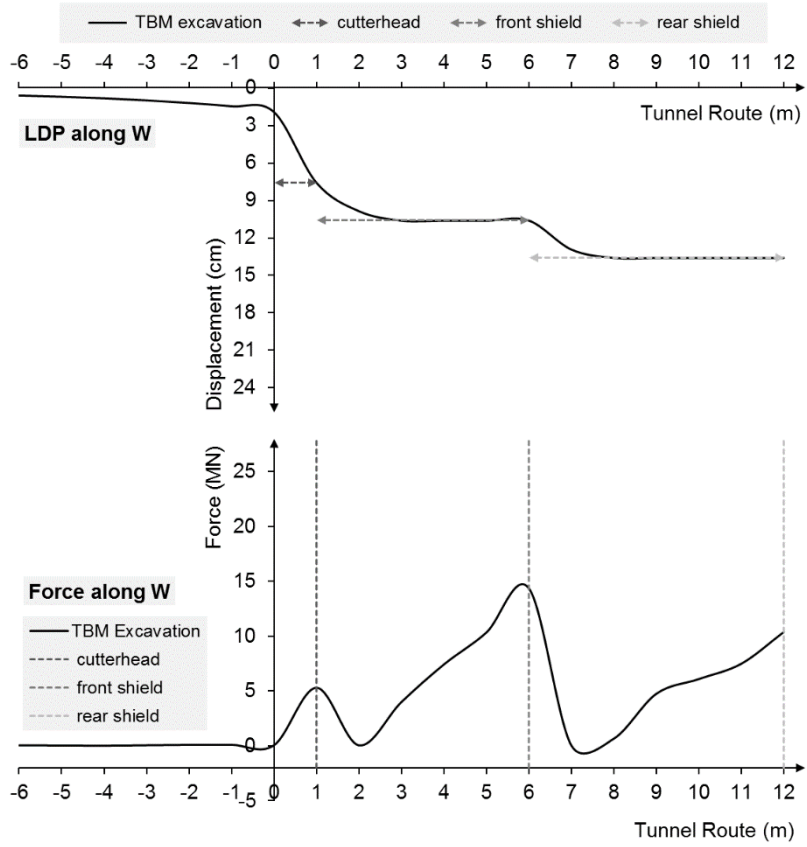


Figure 5.22. LDP and LFP along point W on the shields (tunnel wall)

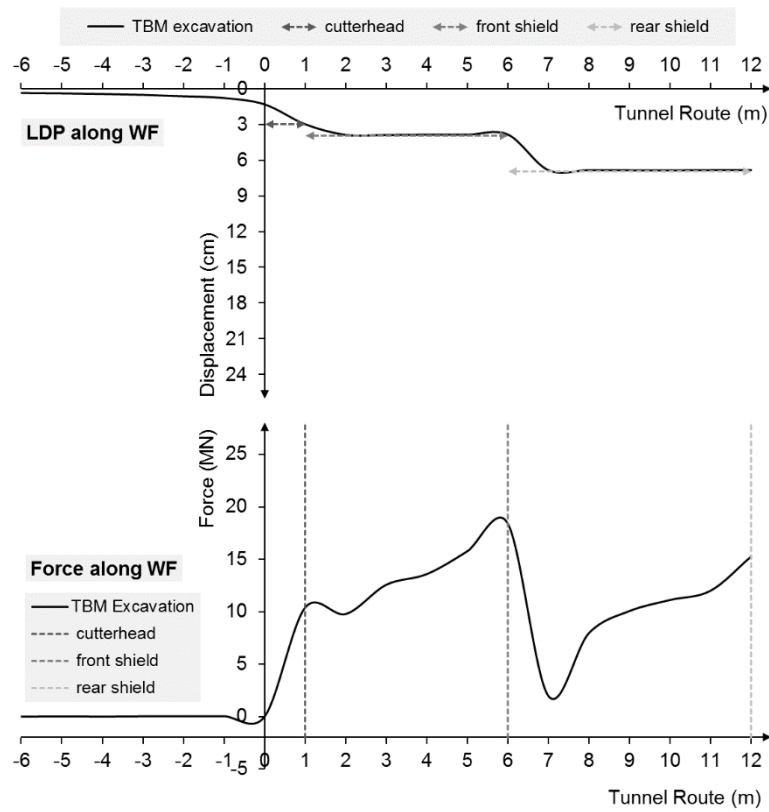


Figure 5.23. LDP and LFP along point WF on the shields

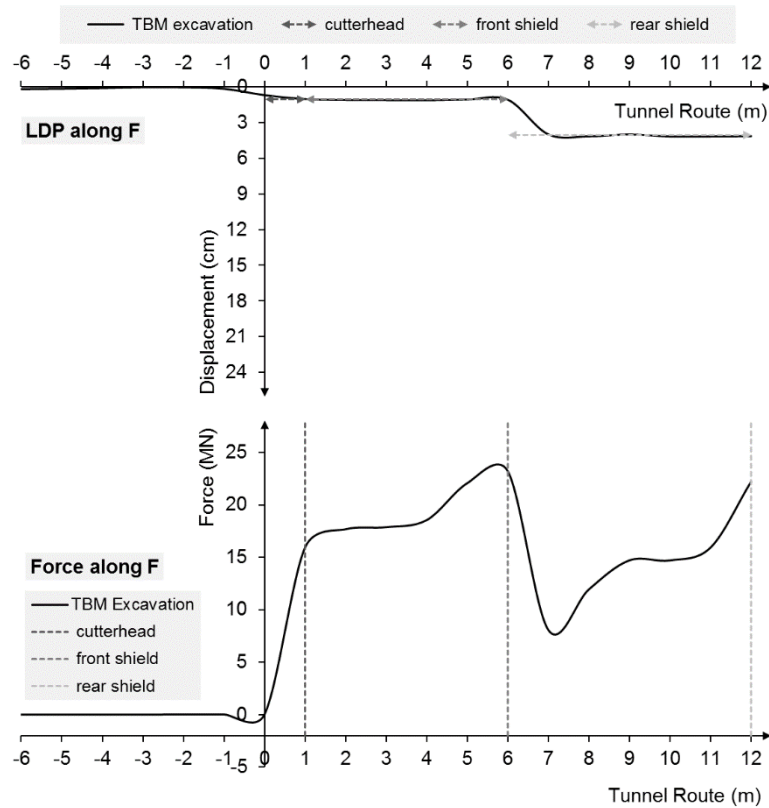


Figure 5.24. LDP and LFP along point F on the shields (tunnel invert)

It is noted that the rock mass experiences three unloading processes during the excavation by TBM. First, as the tunnel walls remain unsupported, the tunnel boundary experiences the first unloading/relaxation process. At the distance of about 1 m behind the face, the invert is confined by the shield and, as soon as the entire gap is closed, loading of the shield takes place. Second, the entire tunnel boundary is unloaded at the front end of the rear shield due to the conical shape of the machine. Finally, as the segments are ejected in the back of the tail shield, the last unloading process occurs [45]. On the other hand, due to the very high in situ stress, large convergence will take place. Thus it is necessary to consider the possible uplift in the invert which could move the machine. This effect could lead to a reduction of the gap at the crown [34].

5.7.3. Result of Analysis for Total Tunnel Excavation with DS-TBM

The longitudinal maximum principle stress history of the ground as well as the deformation at five reference points for a 35 m excavation of tunnel by a double shield TBM are illustrated in Figures 5.25 to 5.29.

As can be seen in these Figures, the stress of the ground at crown of tunnel decreases because a larger overcut is provided in this point. The reduction of stress in this point where the segmental linings are installed is calculated as 20.5 MPa ($26-5.5=20.5$). In the

case of small over cut, especially in the invert and lower shoulders, the gap between ground and machine components is closed instantly after excavation and relaxation of stress in these points are lower than the points with larger overcut. For example, stress reduction of ground in the invert of tunnel is 15 MPa.

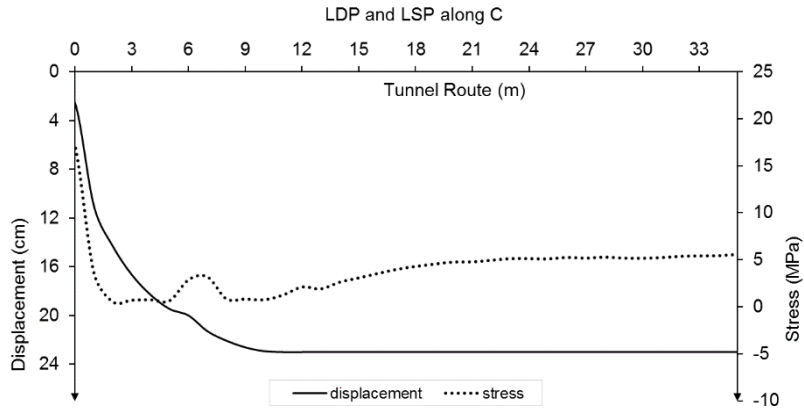


Figure 5.25. LDP and Maximum principal stress history of the ground along point C

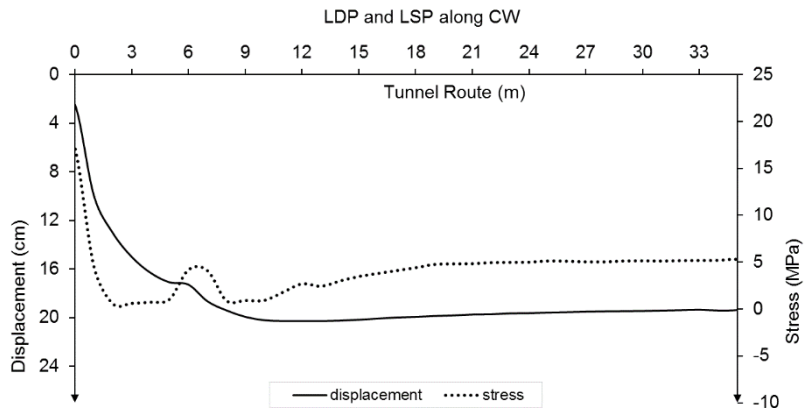


Figure 5.26. LDP and Maximum principal stress history of the ground along point CW

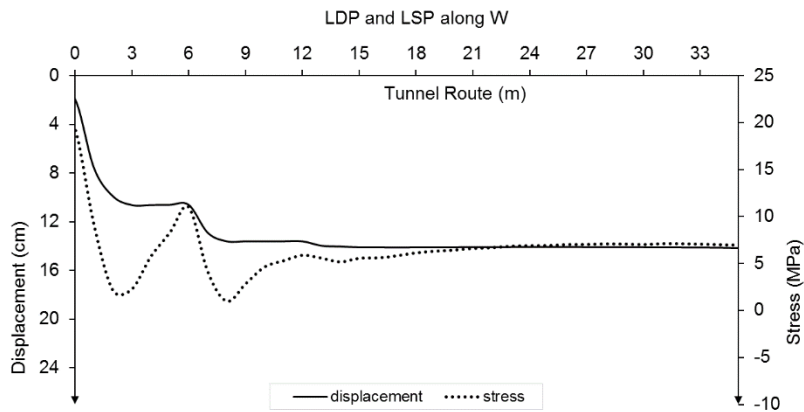


Figure 5.27. LDP and Maximum principal stress history of the ground along point W

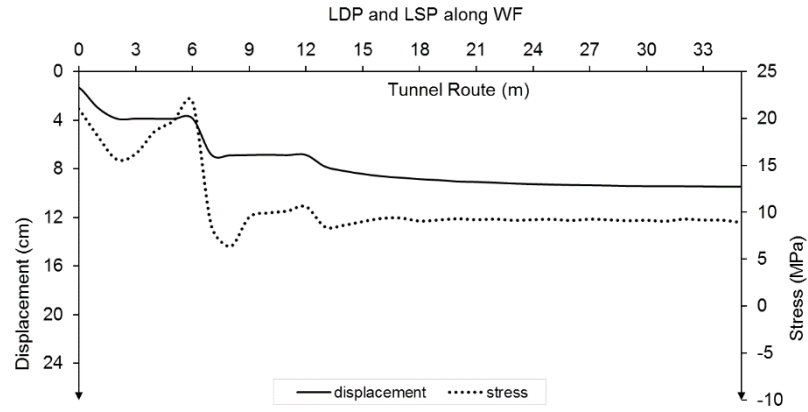


Figure 5.28. LDP and Maximum principal stress history of the ground along point WF

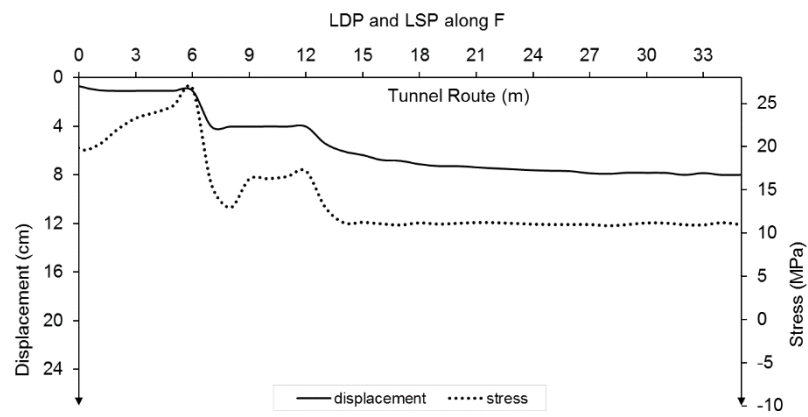


Figure 5.29. LDP and Maximum principal stress history of the ground along point F

5.7.4. Thrust Force Calculations

The thrust force required to overcome shield skin frictional forces are investigated by extracting of sectional profile of contact forces on both front and rear shields. For this purpose, the profile of sectional contact forces between ground and front shield as well as between ground and rear shield are extracted from numerical analysis results as shown in Figure 5.30. According to Figure 5.30, total contact forces over the shields are determined by integrating the contact forces F_i over the shields individually.

Maximum thrust force to overcome friction and drive TBM forward is calculated by multiplying the integral total contact force by the skin friction coefficient μ and the reduction coefficient β which is the ratio of the real shield radius r over the tunnel radius R . Then the required maximum thrust force obtains by the following relationship:

$$F_f = \beta \cdot \mu \sum_{i=1}^N F_i \quad (5.2)$$

where N is the number of contact points on the shield surface [34]. The calculation results for each component of TBM are given in Table 5.4.

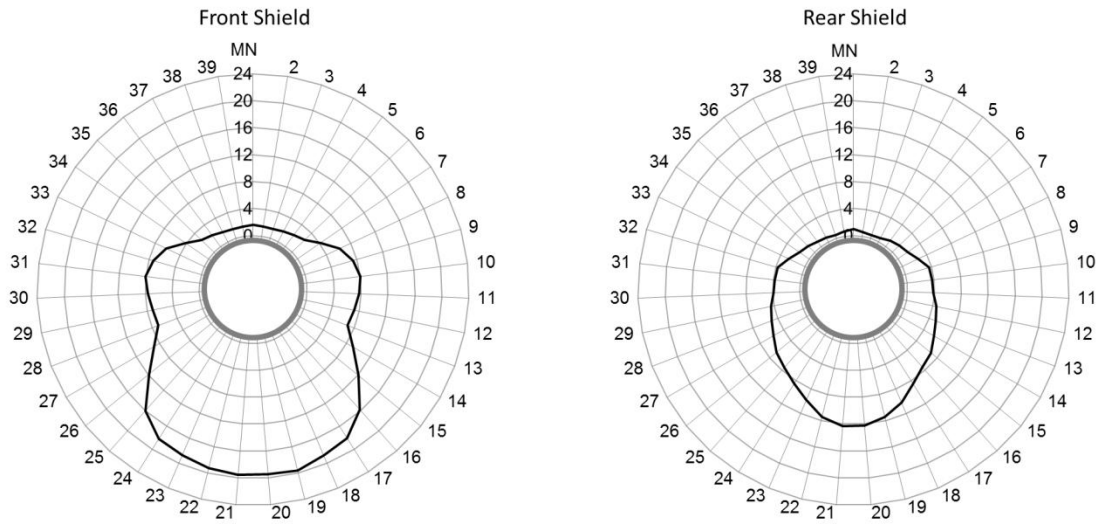


Figure 5.30. Sectional contact forces profile between ground and shields

The maximum total thrust force by the auxiliary thrust cylinders is the sum of the maximum cutter-head thrust F_N and the thrust to overcome friction as follows:

For front shield: $F = F_N + F_f = 17 + 134.1 = 151.1 \text{ MN}$

For rear shield: $F = F_N + F_f = 17 + 72 = 89 \text{ MN}$

Table 5.4. Parameters used for calculation of required thrust force

front shield		rear shield	
$r \text{ (m)}$	9.23	$r \text{ (m)}$	9.17
$R \text{ (m)}$	9.44	$R \text{ (m)}$	9.44
β	0.98	β	0.97
μ	0.40	μ	0.40
$F_i \text{ (MN)}$	342.9	$F_i \text{ (MN)}$	185.3
$F_f \text{ (MN)}$	134.1	$F_f \text{ (MN)}$	72

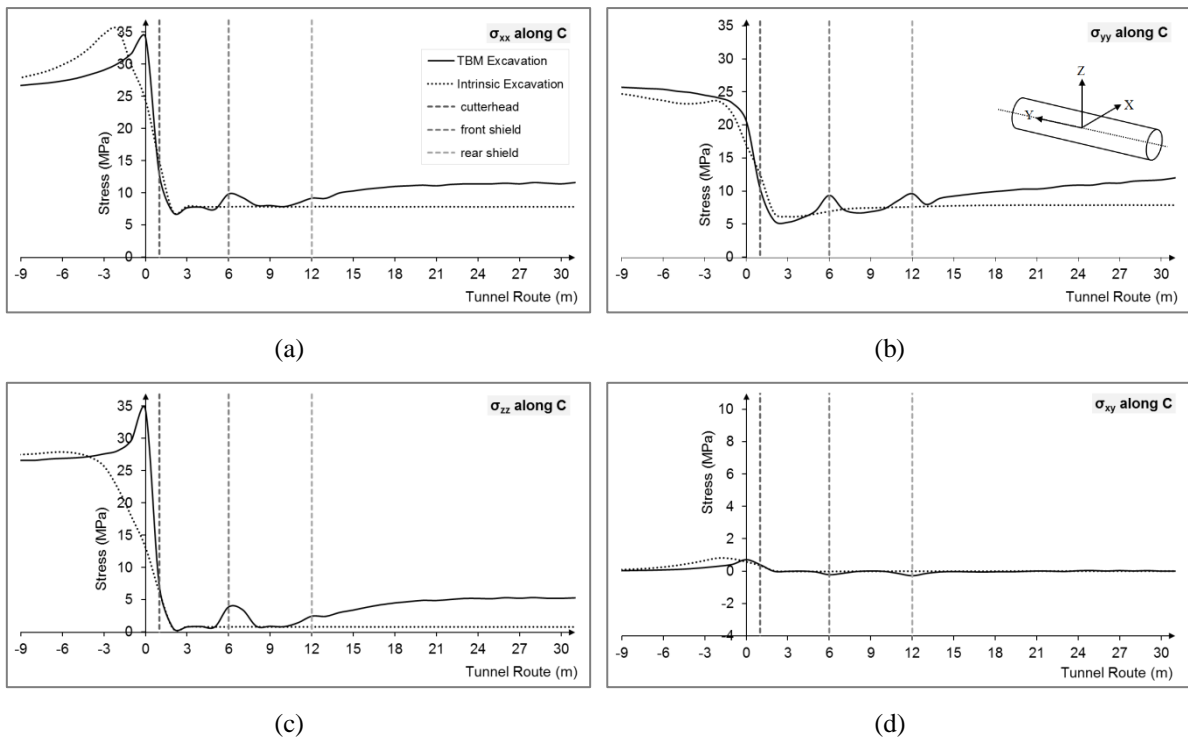
This is equivalent to 134,100 ton of thrust that needs to be applied to avoid machine entrapment and push the machine forward. The relatively high value of required thrust could mean machine jamming if the auxiliary thrust system of the machine cannot deliver such high propel force or the size of the lining does not support such thrust levels. One can think about possible mitigation plans to avoid machine jamming by reducing the required auxiliary thrust force. This could include application an appropriate ground improvement

method to strengthen the ground and prevent or slow down ground convergence. Also applying shield lubricants such as bentonite can be considered to reduce the friction and allow the shield to move forward.

Another approach is to increase the gap between the rock and rear shield. The stepwise increasing of the annular space gap by decreasing the diameter of the rear shield relative to the front shield can be another solution. With this plan the reduction of shield diameter could increase from 3 cm to 5-6 cm, so that the contact between the rock mass and the rear shields would occur mainly at the end of the front shield and the required thrust force would be lowered. These possibilities will be examined in the continuation of the current study.

5.8. Stress History of the Ground

Figure 5.31 and 5.32 provides a complete stress history of the ground along the crown and sidewall of tunnel. At the crown near the tunnel face, the axial stresses become so large that the plastic deformations start to develop in this part. Shear stresses σ_{xy} and σ_{xz} are zero along tunnel. At a certain distance behind the face, the converging ground closes the gap and the shield starts to develop support pressure upon the tunnel boundary.



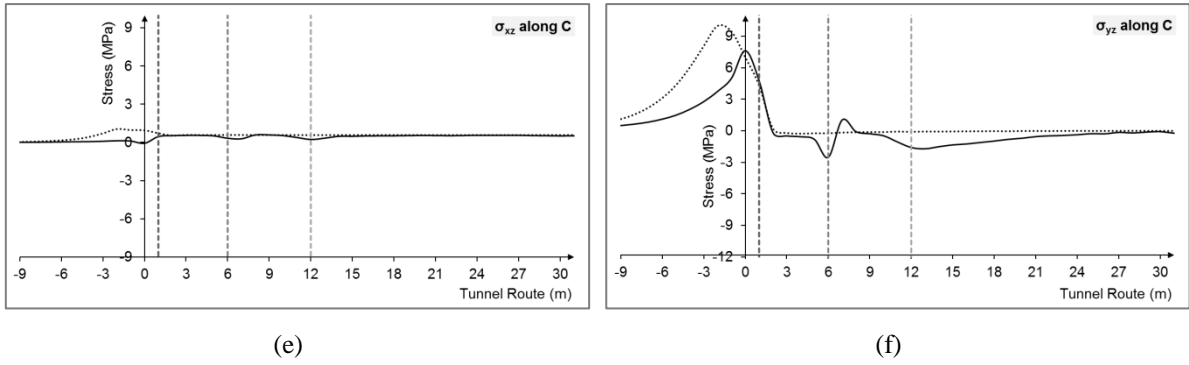
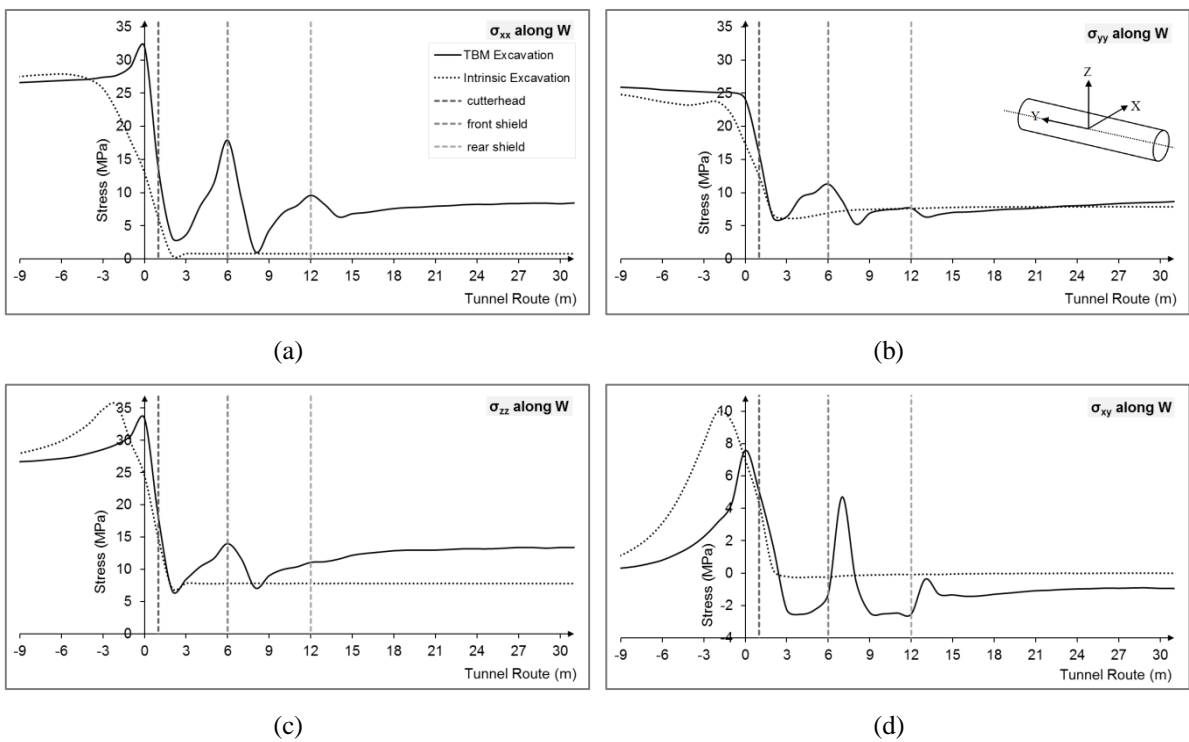


Figure 5.31. Results of numerical computations at crown; a history of the axial stresses a) σ_{xx} b) σ_{yy} c) σ_{zz} and shear stress d) σ_{xy} e) σ_{xz} f) σ_{yz} along the tunnel

As can be seen in the plots, the ground experiences five unloading and reloading cycles, the first unloading being near to the tunnel face until the ground closes the gap and the second reloading is at end of the front shield. The third unloading occurs at end of the front shield and fourth reloading in the middle of rear shield. The fifth unloading is where lining installation takes place at end of rear shield. The same arguments can be considered for description of stress history at sidewall of tunnel according to Figure 5.32.

Figure 5.33 illustrates sectional ground pressure profile at boundary of the segmental linings for three different positions toward to tunnel face.



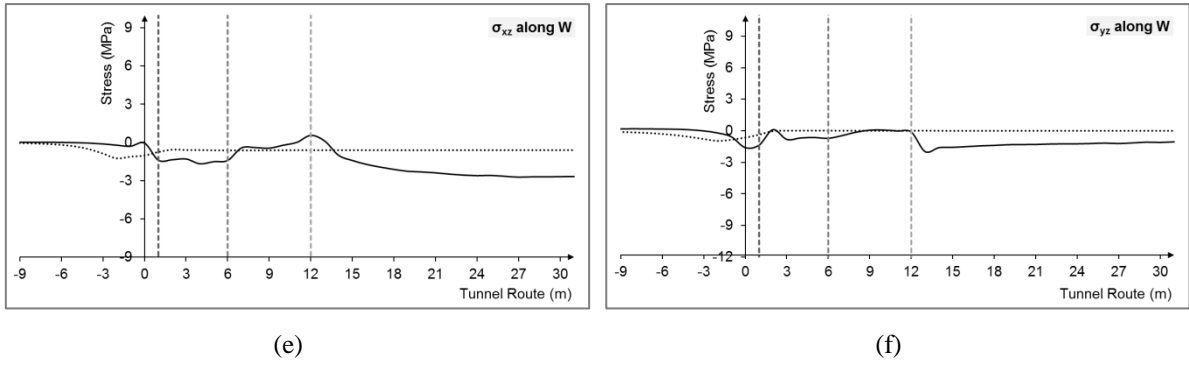


Figure 5.32. Results of numerical computations at sidewall; a history of the axial stresses

a) σ_{xx} b) σ_{yy} c) σ_{zz} and shear stress d) σ_{xy} e) σ_{xz} f) σ_{yz} along the tunnel

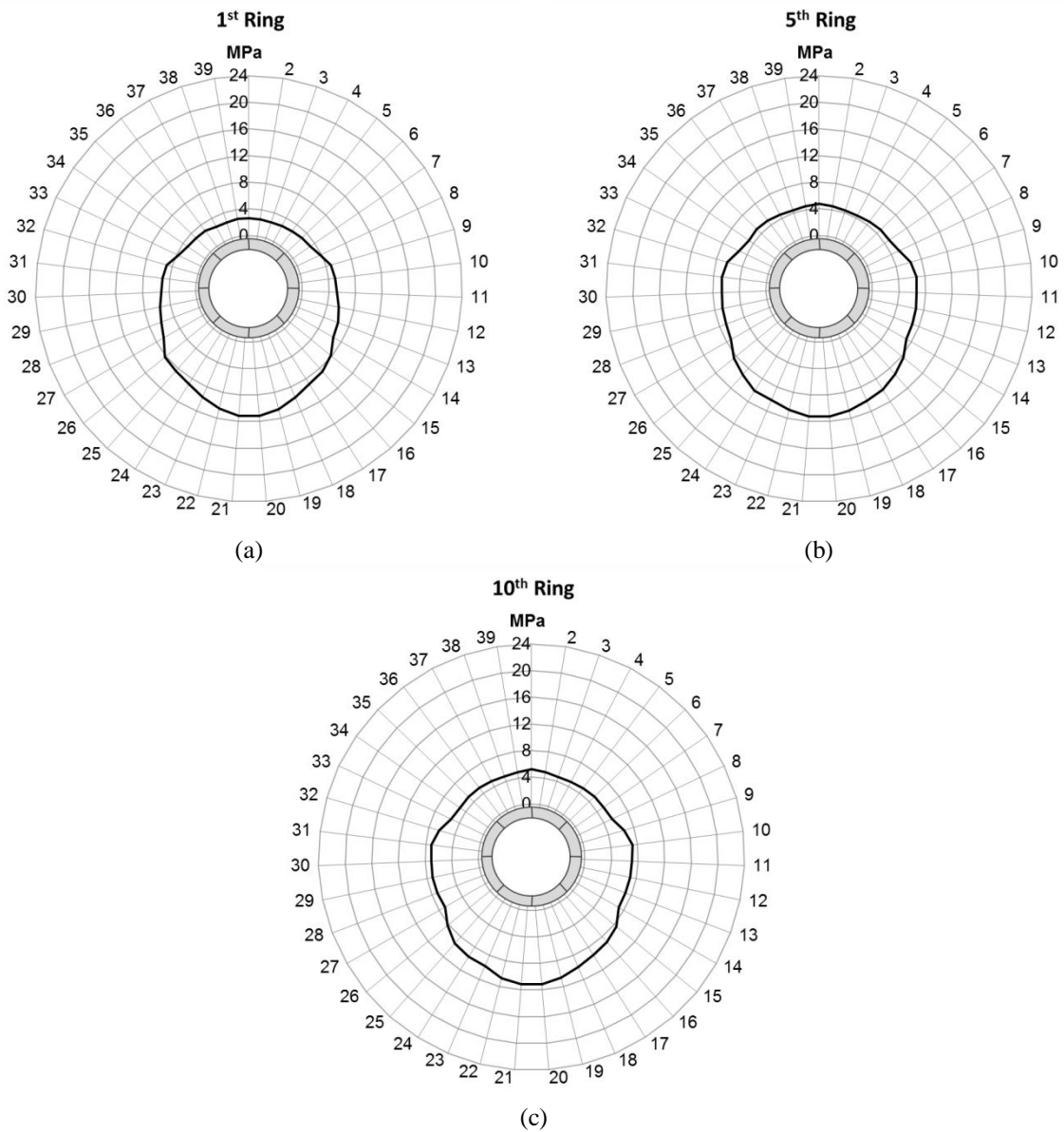


Figure 5.33. Sectional ground pressure at boundary of the segmental rings; a) first ring b)

fifth ring c) tenth ring

According to Figure 5.33, with distance to face, ground pressure upon linings increases partly and being fixed and uniform at a certain distance to face.

It is noted that the high pressure on segmental lining is due to deep tunnel excavation in a ground with squeezing behavior. To avoid failure in the segmental rings and reduce high ground pressure around linings, appropriate ground improvement methods should be applied. Although, uniform distribution of pressures at boundary of the segmental rings may not cause to failure in the segments, however point loading because of a probable faults or other tectonically events will provide breakage in the segments.

6. TIME DEPENDENT ANALYSIS

6.1. Introduction

The tunnel excavation by a shielded TBM is a continuous process, relative to the gradual movement of the ground, unless a major delay in the operation is experienced. Entrapment of shielded TBMs can occur in the squeezing ground due to excessive convergence of the walls during extended machine downtimes, including weekends, stoppages for machine repair or maintenance, or other operational issues. This shows that the "time" factor plays an important role and should be considered when evaluating the stability of the underground opening and designing its support system because considerable amount of deformation and contact pressure may develop with time [1].

There are several cases where shielded TBM was entrapped when there was a slowdown in operation or standstill in the TBM drive. For example, the Nuovo Canale Val Viola (Italy, double shielded TBM, $D=3.60$ m) [1], the Ghomroud Tunnel (Iran, double shielded TBM, $D = 4.50$ m) [17] and the Yindaruqin Irrigation Project (China, double shielded TBM, $D=5.54$ m) [1] are the some cases that the TBM became trapped because of squeezing ground during a one-week holiday stop or during a maintenance stop. This suggests that maintaining a high daily advance rate and reducing downtimes may have a positive effect in avoiding entrapment.

Standstills are unfavorable also with respect to cutter head operation. Depending on the rheological behavior of the ground, high ground pressures acting against the cutter head or an extremely high extrusion rate of the core may develop. In this respect, the Gilgel Gibe II Tunnel (Ethiopia, double shielded TBM, $D = 6.98$ m) is a case history that can be mentioned [1].

As stated by the International Society for Rock Mechanics (ISRM), squeezing rock is the time dependent large deformation related to the progressive yielding, which occurs around the tunnel and is essentially associated with creep, caused by exceeding a threshold shear stress. Deformation may terminate during construction or continue over a long period of time [35]. In engineering practice, the difficulties to deal with squeezing conditions are connected to: (1) the evaluation of the time-dependent characteristics of the rock mass by means of laboratory or in-situ tests, (2) the use of an appropriate constitutive model, and (3) the choice of a suitable excavation and support system [47].

In this chapter, to evaluate the impact of time factor on possibility of machine seizure, time dependent finite difference simulation of a double shield TBM in squeezing ground was performed. The study includes the time effect during advancement of excavation cycle of a shielded TBM to observe the impact of tunneling advance rate on the possibility of machine jamming in the squeezing grounds. The 3D model used in Chapter 5 is utilized in this study with the difference that incorporates the creep properties of rock mass in severe squeezing conditions. Two time dependent constitutive models including a Burger-creep visco-plastic model (CVISC) and a power-law visco-plastic model (CPOW) are applied in the numerical models for describing the tunnel time dependent response associated with severely squeezing conditions. The results estimate tunnel convergence during excavation, compare the longitudinal and sectional maximum principal stresses in the rock mass during TBM excavation for different advance rates, and predict the magnitude of load on the shields in squeezing conditions, allowing to estimate the frictional forces between the rock and shield and thus the required machine thrust to move the machine forward.

6.2. Creep Behavior of Material

Creep is a time-dependent deformation that may occur in materials under constant stress. Creep originates from visco-elastic effects in the solid framework, thus creep unlike consolidation may occur in both dry and saturated rocks. There are three stages of creep following a change in the stress state. First, there is a region where the rate of the time-dependent deformation decreases with time (Figure 6.1). This is called transient (or primary) creep. The process may be associated with minor spreading at decaying rate of “stable” micro fractures. If the applied stress is reduced to zero during the primary creep stage, the deformation will eventually decrease to zero too.

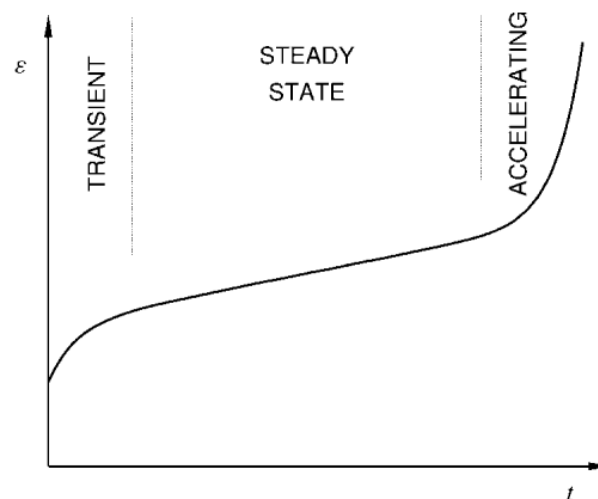


Figure 6.1. Strain versus time for a creeping material [48]

In the next stage, the deformation rate is constant. This is called steady state (or secondary) creep. If the applied stress is reduced to zero during this stage, the deformation will not vanish completely. Steady state creep thus implies a permanent deformation of the material. Finally, the deformation rate may increase with time. This is called accelerating (or tertiary) creep. This stage rapidly leads to failure. The process may be associated with a rapid spreading of “unstable” fractures [48].

The actual creep behavior of a rock depends on the magnitude of the applied stress. For low or moderate stresses, the material may virtually stabilize after a period of transient creep. For high stresses, the material may rapidly run through all three stages of creep and finally fail. The intermediate stress regime, where the material fully develops each stage of creep, may be small and hard to find in practice (Figure 6.2). The time scale of a creep stage may vary over a wide range in some cases it lasts for minutes, in other cases for years. Creep is a molecular process, and the time scale depends on temperature; the process generally speeds up with increasing temperature [49].

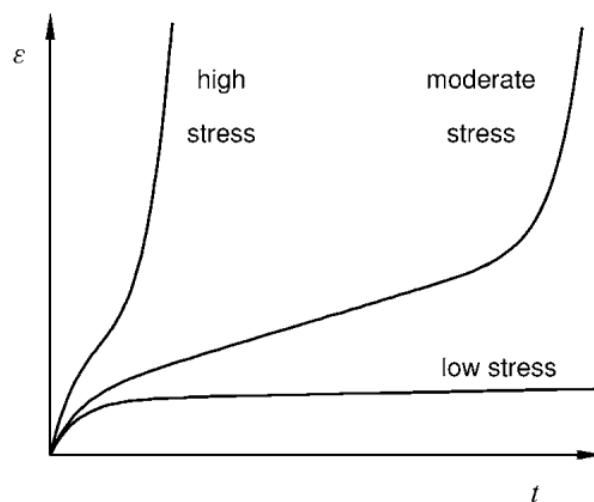


Figure 6.2. The development of creep for different values of the applied stress

The fact that even steady state creep eventually leads to failure, means that a rock which is loaded to a level somewhat below its ultimate strength, may fail after some time, if the load is maintained. This effectively reduces the long-term uniaxial strength to typically 50-70% of the ultimate strength [49].

6.3. Time Dependent Response

Influence of the time-dependent mechanical properties of the rock mass on the response of a tunnel to excavation has been modeled by many authors using visco-elastic and visco-

plastic constitutive equations. Ladanyi [50] and Cristescu [51] give a comprehensive presentation of the available solutions for simple tunneling cases and models of behavior:

- Linear visco-elastic
- Linear elastic - linear viscous
- Linear elastic - nonlinear viscous
- Elastic - visco-plastic

a) A typical simple example of analysis for a linear visco-elastic model consists in using the so called Maxwell model given in Figure 6.3, where an elastic spring and a viscous dashpot are put in series. In such a case, the radial displacement u_r at the tunnel contour (as for the closed form solutions previously discussed for the elasto-plastic case, the tunnel is circular and the rock mass is subjected to a hydrostatic state of stress) is given by:

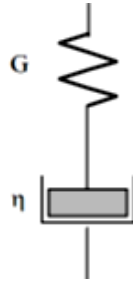


Figure 6.3. Maxwell linear visco-elastic model

$$u_r = \frac{(p_0 - p_i)R}{2G} \left(1 + \frac{t}{T}\right) \quad (6.1)$$

Where:

t = time

$T = \eta/G$, relaxation time.

If a linearly elastic lining (a ring) with stiffness K_l is installed at time t_s , the displacement u_r is:

$$u_r = \frac{p_0 R}{2G} \left(1 + \frac{t}{T}\right) + \frac{p_c R}{K_s} \quad (6.2)$$

with the pressure p_c on the same lining being given by:

$$p_c = p_0 \left[1 - \exp \left[-\frac{t - t_s}{T \left(1 + \frac{2G}{k_l}\right)} \right] \right] \quad (6.3)$$

b) Similarly, with reference to the linear Kelvin-Voigt visco-elastic model of next figure one would obtain for u_r , when no lining is installed yet (Figure 6.4).

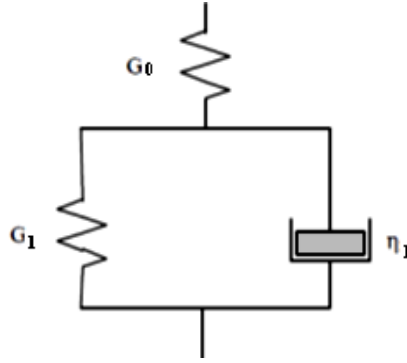


Figure 6.4. Kelvin-Voigt visco-elastic model

$$u_r = \frac{(p_0 - p_i)R}{2G_0} \left[1 + \left(\frac{G_0}{G_f} - 1 \right) \cdot \left(1 - \exp\left(-\frac{t}{T}\right) \right) \right] \quad (6.4)$$

Where;

$$T = \frac{\eta_1}{G_1} \quad (6.5)$$

$$G_f = \frac{1}{G_0} + \frac{1}{G_1} \quad (6.6)$$

with the lining installed at time t_s , the following equations are obtained for u_r and p_c .

$$u_r = \frac{p_0 R}{2G_0} \left[1 + \left(\frac{G_0}{G_f} - 1 \right) \cdot \left(1 - \exp\left(-\frac{t}{T}\right) \right) \right] + \frac{p_c \cdot R}{k_l} \quad (6.7)$$

$$p_c = p_0 \cdot \left[\frac{1 - \frac{G_f}{G_0}}{1 + 2 \frac{G_f}{K_l}} \right] \exp\left(-\frac{t_s}{T}\right) \cdot \left[1 - \exp\left[\frac{2 + \frac{K_l}{G_f}}{2 + \frac{K_l}{G_0}} \cdot \left(-\frac{t - t_s}{T}\right) \right] \right] \quad (6.8)$$

c) If consideration is given to squeezing behavior, the visco-elastic models above, where the assumption is that the time effect can be separated from the stress effect in the general creep formulation, are not appropriate. Therefore, models of the elastic-visco-plastic type should be used.

A simple model of interest, due to Sulem et al. [52], allows the analysis of time-dependent stress and strain fields around a circular tunnel in a creeping rock mass with plastic yielding. Although valid for a monotonic stress path, this model is well suited for the problem considered in this study and allows a closed form solution for the computation of the time-dependent convergence.

As discussed by Sulem [53], the total strain ε is obtained by adding together the time-independent elastic strain ε^e and the time-dependent inelastic strain ε^{ne} :

$$\varepsilon = \varepsilon^e + \varepsilon^{ne} \quad (6.9)$$

where:

$\varepsilon^{ne} = \varepsilon^p + \varepsilon^c$ for ε^p = plastic strain and ε^c = creep strain.

The creep strain is written as an explicit function of stress σ_{ij} and of time t as an explicit parameter:

$$\varepsilon^c = g(\sigma_{ij})f(t) \quad (6.10)$$

where f is an increasing function of time with $f(0) = 0$ and $\lim f(t) = 1$.

If $g(\sigma_{ij})$ is taken as a linear law (the most appropriate form for rock is a power law) and the creep strain is assumed to depend only on the deviatoric stress and to occur at constant volume, the radial strain ε_r^c and the tangential strain ε_θ^c can be written as [53]: (where G_f is a creep modulus)

$$\varepsilon_r^c = -\frac{\sigma_\theta - \sigma_r}{4G_f} f(t) \quad (6.11)$$

$$\varepsilon_\theta^c = \frac{\sigma_\theta - \sigma_r}{4G_f} f(t) \quad (6.12)$$

Let the rock mass follow a Mohr-Coloumb yield criterion in which peak and residual strength coincide ($c_p = c_r = c$; $f_p = f_r = f$), and the deformations subsequent to yielding occur at constant volume ($\psi = 0$). As demonstrated by Sulem et al. [52], under these conditions the linearity of the creep law with stress leads for the stress field around the tunnel to the same results as for the simple elastic perfectly plastic model. The plastic radius R_p and the critical pressure p_{cr} , defined by the initiation of plastic failure of the rock around the tunnel, are given by the same expressions below.

The radial displacement at the tunnel wall is:

- For $p_i > p_{cr}$

$$u_r = \frac{p_0 R}{2G} \left(1 + \frac{G}{G_f} f(t) \right) \quad (6.13)$$

- For $p_i < p_{cr}$

$$u_r = \frac{p_0 R}{2G} \left(\frac{R_p}{R} \right)^2 \left(1 + \frac{G}{G_f} f(t) \right) \lambda_e \quad (6.14)$$

Where;

$$\lambda_e = \sin\varphi + \frac{c \cos\varphi}{p_0} \quad (6.15)$$

6.4. Time Dependent Numerical Modeling

To analyze the time dependent behavior of rock mass in a tunnel excavation with a double shield TBM, a 3D model of DS-TBM used in Chapter 5 was applied. However, rock mass and creep parameters are provided along the tunnel at depth of nearly 600 m. Rock mass parameters in this location are different from parameters that are used in the previous Chapter.

6.4.1 Assumptions for Numerical Model

In the model, the presence of water pressure and consolidation problems is ignored. Moreover, the in situ state of stress is assumed to vary linearly with depth and it represents the conditions along the Base Tunnel at depth of nearly 600 m. The ratio between the horizontal and vertical stress components (σ_h/σ_v) in the rock mass is assumed to be $K_0=1$. The rock mass is assumed to follow a linear elastic and perfectly plastic behavior according to Mohr-Coulomb failure criterion. The rock mass parameters are shown in Table 6.1.

Table 6.1. Rock mass parameters from Lyon–Turin Base Tunnel [47]

Rock mass parameters		
Elastic modulus, E	GPa	0.942
Poisson's ratio, ν	-	0.25
Cohesion, c	MPa	0.61
Friction angle, ϕ	°	28
Dilatancy angle, φ	°	8

6.4.2 Creep Model of the Analysis

Two time dependent constitutive creep models including a Burger-creep visco-plastic model (CVISC) and a power-law visco-plastic model (CPOW) are applied to the numerical models for describing the tunnel time dependent response associated with severely

squeezing conditions. These two creep models were used because they are available in FLAC^{3D} software package and they can be used directly in the analysis.

6.4.2.1. CVISC model

The CVISC model is an analogical model which couples, in series, the Burgers viscoelastic model (i.e. Kelvin and Maxwell models in series) with a plastic flow rule, based on the Mohr-Coulomb yield criterion [54]. Creep parameters of CVISC model were derived from the Lyon-Turin Base Tunnel [47]. Table 6.2 summarized the creep parameters that were used in the analyses.

Table 6.2. Creep Constitutive parameters, CVISC model, [47]

CVISC model		
Maxwell shear modulus, G^M	[MPa]	566
Maxwell viscosity, η^M	[MPa.year]	27.98
Kelvin viscosity, η^K	[MPa.year]	4.26
Kelvin shear modulus, G^K	[MPa]	498.1
Tensile strength, σ_t	[MPa]	8.5e-3

6.4.2.2. Power Law Creep Model (CPOW Model)

Power law creep model correlates the strain rate according to the following equation:

$$\dot{\epsilon} = A\sigma^n \quad (6.16)$$

where $\dot{\epsilon}$ is the strain rate versus time, σ the deviator stress = $\sigma_1 - \sigma_3$, A and n are the creep model parameters and can be evaluated from laboratory tests. The rock mass creep parameters for this model have been selected according to studies from Shalabi [22]. Table 6.3 summarized the creep parameters that were used in the analyses.

Table 6.3. Creep Constitutive parameters; CPOW model, [22]

CPOW model		
power-law constant, A	-	2.783e-18
power-law exponent, n	-	2.19
tensile strength, σ_t	[MPa]	2

6.5. Results of Numerical Analysis

The result of numerical analysis includes the deformation and history of maximum principal stresses in the rock mass as well and contact forces between ground and machine components for different advance rates by considering the gap between the shields and the rock mass that is not uniform. Two monitoring points at the crown and the sidewall of tunnel have been selected for evaluation of longitudinal profiles.

6.5.1. DS-TBM Time Dependent Excavation Results for CVISC Model

Figure 6.5 depicts the longitudinal displacement profile (LDP) and longitudinal contact force profile (LFP) at the crown of tunnel (point C) based on CVISC model in the contact and non-contact points between rock mass and machine when TBM advance rate (AR) is 24 m/day. As displayed in the Figure, the closure of gap between cutter-head and the ground would not take place; therefore the contact force on the cutter-head is nearly zero. Also the closure of gap between the front shield and the ground occurs at about 4.0 m distance to face, and rock mass starts to load on the front shield up to 6.4 MN. Due to conical shape of the shields, the contact stress between ground and rear shield is initially reduced to zero. After a few time steps that equals 2 hours, contact between ground and rear shield occurs and ground starts to load on the rear shield with up to 3.6 MN of forces.

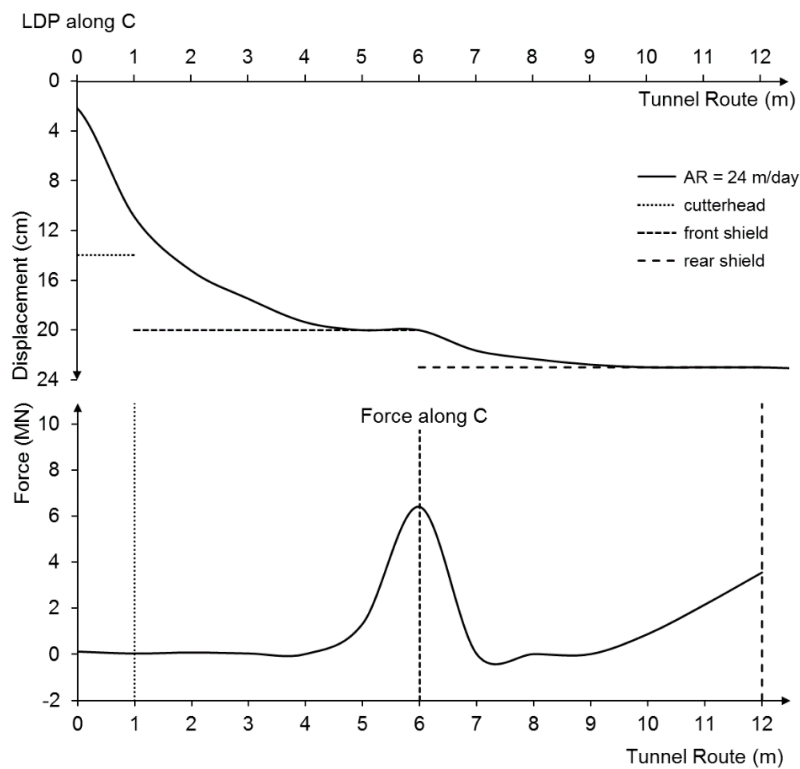


Figure 6.5. LDP at tunnel circumference and LFP on shields along tunnel crown (point C)

Longitudinal maximum principle stress profile (LSP) in the ground at the crown of tunnel based on CVISC model is illustrated in Figure 6.6. Redistribution of stresses due to excavation of tunnel occurs and ground stress decreases from in situ stress 13.8 MPa to 0.12 MPa in area of the front shield. When contact between the front shield and rock mass starts, shield supports the ground. With advancing of tunnel, stress in the ground increases up to 2.8 MPa.

Due to conical shape of rear shield, stress in the ground decreases again under 0.16 MPa. Contact between rear shield and ground takes place with advancing of tunnel, hence stress in the ground around tunnel increase to 2.11 MPa. Installation of segmental lining and subsequent application of backfilling allow contacting between ground and lining by backfill. Therefore internal pressure from lining to rock mass is created and growth with advancing of tunnel and fixed at a distance to face that is about 30 m.

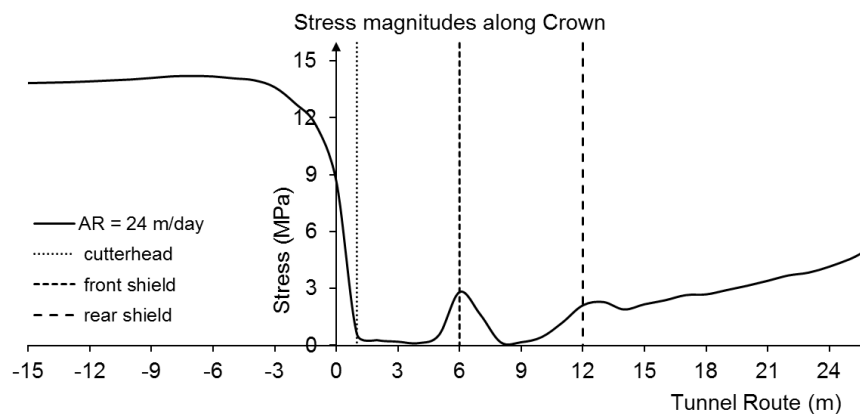


Figure 6.6. LSP at the tunnel circumference along tunnel crown (point C)

Numerical results for investigation of LDP and LFP at the sidewall of tunnel are shown in the Figure 6.7. As can be seen in the Figure, the contact between cutter-head and ground started in last solving time step at sidewall, hence the minimal forces from rock is applied to the cutter-head. This contact because of smaller gap between rock mass and TBM components at the sidewall because of non-uniform overcut that case to closure of gap instantly after boring comparing to conditions at the crown of tunnel. On the other hand, a slowdown or standstill in TBM advance may cause extended area of contact between rock and cutter-head in the wall, and hence higher frictional forces. Contact between rock mass and shields occurs right after the advance of the machine behind the face. Contact forces on both front and rear shield increase to 9.7 and 9.1 MN respectively.

Longitudinal maximum principle stress profile (LSP) at the tunnel circumference along tunnel sidewall is shown in the Figure 6.8. Mechanism of redistribution of stresses in the sidewall due to some loading and unloading processes is similar to mechanism in the crown as discussed for Figure 6.6.

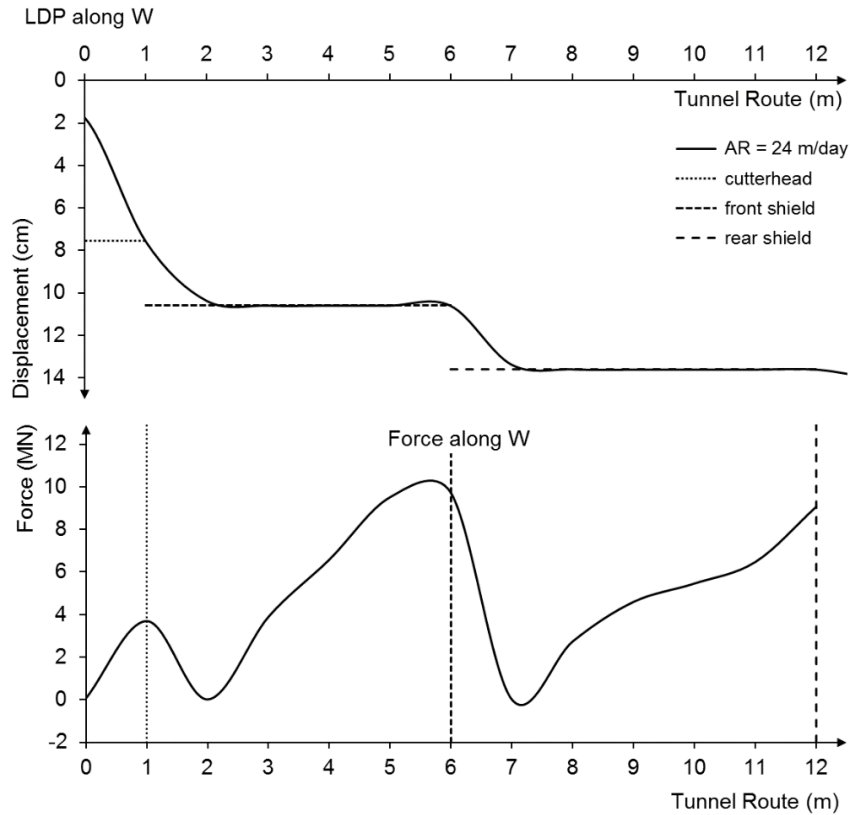


Figure 6.7. LDP at tunnel circumference and LFP on TBM components along tunnel sidewall (point W)

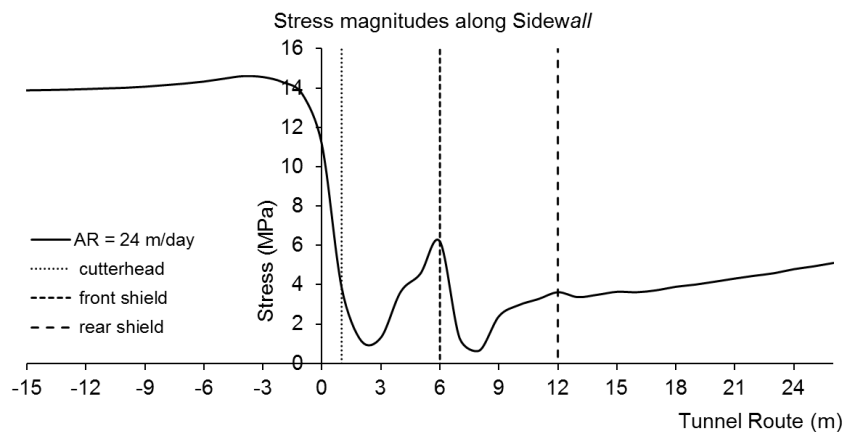


Figure 6.8. LSP at the tunnel circumference along tunnel sidewall (point W)

Sectional contact forces between ground and front shield as well as between ground and rear shield are shown in the Figure 6.9. The required thrust force to overcome friction on shields and drive TBM forward is calculated by integrating of contact forces in the Figure and multiplying them to friction coefficient when AR=24 m/day. The skin friction coefficient, μ , is assumed 0.4 for a condition “restart after standstill”. The maximum total thrust force by the auxiliary thrust cylinders is the sum of the maximum cutter-head thrust F_N and the required thrust to overcome friction F_f as follows:

For front shield: $F = F_N + F_f = 11 + 85.6 = 96.6 \text{ MN}$

For rear shield: $F = F_N + F_f = 11 + 42.8 = 53.8 \text{ MN}$

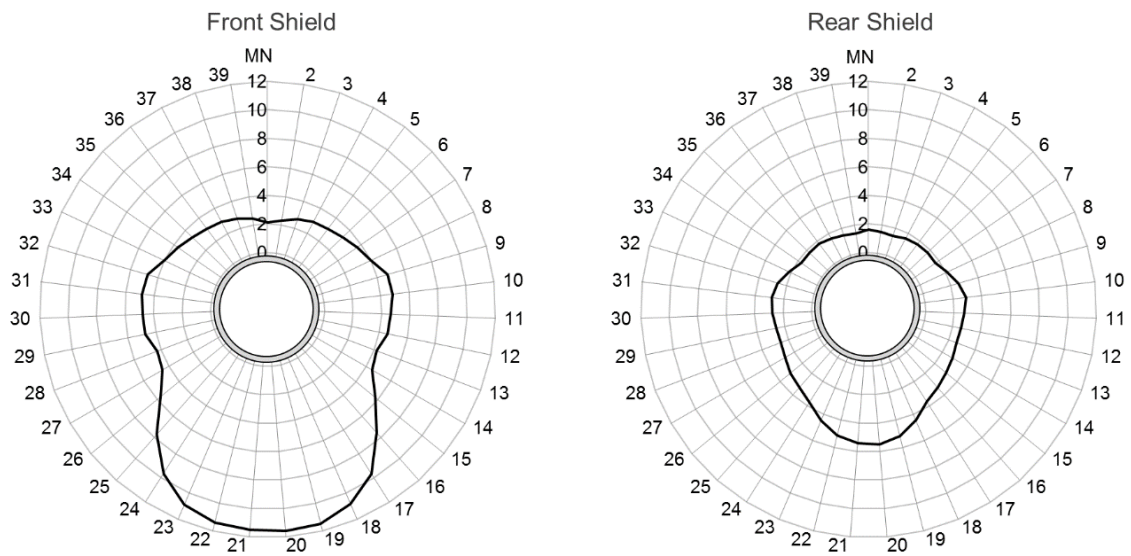


Figure 6.9. Sectional contact forces profile between ground and shields

6.5.2. Effect of Advance Rate

For evaluation of different advance rates on behavior of rock mass as well as loadings on machine components, LFP in the contact forces on machine elements at the tunnel crown and sidewall are investigated. Figure 6.10 shows the impact of different advance rates on deformation and applied stress on TBM components.

As shown in Figure 6.10, at point W, the front shield, when the advance rate is 6 m/day, is loaded 1.2 MN more than when advance rate equal to 48 m/day. This value is 1.7 MN for rear shield. Also for advance rate of 48 m/day the segment experiences 2.5 MN load less than the same segment when the advance rate is 6 m/day during the course of excavation. Therefore the entrapment of shielded TBMs can occurs in the squeezing ground during extended machine downtimes or in the lower advance rates.

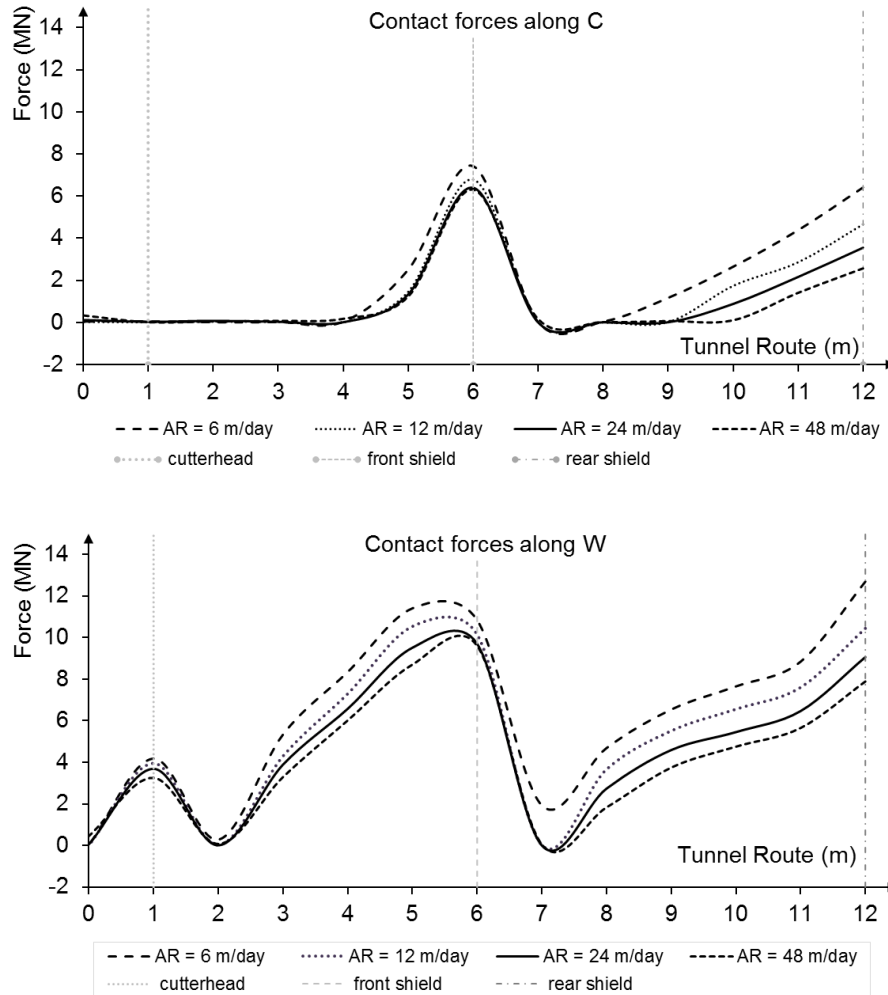


Figure 6.10. LFP for different advance rates at crown and sidewall (point C and W)

6.5.3. Evaluation of TBM Entrapment Risks

Figure 6.11 shows the sectional principal stresses or ground pressure in the ground around the machine components for various advance rates. In this case, the maximum principal stress is observed in the invert. This is due to non-uniform overcut with smallest amount in the invert cause to closure of gap early so that the cutter-head and shields start to support the excavation walls. Also the weight of the machine provides additional confinement to the excavation surface near the tunnel face.

On the other hand, as shown in Figure 6.11, the impact of advance rate on applied stress from rock mass to cutter-head and front shield where there is contact between them is not pronounced, but the rear shield experiences lower magnitudes of load in high speed TBM excavation.

For assessment of shield entrapment risk and prediction of thrust force, maximum required thrust forces on machine components in the contact points is calculated for different

advance rates (Figure 6.12). By using this diagram, the maximum required thrust force on machine elements is easily specified for different advance rates.

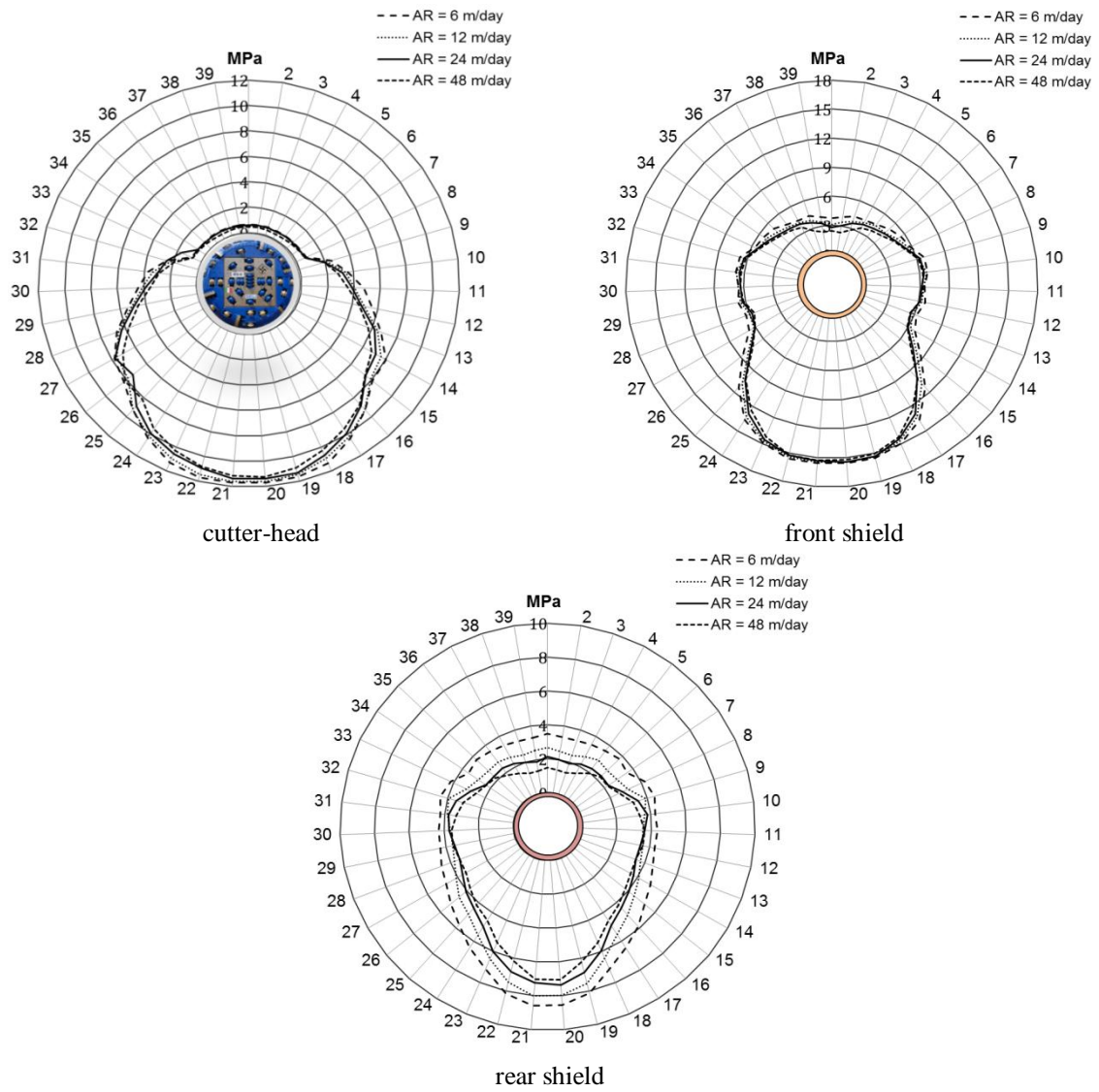


Figure 6.11. Maximum sectional principal stresses on TBM components for different advance rates

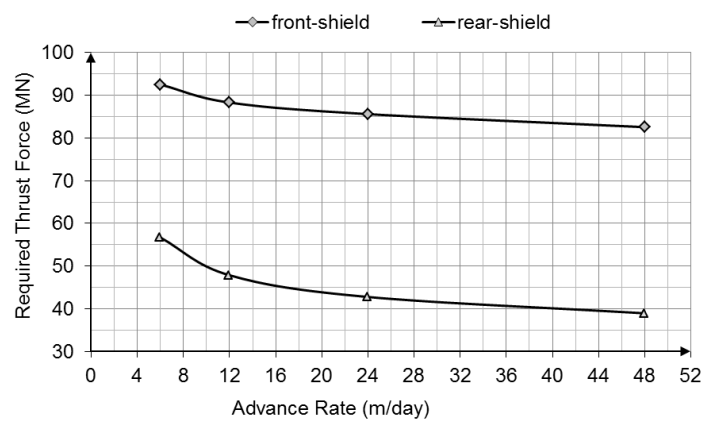


Figure 6.12. Required thrust force diagram versus different advance rates

6.5.4. Effect of Advance Rate on Loading of Segmental Lining

As illustrated in Figure 6.13a, after installation of segmental lining, ground pressure is transferred uniformly to the ring by backfill. This shows the importance of backfill. Moreover, the role of advance rate on the loading of lining is significant. In this case, for advance rate of 48 m/day the segmental ring experiences about 2.5 MPa less than when the advance rate is 6 m/day.

Figure 6.13b depicts the diagram that is used for prediction of maximum principal stress in the ground at the boundary of the segmental ring at the variable advance rates. According to this diagram, average stress on the lining ring mainly depends on advance rates. By developing such diagrams for a specified tunnel, one can calculate the magnitude of stress on the lining for a given advance rate and apply this value for designing of the segmental lining.

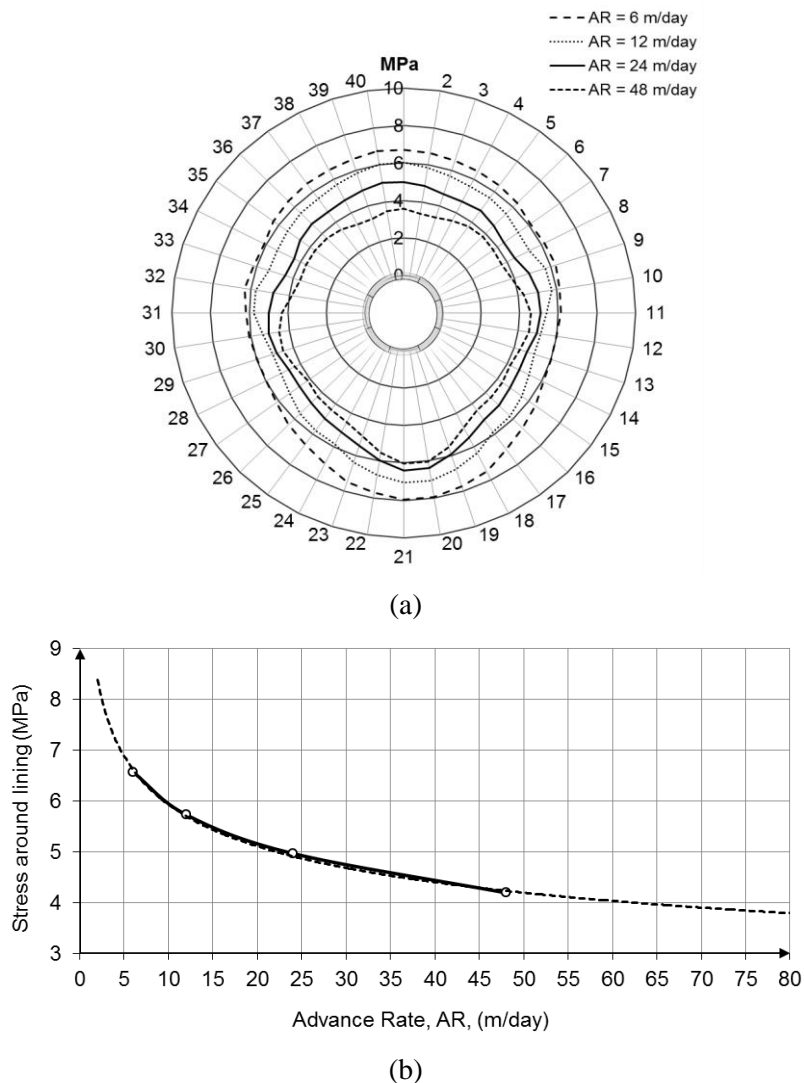


Figure 6.13. a) Sectional principal stress on the segmental ring b) average stress-advance rate diagram for lining

The results of numerical simulation prove the importance of advance rate on prediction of potential for TBM jamming. The analysis has been performed by using CVISC model, but it is noted that the CVISC model simulates the tunnel “short term” response. The model does not predict the observed deformation when the tunnel exhibits a gradual decrease in the rate of convergence, reaching a near stable condition. This is essentially due to the rather simple mathematical formulation of the CVISC model [47].

6.6. Results of Numerical Analysis for CPOW Model

The same analyses have been performed to investigate the impact of different advance rate values (AR) by using the CPOW Model. The results of this analysis are given in Appendix A.

7. IMPACT OF OVERCUT ON INTERACTION BETWEEN SHIELD, GROUND AND SUPPORT

7.1. Introduction

The ground pressure acting upon the shields as contact pressure is of paramount importance both for the structural design of the machine and for the calculation of the frictional resistance to be overcome when advancing the TBM. After a certain amount of deformation has occurred, the ground starts to load the shields. In this chapter, influence of different non-uniform overcut values on the deformation and contact forces developing along the tunnel in a 3D space is examined. The created plastic zone in the ground due to redistribution of stresses as well as the thrust force required in order to overcome friction are evaluated with respect to different amounts of overcut. Specifically, this Chapter shows that the ground at the excavation boundary experiences several unloading and reloading cycles and a stepwise reduction of the shield diameter may be very favorable with respect to the ground pressure.

In order to evaluate the 3D impact of non-uniform overcuts for determining possibility of DS-TBM entrapments, the interaction between ground with cutter-head, shields, and the tunnel support has been analyzed by using 3D numerical analysis for the tunnel excavation case simulated in Chapter 5, excavation of a 1000 m deep long tunnel with a boring diameter of 9.44 m. Information about rock mass, tunnel and machine parameters are given in Chapter 5.

7.2. Shield–Ground Interaction

Similar to Chapter 5, five reference points are selected on tunnel circumference as well as on shield boundaries for extracting the results of numerical analysis. Since it may not be practical to present results for all of five points; therefore in this section and hereinafter, numerical results will be given for crown and spring-line of tunnel (points C and W). On the other hand, results of numerical calculations for other points are given at Appendix B.

In this thesis, over boring or so-called overcut is defined as the gap between ground and front shield at the crown. Moreover, the overcut in the nominal diameter of the cutter-head between ground and rear shield increases due to conical shape of shields. The shield thickness is considered to be 3 cm. The gap between rock mass and cutter-head is about 6 centimeter that is smaller than overcut for the front shield where the crown overcut is 20 cm. For other overcut values, this magnitude is different and it referenced with respect to

overcut on the front shield. Figure 7.1 depicts the different overcut values ΔR on the main components of a double shield TBM that are studied in this section.

Since the overcut is non-uniform for a cross section between ground and shields, hence we have different sizes of overcut at tunnel sectional boundaries, so that the overcut in the crown has the maximum value and minimum in the invert. Numerical analysis model has been set up to account for the non-uniform overcut on TBM main components.

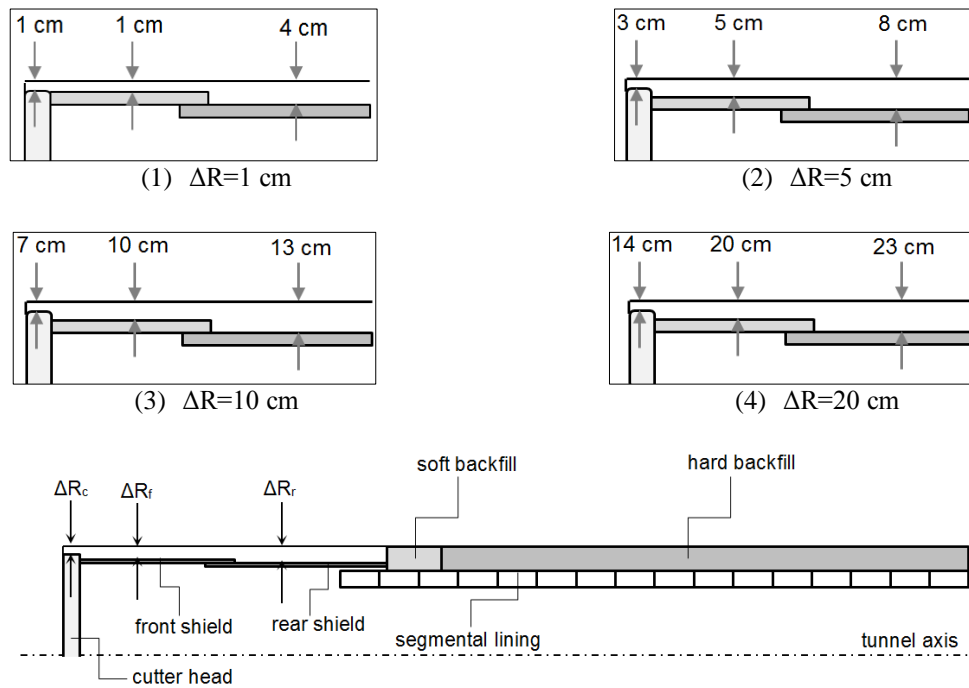


Figure 7.1. Illustration of 4 different overcut values

7.2.1. Shield-Ground Interaction at the Tunnel Crown

Figure 7.2 shows the longitudinal radial displacement of the ground at the tunnel crown for four values of the overcut, ΔR , between ground and shields. In the case of minimum overcutting equal to 1 cm ($\Delta R=1$ cm) the ground closes the gap between cutter-head and rock mass instantly after tunnel boring passes the monitoring point (point A) which is very close to the back of the cutter-head. When $\Delta R=5$ cm, the closure of gap occurs at point B between ground and front shield. Point C is where that contact between rock mass and front shield take place in the middle of the front shield with $\Delta R=10$ cm. A larger gap ($\Delta R=20$ cm) remains open for a longer interval for length of the front shield (up to point D). Contact between rock mass and rear shield occurs after passing through conicity in the same point for each four state. After closing the gaps, the ground starts to load the shields.

One of the most important parameter in DS-TBM design is the so-called ‘‘conicity’’ of the shields, and thus the variation ΔR of the radial gap size along the shield. The positive effect of a conicity or stepwise construction of the shield is reducing the contact forces (which governs the required thrust force) acting upon the shields. Figure 7.3 illustrates the simulation results along the tunnel crown in terms of longitudinal contact forces profile (LFP) proportional to LDP at tunnel circumference. As expected, the contact forces are considerably lower (both for the front and rear shields) when a larger over boring is applied. In the case of a very large over boring of $\Delta R=20$ cm the gap between ground and shield is closed late and the shield remains with lower contact forces.

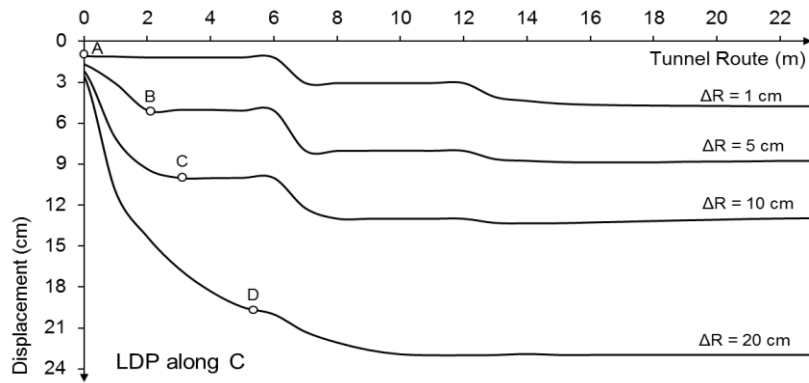


Figure 7.2. Radial displacement of the ground at the tunnel circumference for different overcut, ΔR , of 1, 5, 10 or 20 cm at the crown

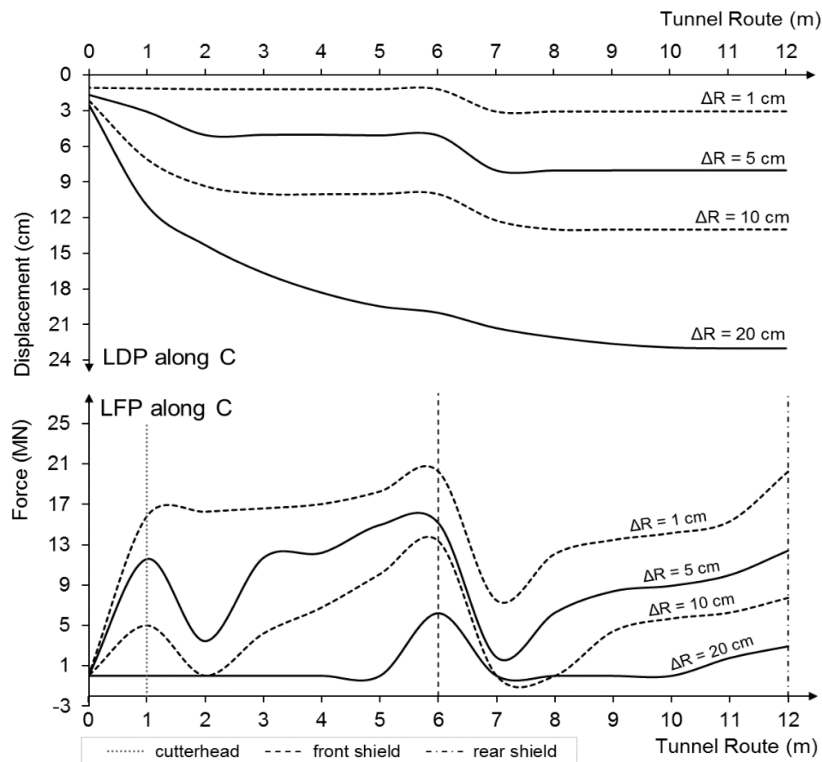


Figure 7.3. Radial displacement of the ground at the tunnel circumference and contact forces for a 1 m cutter-head length, 5 m front shield and 6m rear shield at different overcut ΔR of 1, 5, 10 or 20 cm at the crown

Figure 7.4 shows the redistribution of the maximum principal stress for four different overcut sizes acting upon the shields and the segmental linings. The ground stress increases with the distance from the tunnel face and stabilized at a certain distance. As can be seen from Figure 7.4, unloading–reloading cycles occur several times for the shields having a stepwise decreasing diameter (conical shield). The Figure shows that ground pressure acting on the front shield decreases from 23.3 MPa where $\Delta R=1$ cm to 4.2 MPa at $\Delta R=20$ cm correspondingly to a decline of about 81.9%. This percentage is about 86.3% for rear shield where the ground pressure reduced from 19.6 MPa to 2.7 MPa. Table 7.1 presents the effect of conicity on decreasing of ground pressures acting upon shields for different values of overcut. A wide gap is more important for the rear part of the shield because the convergence of the ground increases with the distance behind the face.

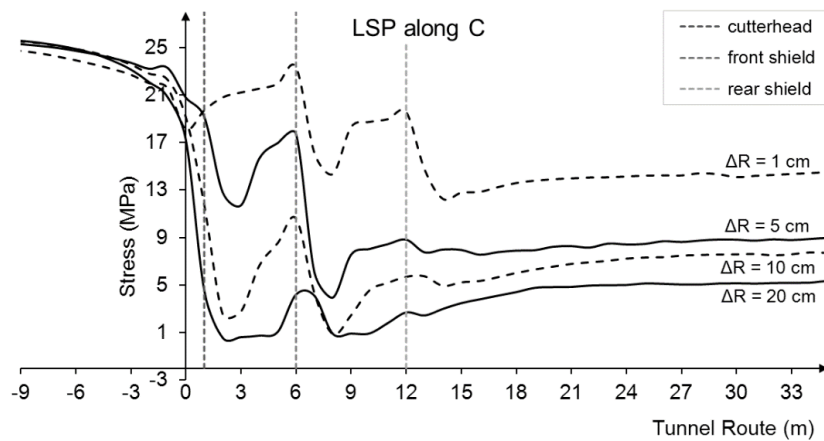


Figure 7.4. Maximum principal stress of the ground around machine components

Table 7.1. Ground pressure acting upon machine components

overcut, ΔR , (cm)	Ground pressure (MPa) acting on			Pressure reduction comparing to 1 cm overcut (%) on		
	cutter head	front shield	rear shield	cutter head	front shield	rear shield
1	19.7	23.3	19.6	0	0	0
5	19.2	17.7	8.8	2.5	24	55.1
10	11.7	10.6	5.7	40.6	54.5	70.9
20	4.5	4.2	2.7	77.2	81.9	86.2

It should be noted, however, that over boring technology is not yet well developed and, as shown from tunneling experience, may be of limited reliability. Feasibility and reliability of a large over boring have to be checked carefully particularly for hard rocks because very high loads act upon the extended gauge cutters in this case and may endanger their structural safety [55].

7.2.2. Shield-Ground Interaction at the Tunnel Wall

Similar to the simulated mentioned earlier, numerical models have been utilized to study interaction between shield and ground along the sidewall of tunnel. The analysis results include longitudinal radial displacement of the ground and contact forces profile acting upon the TBM components and maximum principal stress of the ground provided in Figures 7.5 to 7.7. According to Figure 7.5 and 7.6, closure of gap at sidewall for variation of overcuts occurs earlier than the crown due to smaller gap in this point. Therefore calculated contact forces in this point are larger than forces at the crown. For example, when overcut in the crown is 10 cm ($\Delta R=10$ cm), in the sidewall due to non-uniformity, this value is calculated as 5.55 cm. Hence overcut in the sidewall of the tunnel is closed before than overcut in the crown and provided more contact forces on machine main elements. This deduction is also true for evaluation of ground stress (pressure) acting upon the cutter-head and shields (Figure 7.7).

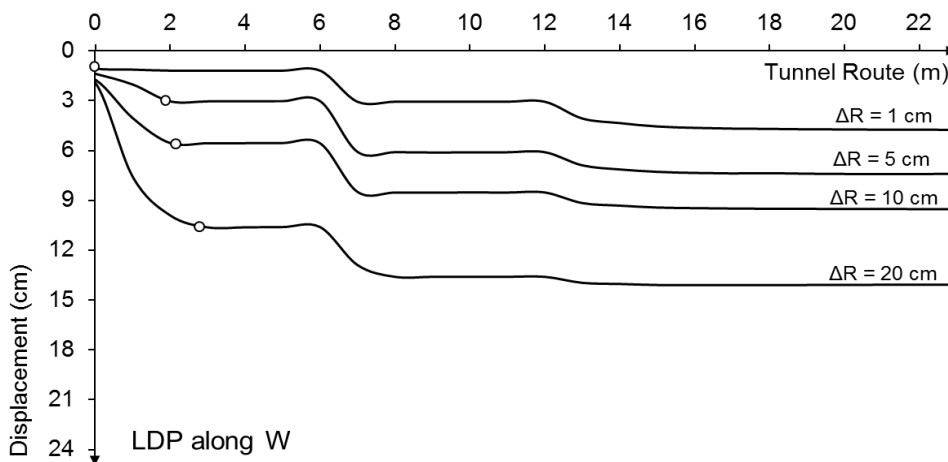


Figure 7.5. Radial displacement of the ground at the tunnel circumference for four different overcut at sidewall when ΔR at the crown are equal to 1, 5, 10 or 20 cm

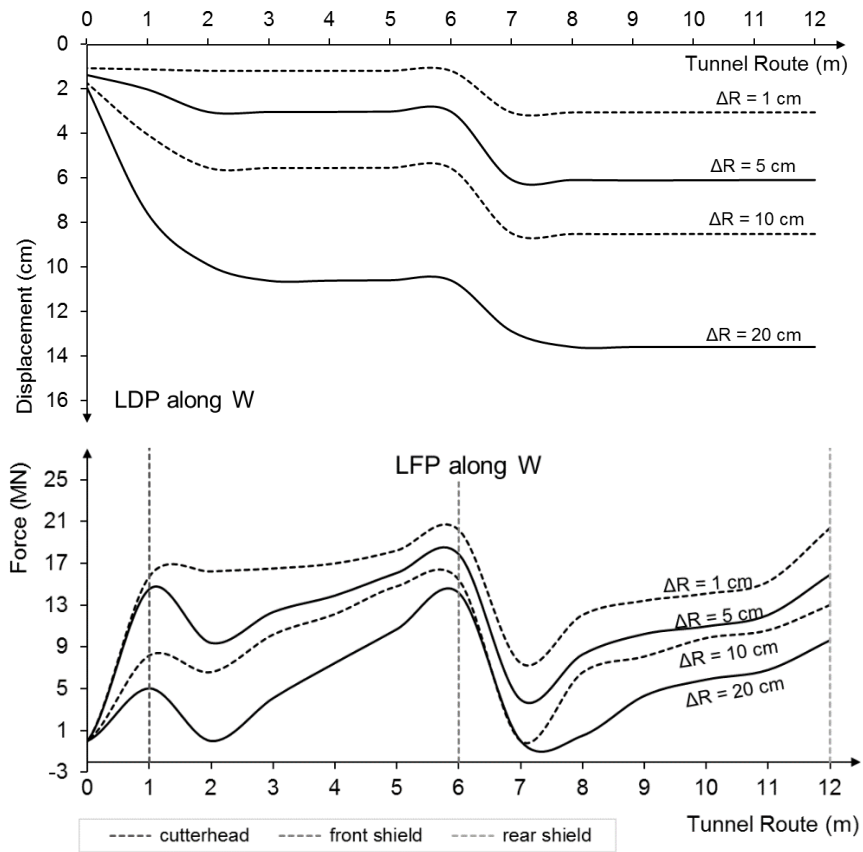


Figure 7.6. Radial displacement of the ground at the tunnel circumference and contact forces for a 1 m cutter-head, 5 m front shield and 6m rear shield at variable ΔR at the crown are equal to 1, 5, 10 or 20 cm

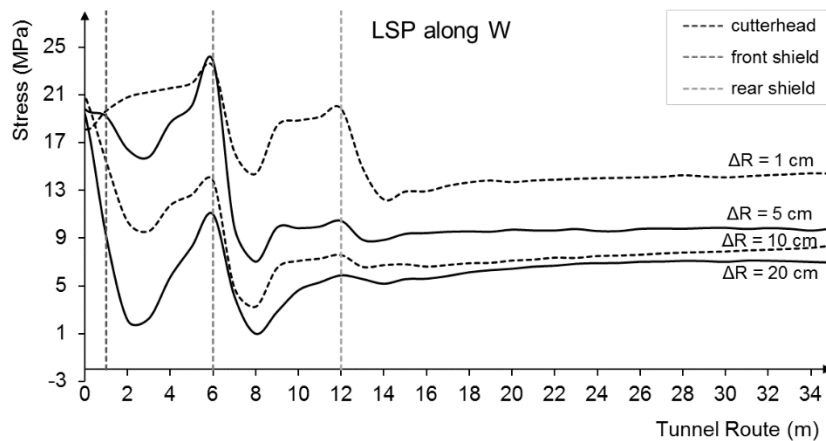


Figure 7.7. Maximum principal stress of the ground around machine components

7.3. Comparison of the Extent of the Plastic Zone

In this study, the extent of plastic zone around tunnel has been investigated for different size of overcut. According to Figure 7.8, the size of plastic zone for different overcut is practically linearly with the size ΔR of the radial gap ($\Delta R = 1, 5, 10$ and 20 cm). The larger

overcut allows for more time to close the gap, leading to a bigger plastic zone in the longitudinal direction (Figure 7.8, $\Delta R = 20$ cm). Therefore, for example, if $\Delta R = 20$ cm the gap remains open for extended shield length L and the plastic zone extends up to the end of the shield.

It has to be noted that providing a larger over boring leads to a lower shield loading and therefore to a lower frictional resistance during shield advance. On the other hand, a larger radial gap allows a larger deformation to occur and, therefore, there is a more extended zone of overstressed ground around the tunnel [44]. In a ground exhibiting brittle behavior, the deformations and the overstressing may enhance loosening and softening of the ground, thus favoring gravity-driven instabilities. This may lead to problems during the backfilling of the segmental lining in the shielded TBMs. The issue of loosening and softening is particularly important for the design of a yielding support, because both strength loss and major loosening call for a higher yield pressure in the support system [56].

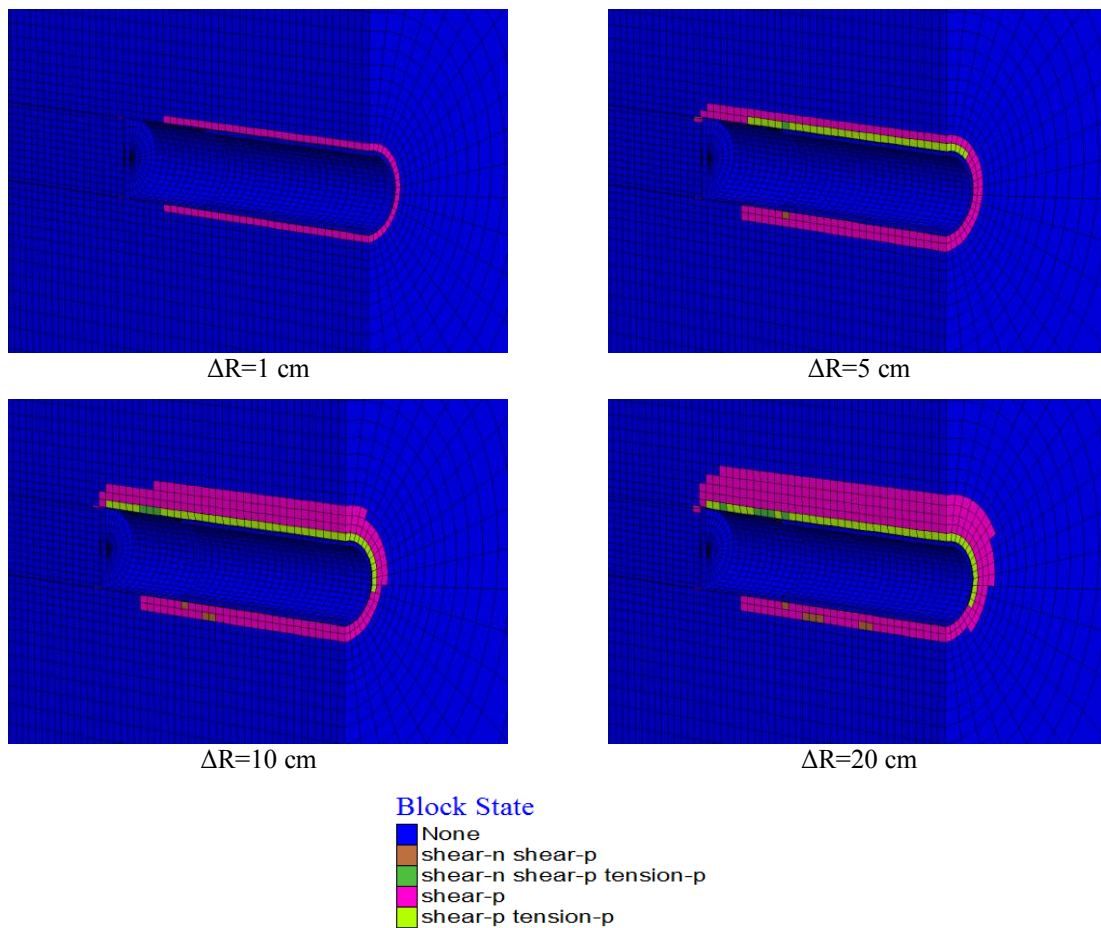


Figure 7.8. Plastic zone for a 1 m cutter-head, 5 m front shield and 6m rear shield at variable ΔR a) 1 cm, b) 5 cm, c) 10 cm d) 20 cm

On the other hand, overcut may be artificially created in the tunneling with shielded TBM in the weak grounds. This phenomenon is due to over excavation resulting in creation of large cavity. Because of loosening of the ground, gravity-driven instabilities can occur and dead load pressure against the shield is anticipated as development of weak loosening material on the shield or on the segmental linings takes place. Some case histories show that this could cause serious failure in the segments or resulted to the entrapment of the shields.

7.4. Thrust Force Calculations

The thrust force required to overcome shield skin friction can be calculated by integrating the contact pressure over the shield surface and multiplying the results by the skin friction coefficient. For this purpose, sectional contact pressure profile between ground and front shield as well as between ground and rear shield are extracted from numerical analysis results as shown in Figure 7.9. According to the Figure, contact pressure over the front shield and rear shield are determined by integrating the contact stresses P_i over the shields individually.

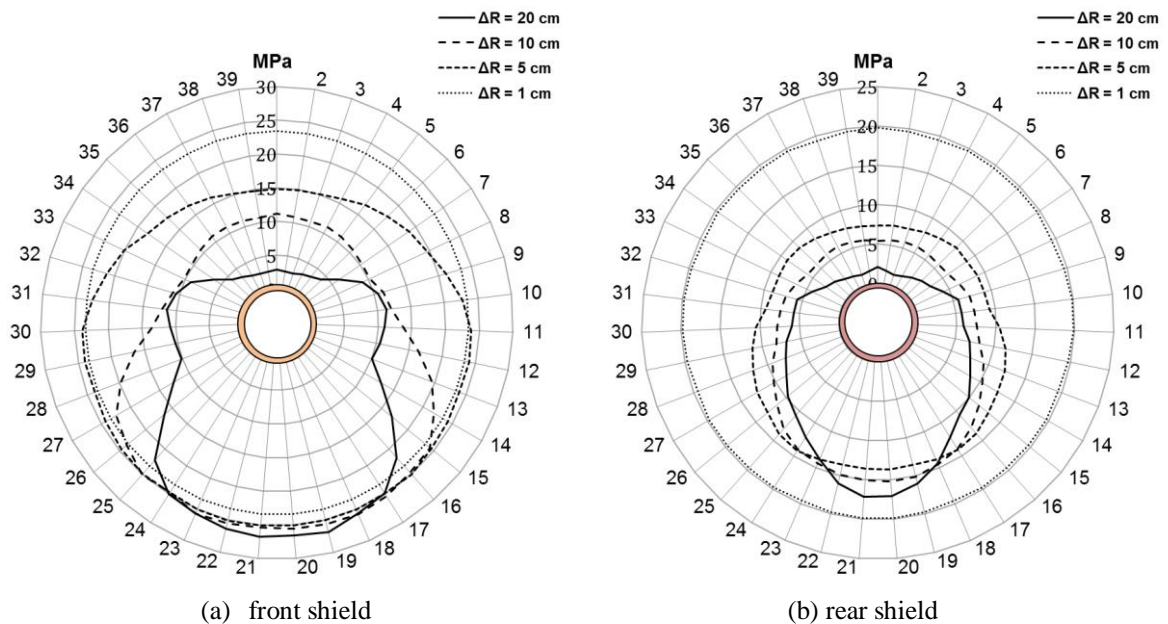


Figure 7.9. Sectional contact pressure profile between ground and a) front shield b) rear shield

There are two operational stages for calculation of required thrust force due to interaction between shield and ground that includes ‘ongoing excavation’ and ‘restart after a standstill’ where the skin friction coefficient for ongoing excavation stage (sliding friction) is smaller than for restart after a standstill stage (static friction). During the excavation TBM has to

overcome sliding instead of static friction. The required thrust force for overcoming to skin friction depends on the shield length and the overcut on one hand, and the ground convergence and time on the other. The skin friction coefficient was taken to be $\mu=0.15-0.30$ for sliding friction and $\mu=0.25-0.45$ for static friction, where the lower friction coefficient values aim to illustrate the positive effects of lubrication of the shield extrados, e.g., by bentonit or other lubricants [1].

Figure 7.10 shows the required thrust force F_r to overcome frictional forces on machine main components as a function of the overcut for the two operational stages and an overcut between 1 and 20 cm. The diagram illustrates the positive effect of a larger overcut.

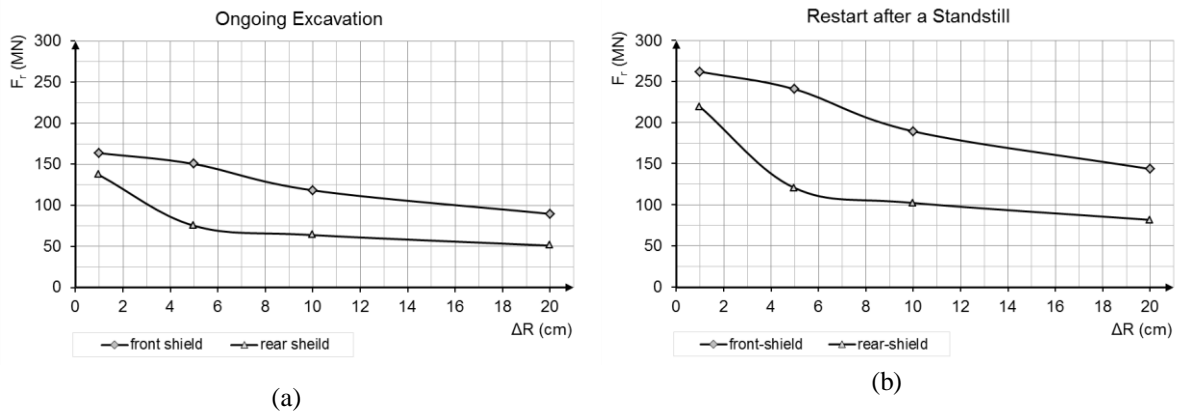


Figure 7.10. Required thrust force for the two operational stages a) Ongoing excavation, $\mu=0.25$ b) Restart after standstill, $\mu=0.40$

7.5. Interaction between Ground and Segmental Lining

In DS-TBM tunneling, installation of segmental linings is implemented inside the rear shield and the segmental ring is subjected to ground loading that start from a certain distance behind the machine. Simultaneously, the injection of backfill into the annular space between rock mass and lining is applied. Ground pressure is transferred to the segmental lining from backfill. Figure 7.11 shows the redistribution of ground pressure around segmental lining versus different size of overcuts after backfilling. Comparing to contact pressure upon shields in Figure 7.9, this Figure proves that the important role of backfill that cause to uniform distribution of stresses at boundary of lining.

Figure 7.12 depicts the diagram that is used for prediction of average ground pressure on the segmental rings at the variable over boring amounts. According to this diagram, ground pressure around the lining is mainly dependent upon overcut sizes. By developing such diagrams for a specified tunnel and ground conditions, one can calculate the magnitude of

ground pressure on the lining for variable overcuts and implement for design of TBM as well segmental rings.

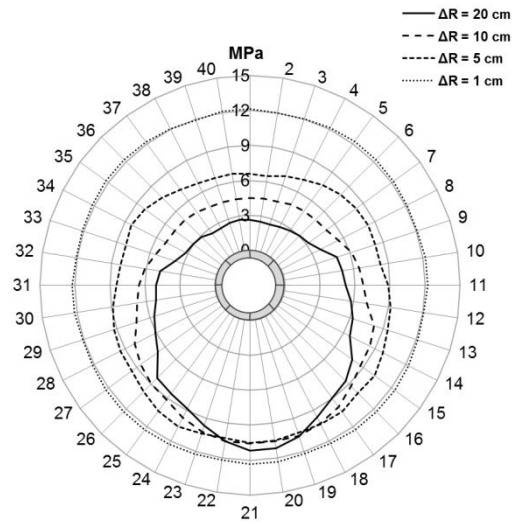


Figure 7.11. Ground pressure around segmental lining

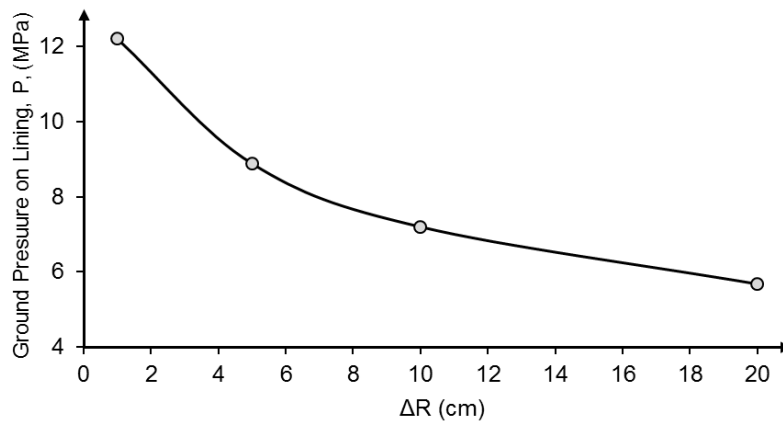


Figure 7.12. Ground pressure – overcut diagram

8. APPLYING IMPROVEMENT METHODS FOR PREVENTING TBM ENTRAPMENTS

8.1. Introduction

The main concern in using a shielded tunnel boring machine in deep rock tunnels with high stress is the possibility of the machine seizure in squeezing ground. For coping with squeezing condition, there are some ground improvement methods that can be implemented to shielded TBM design in order to further increase their capability to cope with squeezing ground conditions.

To face particular adverse tunneling conditions especially tunneling through squeezing grounds, new DS-TBM design has been developed in recent years. The new generation of DS-TBMs is equipped with additional measures to treat the ground in front of the machine (through the shields and through the cutter-head). This configuration can prove to be very important and useful when the tunnel crosses through a disturbed rock formation under high overburden. The high power and torque up to 4900 kW and 18700 kNm, the high main and auxiliary thrust respectively 82500 kN and 152500 kN, the 30 cm standard clearance between the excavation and the segmental lining outer diameter, the possibility of additional over-cut of 20 cm on diameter, the possibility to displace the cutter-head in vertical and horizontal directions with respect to the shield, and possibility of drilling probe/pipe ahead of the machine in the upper 180° or full 360° around the tunnel at the gripper shield, drilling at a 7° angle to the tunnel wall are the most recent development characteristics and design features of new DS-TBMs [57].

In this Chapter, to realistically evaluate the possibility of machine seizure in squeezing grounds and the impact of ground improvement to prevent such possibility or reduce the risks, 3D finite difference simulation of a double shield TBM in squeezing ground was performed. The results of the modeling include evaluation of ground improvement methods and lubrication mechanism by comparing the numerical results between the DS-TBM tunneling with and without applying such treatment methods. Furthermore the combined results allow for estimation of the required thrust force when different lubricant was used between rock and shield to propel the machine forward in case of encountering squeezing grounds. The results show the ground improvement methods can be very useful for preventing of shield jamming when shield is subjected to high stress from rock mass.

8.2. Ground Improvement Methods

Some ground improvement methods that are applied during tunnel excavation as well numerical analysis of these methods are reviewed in this section. The simulation results include evaluation of applying probe drilling and rock bolts in deep tunnels. The results are compared with outcomes from a DS-TBM tunneling without ground modification or improvement and shown for sidewall of tunnel.

8.2.1. Grouting from Probe Drilling Holes

Grouting involves the process of injecting a material into the ground with the following two principal objectives:

- to reduce the permeability of the ground;
- to strengthen and stabilize the ground. In soft ground this leads to an increase in its ‘strength’ and in jointed rock in its ‘stiffness’.

Grouting operations can be carried out either from the ground surface (or from within an adjacent shaft to the tunnel operation) or from within the tunnel during the construction. They can also be applied to locally stabilize the foundations of structures likely to be affected by the tunneling works in the form of settlements. For tunnel grouting, the grouting holes are drilled ahead of the advancing tunnel in a pattern of diverging holes at an acute angle of about 5-7 degrees to the tunnel axis to form overlapping cones of treated ground [58]. This creates an umbrella or shell around the tunnel to strengthen the ground and improve its characteristics relative to the objectives of the grouting, bit control of ground water or reinforcement of the ground, or both.

For tunneling with TBMs the holes can be drilled forward from the gripper or rear shield of the machine, to avoid affecting the cutter wheel, but direct grouting of the face through the cutter wheel is also possible. In addition, grouting is regularly conducted radially through the lining to fill any voids and to lock the segmental lining with respect to the ground as well as cementation of the pea gravel injected behind the lining. In some cases, a secondary grouting is also used to go beyond the annular space and control the water ingress into the tunnel. In particular in the case of TBMs with a diameter of up to 4-5 meters, there is limited space in the machine area to install probe drilling equipment and it is necessary to have specially adapted drilling equipment. In the case of larger machines, the space in the machine area is not as tight and thus conditions are better and adaptation of

the equipment into the work environment is simpler [59]. Figure 8.1 shows some examples of grouting during tunnel construction.

The possibility of varying the hole locations is different machine configuration depends on the type and diameter of the machine. Normally, it will be easiest to adapt the drilling equipment in an open machine. In shielded machines, the space is smaller and it may be necessary to draw the collaring of the grouting holes slightly further back in the machine area. The retrofitting of equipment results in complex and inexpedient solutions, thus it is crucial to identify the need for probe drilling and integrate that into the design of the machine at the early stage of defining machine configuration.

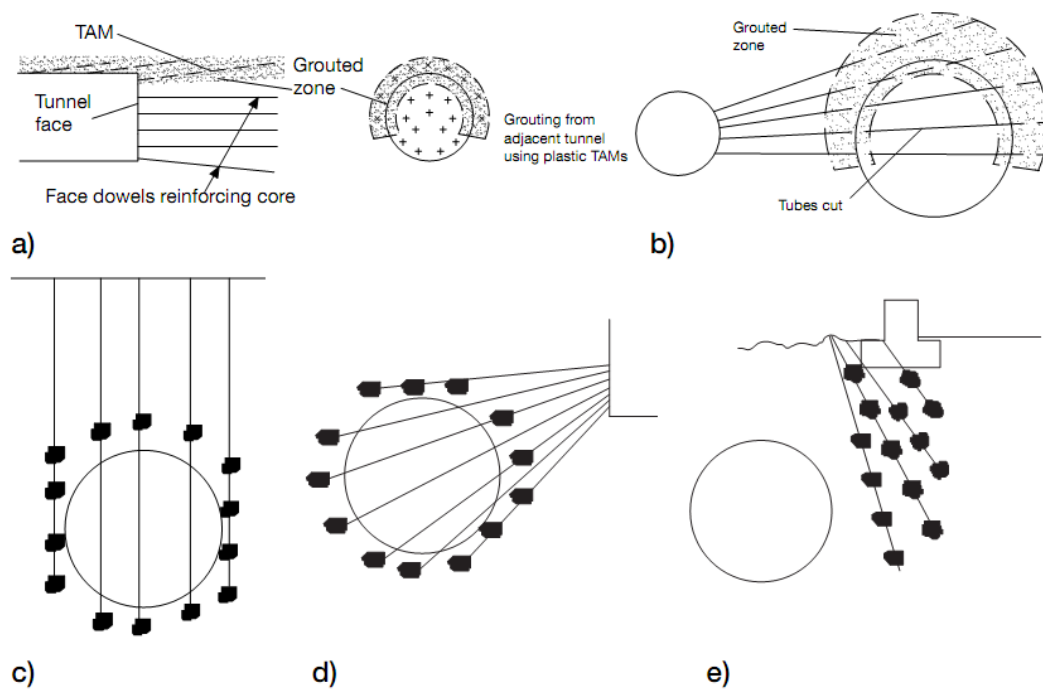


Figure 8.1. Examples of grouting tunnels during construction, a) from within a tunnel, b) using an adjacent tunnel [60], c) from the ground surface, d) from an adjacent shaft, or e) as protection to adjacent structures [61]

Long TBM tunnels sometimes pass through the complex geological conditions particularly in case of deep tunnel. Geological predictions in deep tunnel are hard to make on the basis of surface observations. If the site conditions require, probe holes may be drilled on the sides (or rarely at the face) of the tunnel for certain length to investigate the ground conditions ahead of the machine. In addition, it may often be necessary to drill probe holes for ground improvements.

The drilling of the injection holes for the consolidation of the ground (probe drilling) immediately in front of the cutter head can no longer be done through the stator of the TBM with machines of large diameter. The only possibility is to drill the holes for the injection lances in a close pattern out of the cutter head itself. This requires small drills and drilling equipment, which also functions as injection lances. These represent no hindrance for boring with the TBM after the injection measures are complete, or catch up in the cutter head, which would tear out the rock again with the rotation. Very suitable tools for this purpose are extension tubes made of glass fiber reinforced plastic with a throwaway drilling head (Figure 8.2). These extension tubes can be excavated by the cutter discs if there were to be installed in the face for face stabilization [33].

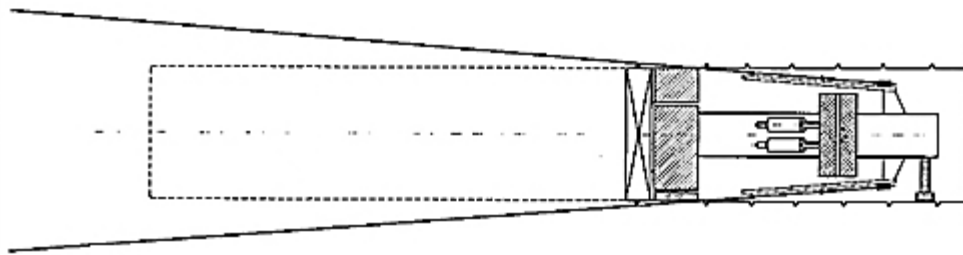


Figure 8.2. Positioning the drilling equipment for ground investigation or for drilling injection holes with a TBM [33]

Injections through the cutter head are best carried out with relatively rapidly hardening artificial resins e.g. PU and Acrylic resins. The cutter head does not stick in this type of material and the injected substances do not run down to the invert of the excavation area of the TBM. In some cases large fault zones may be difficult to drive through, and here one solution is to pre-grout these zones so as to increase stability. In such conditions, it may be necessary to use different grouts, depending on the local conditions [58].

Probe Drilling Method: Numerical Simulation

For numerical analysis of ground improvement by probe drill holes, it is assumed that application of ground treatment, i.e. grouting, can lead to increase in cohesion of ground to a certain radial distance around the tunnel. For this purpose, application of 20 m holes with 10 m overlap was integrated into simulated model around tunnel. Furthermore, cohesion of rock mass was increased to 4 MPa for zones around probe drills with respect to length of holes (In the reference model, cohesion of ground is equal to 2 MPa). The results of analysis were compared with outcomes from reference model (model without ground improvement method) to investigate how application of ground improvement through

probe drilling affects ground behavior around tunnel. Probe drills and grouting by holes during excavation of tunnel by a double shield TBM is illustrated in Figure 8.3.

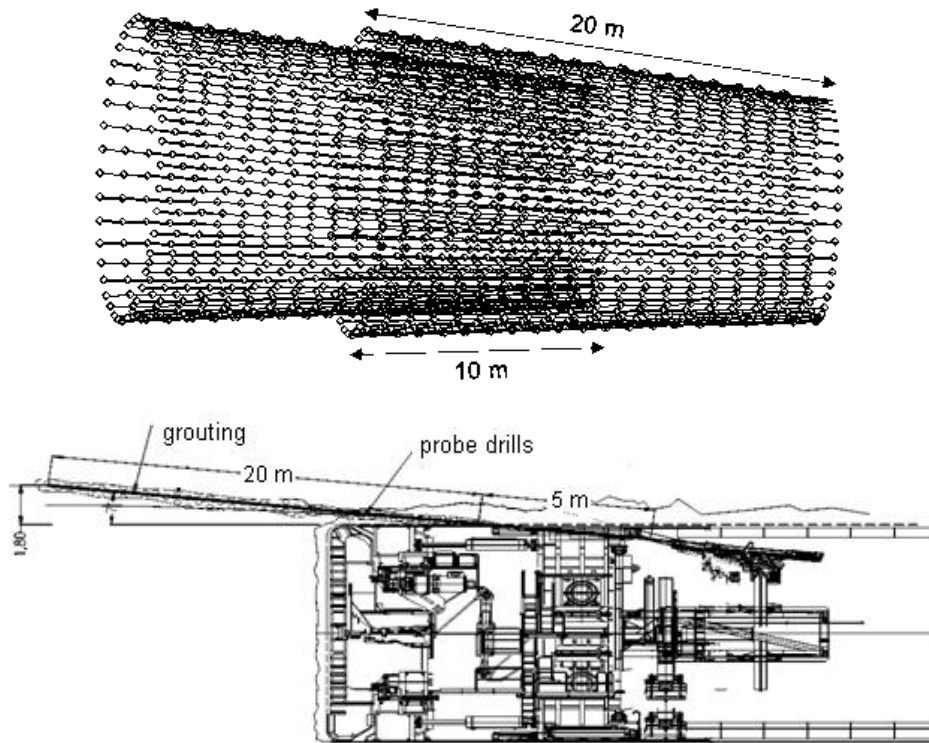
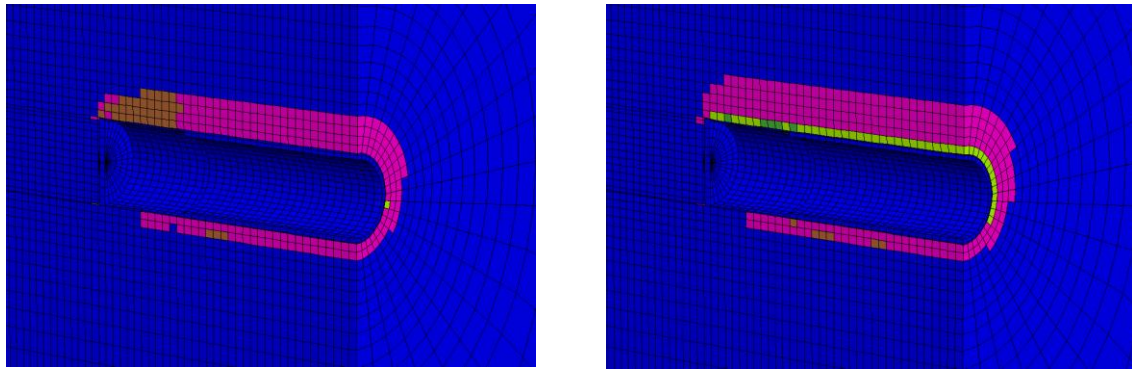


Figure 8.3. Configuration of applied probe drilling method in numerical analysis

In order to evaluation efficiency of probe drilling method in numerical investigations, the plastic zone around tunnel has been examined for two different conditions of tunnel excavation. As can be seen in the Figure 8.4, whereas the size of plastic zone is smaller for improved ground, a shear zone is created in the past (brown zone) on shields, which with advancing of tunnel, creates new shear zones (pink zones) but their impact and loading on the shield are negligible.

Figure 8.5 shows the longitudinal displacement of the ground at sidewall of tunnel for models with and without applying probe drilling method. In the case of model with applying ground improvement, there is no contact between ground and shields at sidewall of tunnel. This means that contact forces along tunnel at sidewall of tunnel are zero. However closure of gap occurs between ground and front shield as well as between ground and rear shield when tunnel is bored without any ground improvement. After closing the gaps, the ground starts to load the shields at the spring-lines (sidewalls) shortly after the excavation in the model without applying grouting.



model with applied probe drilling (improved model)

reference model

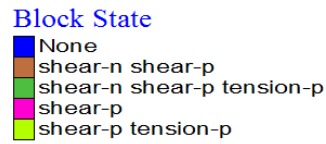


Figure 8.4. Plastic zones created around tunnel for two different simulated models

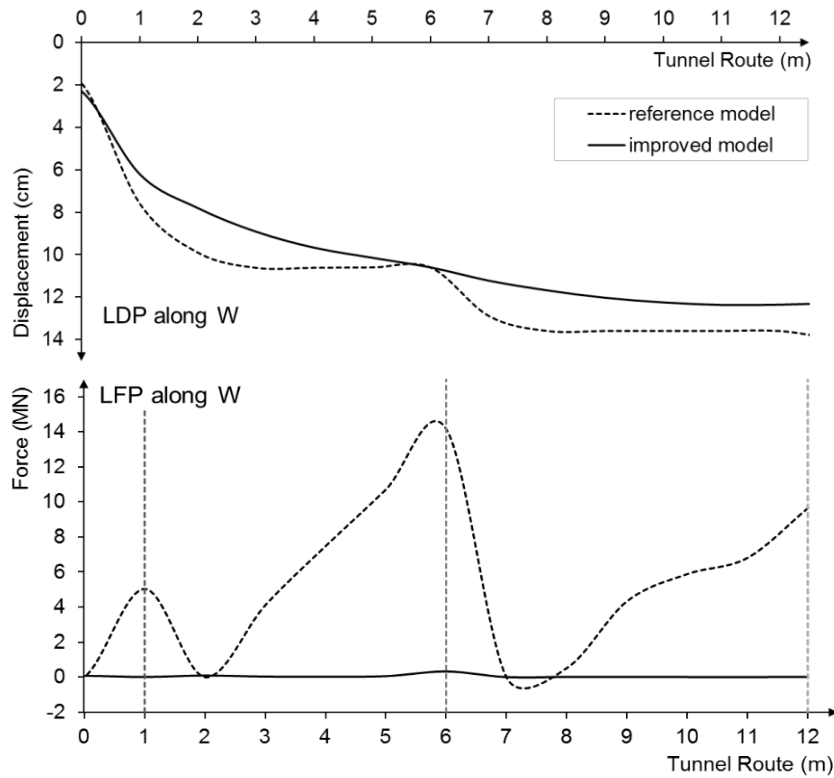


Figure 8.5. Radial displacement of the ground at the tunnel spring-wall and contact forces for two numerical models

Sectional contact pressure profile between ground and front shield as well as between ground and rear shield are extracted from numerical analysis results as shown in Figure 8.6. This Figure shows that the required thrust force to overcome frictional forces on machine main components for improved ground is smaller than reference model. The maximum required thrust force that is calculated on the front shield is 107.7 MN for model

with ground improvement whereas this value was 134.1 MN for reference model. The maximum total thrust force by the auxiliary thrust cylinders for improved ground is estimated to be 124.7 rather than 151.1 MN for reference model. This means that for a DS-TBM, if maximum installed auxiliary thrust force was 140 MN, machine will seize if ground improvement is not used.

Figure 8.7 shows the redistribution of ground pressure around segmental lining for both reference and grouted rock mass. It clearly indicates that grouting of probe drilled holes results in a uniform distribution of ground pressures at the boundary of segmental lining. Moreover, pressures around lining in the model treated ground will be smaller than reference model.

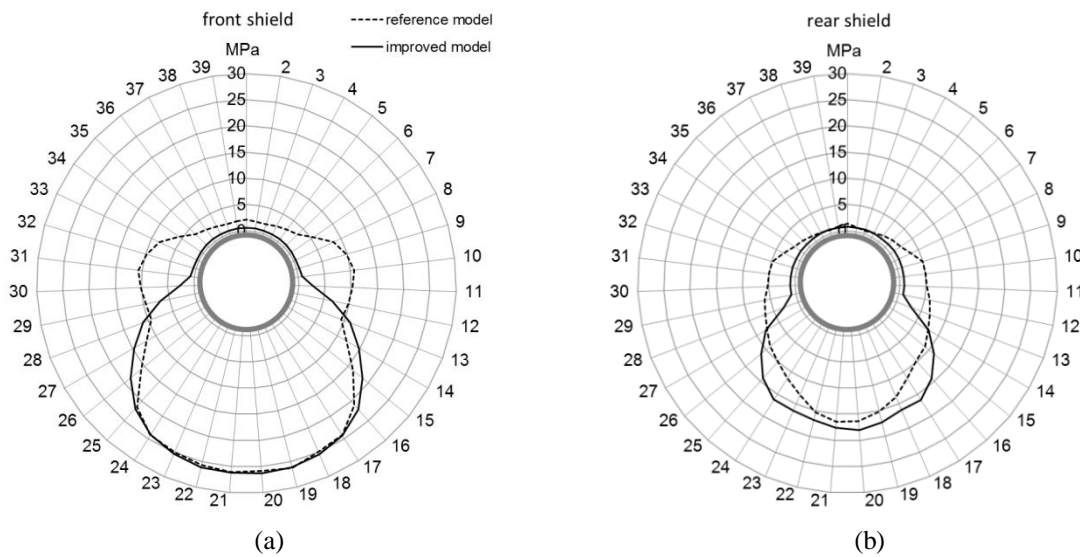
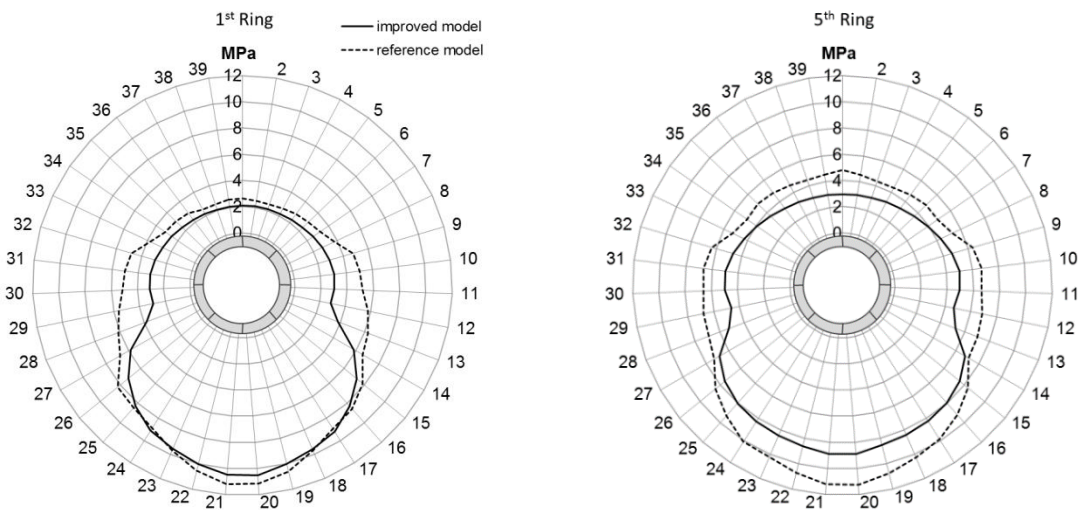


Figure 8.6. Sectional contact pressure profile between ground and a) front shield b) rear shield



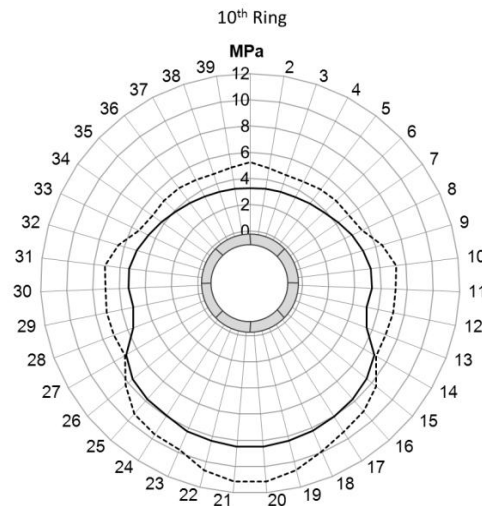


Figure 8.7. Ground pressure around segmental lining at different positions

8.2.2. Ground Reinforcement

There are three distinct types of ground reinforcement methods: rock dowels, rock bolts and rock anchors. Rock dowels are reinforcing elements with no installed tension. Rock bolts are reinforcing elements which are tensioned during installation. Anchors are reinforcing elements which are tensioned following installation and are of higher capacity and generally of greater length than rock bolts [60].

There are four generally accepted mechanisms by which rock reinforcement can improve the stability of the ground [62].

1. By stabilizing individual blocks of material that may detach due to gravity in relatively competent and well-jointed rocks, by using rock bolts with an anchorage force capacity greater than the weight of the block
2. By using tensioned or untensioned bolts to maintain the shear strength of the ground along discontinuities in weaker fractured ground conditions
3. By using fully grouted untensioned rock bolts in laminated or stratified rocks to preserve the inter-strata shear strength
4. By using tensioned rock bolts installed relatively quickly after excavation to improve the degree of confinement or the minor principal stress (this is normally perpendicular to the tunnel wall) in overstressed rocks.

Rock reinforcement alone is unlikely to be appropriate if [60]:

- the support pressure required is greater than 600 kN/m^2 ;

- the spacing of dominant discontinuities is greater than 600 mm;
- the rock strength is inadequate for anchorages;
- the RQD is low or there are unfilled joints or high water flow.

Applying Rock Bolt: Numerical Simulation

Although rock bolts may be applied for improvement of ground, however the application of rock bolts in squeezing ground and in weak rocks for long deep tunnels with high in situ stress may not be effective. Before deciding on the use of reinforcement methods, rock mass properties and applicability of reinforcement in such grounds should be carefully evaluated by using lab or in situ tests.

Evaluation impact of applying rock bolts for preventing of shield jamming and reduction of the ground pressure exerted on the segmental lining have been investigated by means of numerical studies. For this purpose, application of 10 m long rock bolts is simulated (Figure 8.8). It should be noted that the rock bolt length is selected by considering plastic zone radius and for the bolts to be effective, a length 2 times the plastic zone is selected to allow for sufficient anchorage in undisturbed ground. Bolts spacing were selected to be 1 and 2.5 m in the longitudinal and cross sectional directions respectively and bolt pattern was staggered.

The main idea for application of rock bolts is to help the surrounding rock mass to support itself. According to Figure 8.9, use of rock bolts for supporting of rock mass around shields are not effective. However, impact of rock bolts for decreasing the ground pressure around segmental linings is evident. It is assumed that the rock bolts can be installed from inside of rear shield by creating holes in the shield skin.

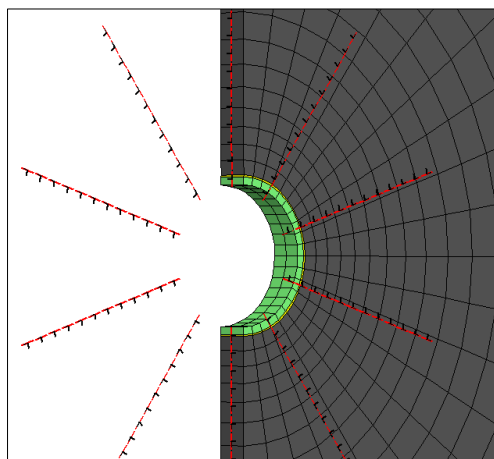


Figure 8.8. Application of 10 m long rock bolts to the simulated model

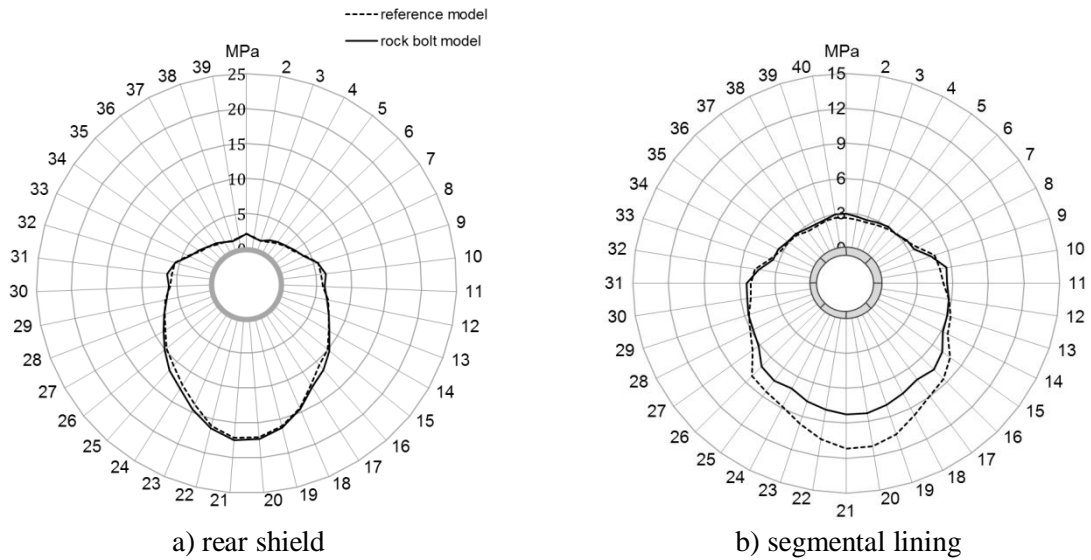


Figure 8.9. Sectional a) contact pressure on rear shield and b) ground pressure around segmental lining

8.2.3. Forepoling

This technique is aimed at limiting the decompression in the crown immediately ahead of the face [63]. Longitudinal bars (dowels) or steel plates (forepoling plates) are installed ahead of the tunnel from the periphery of the face, typically over the upper third or quarter of the excavated profile. In rock, the plates or dowels driven ahead of the excavation are also known as spiles (Figure 8.10).

Face dowels can be used to improve the stability of an excavated tunnel face. The technique involves installing an array of dowels over the cross section of the tunnel face. This method is especially useful for shallow tunneling. This method is good for controlling the loose ground ahead of the shallow excavations for SEM or NATM and is not for squeezing ground.

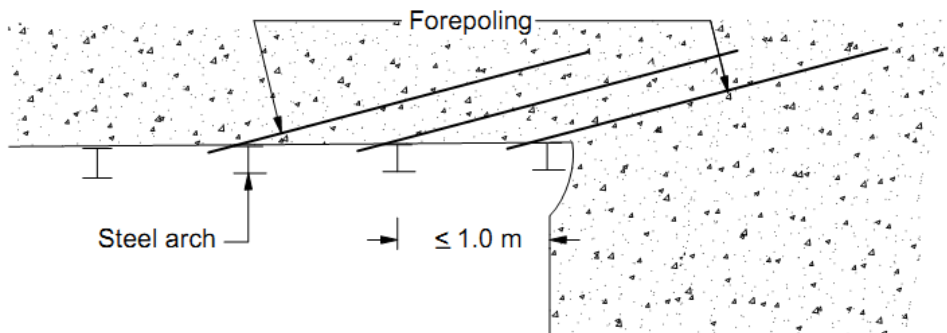


Figure 8.10. Basic arrangement of fore-poling using dowels [63]

8.2.4. Lowering of the Groundwater Table

If groundwater lowering can be achieved successfully, a marked improvement is possible in the ground properties. There are two principle methods of groundwater lowering: well points and deep filter wells. Further details on the design of groundwater lowering can be found in Woodward [60]. The lowering of the groundwater pressure in the surrounding medium can reduce the pore pressure and thus effectively increase the effective stresses in the ground and in some cases; it can increase the shear strength of the rock. This ground improvement method is not used in the modeling for this study.

8.3. Application of Lubricants Such as Bentonit

The high advance speeds attainable by a double shield TBM is favorable in squeezing ground. This advantage only exists if the machine is constantly moving forward and not standing. The double shield TBM is, due to the machine concept with its long shield, in danger of jamming if it encounters squeezing rock. Lubrication systems on the shields can reduce the skin friction of the shield by providing a low friction medium during the stroke as well as injection of the lubricants through the shield as it moves forward.

In this section, for assessment of the impact of lubrication on interaction between shield and ground, two stages of excavations including ongoing excavation and restart after a standstill are considered in the calculations. Skin friction coefficient for ongoing excavation stage is smaller than for restart after a standstill stage. During the excavation, TBM has to overcome sliding instead of static friction. In high contact pressures when shield is jamming, applying a pressurized lubricant such as bentonit, when shield is subjected to ground convergence pressure can reduce the friction and allow the shield to move forward. It is noted that skin friction coefficient during ongoing excavation so called sliding friction was taken to be $\mu=0.15-0.30$. Also skin friction coefficient during restart after a standstill named static friction is assumed to be $\mu=0.25-0.45$ where the lower friction coefficient values aim to illustrate the positive effects of lubrication of the shield extrados by bentonit or other lubricants.

Numerical analysis has been performed for determination of required thrust force F_r , as a function of skin friction coefficient during ongoing excavation as well as for restarting TBM after a standstill. The result of analysis is illustrated in Figure 8.11.

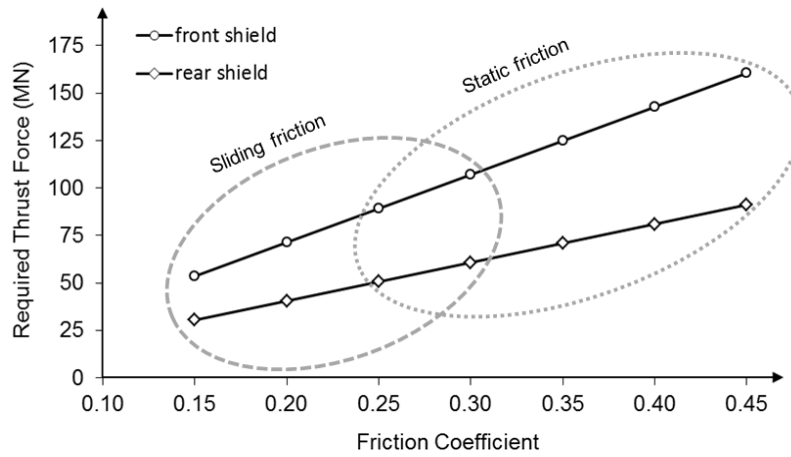


Figure 8.11. Required thrust force versus friction coefficient for two stages of excavation

Relating to rock mass properties, in-situ stresses and machine components, a combination of ground improvement methods with applying appropriate lubricant can be useful for preventing of TBM entrapment.

9. CONCLUSIONS AND RECOMMENDATIONS

This thesis is an attempt to develop a comprehensive numerical simulation for evaluation of applicability of Double Shield Tunnel Boring Machines (DS-TBM) in squeezing grounds. The systematic evaluation of potential of excessive ground convergence and of encountering ground squeezing has been performed relative to the application of DS-TBMs in such grounds to assess the possibility of machine entrapment. The 3D numerical modeling was subsequently used for evaluation of the possibility of using ground improvement or lubrications to avoid shield jamming in such cases.

The main emphasis of this research is on numerical analysis to allow for modeling the detailed configuration of the machine and its interaction with the intruding ground in a true 3D simulation. The simulation results have been examined at five reference points on the tunnel circumference along the tunnel or longitudinal displacement profile (LDP) as well as contact force profiles (LFP) on both front and rear shields. Also, maximum thrust force required to overcome friction and drive TBM forward is calculated.

It is concluded that:

1. A simple numerical model based on Hoek and Brown failure criterion has been developed. The model simulates intrinsic excavation of tunnel in squeezing ground conditions. Furthermore a comparison of numerical modeling results with Hoek and Marinos semi empirical approach has been carried out for verification purposes. It has been found that numerical modeling and Hoek and Marinos approach results were in good agreement for evaluation of the ground behavior in simple tunneling scenarios. Therefore the result of the numerical simulation was deemed reliable for use in modeling ground behavior in squeezing ground conditions.
2. A comprehensive 3D modeling of excavation of tunnel by considering the DS-TBM main components was developed to allow for assessment of the ground shield interaction at various points along the shield. The numerical analysis was based on the finite difference method and FLAC^{3D} commercial software was used to simulate the ground movements, tunnel convergence, the contact forces and ground pressures between the tunnel walls and the shields and between ground and segmental lining. To accurately model the ground behavior in this application, a full 3D model was created to account for the correct geometry of tunnel excavation

relative to shield dimensions together with incorporating all stages of tunneling process. Moreover, the developed 3D model is capable of applying proper material and geometric characteristics to represent the shield, annular space, soft and hard backfill behind the segments, and segmental lining. Machine advance rate was also implemented by allowing controlled relaxation of ground pressure and step by step movement of the main components of machine. The models created for the thesis can encounter various rock and ground conditions together with different in situ loading situations. Another feature of the modeling is that the software used in 3D simulation allows for large strain, however sometimes unforeseen errors such as penetration of rock mass into shield elements can occur within numerical calculations. To avoid this problem related to large displacements in squeezing grounds, displacement control has been applied at contact surfaces. For this purpose, a FISH code was developed in FLAC^{3D} that controls all displacements with respect to non-uniform overcut at each solving step of numerical analysis.

3. Increasing of gap due to conical shape of the shields is considered in the simulations. This property of model distinguishes the model from other 3D models that have been developed for numerical simulation of shield TBMs in the past. Another advantages of model developed for this study is the use of Mohr-Coulomb and Hoek-Brown failure criterion as constitutive models defining the material properties depending on the field measurements and ground conditions. In order to perform numerical analysis of tunnel excavation in the rock mass, a series of FLAC^{3D} models have been developed which uses the Mohr-Coulomb failure criterion. However, to use Hoek–Brown failure criterion in the model, a FISH code was written in FLAC^{3D} to implement Hoek–Brown parameters as input data and map the anticipated rock behavior into Mohr-Coulomb parameters.
4. Based on the results of numerical modeling, longitudinal displacement and contact force profiles were calculated for both transient conditions and for the final equilibrium of the ground in the model. The results indicated that for the given machine and rock conditions, the initial contact between the shield and rock occurs towards the end of the front shield at relatively low levels of contact pressures and forces. The continued ground convergence will increase the area of contact between the rock and the rear shield, subsequently leading to higher contact forces. In

addition, the modeling allows for extracting the history of the axial stresses, shear stresses and principal stress paths along the tunnel boundary.

5. There has been an ongoing discussion on the effect of time in relation to machine jamming in the squeezing grounds. The impact of tunneling advance rate on the possibility of machine jamming has been studied. For this purpose, two time dependent creep constitutive models including a Burger-creep viscoplastic model and a Power-law viscoplastic model were applied to the numerical models for describing the tunnel time dependent response associated with severely squeezing conditions. Longitudinal displacement and contact stress profiles together with sectional principal stresses were calculated for different advance rates. The maximum required thrust force on machine elements and the average stress on the lining rings at different advance rates are presented as load diagrams. The results show that the effect of advance rate on relaxation of loading on shields is more considerable in the rear shield in comparison to front shield. Also the average stress on the lining ring is heavily impacted by the advance rate. The loading diagrams can be utilized to determine the magnitude of loads on the lining at specified advance rates. Moreover, the results can also be used to evaluate the potential for entrapment of shielded TBMs in the squeezing ground during extended machine downtimes or for lower advance rates.
6. Numerical analysis was also performed to evaluate the impact of over boring (overcut) on TBM jamming. Effect of conicity or stepwise construction of the shields on decreasing of ground pressures acting upon shields for different values of overcut was investigated. A larger over boring decreases shield loading and therefore would lead to a lower frictional resistance during shield advance. Consequently the required thrust force to overcome frictional forces was determined for various overcuts and for two operational stages (ongoing excavation stage and standstill stage).
7. The impact of ground improvement methods including probe drilling and ground improvement by using grouting techniques were simulated to see if such measures could reduce the magnitude of the ground convergence. Hence entrapment risks of TBM in potentially squeezing grounds could be reduced and machine jamming be prevented. The results proved that applying ground improvements in squeezing ground, where there is shield jamming risks, will significantly be effective in

reducing the convergence, shield loading, and hence the required thrust for propelling the machine forward. The use of rock bolts for this purpose is not going to be effective since the reinforcement mechanisms of the rock bolts are appropriate for squeezing ground where large plastic deformation is anticipated. However, impact of rock bolts for decreasing the ground pressure around segmental linings on a temporary basis is evident.

8. The use of lubricants to decrease the required thrust force as a function of skin friction coefficient during ongoing excavation and restarting machine after a standstill were examined in the simulation by using reduced shield-ground friction factors. The results show that the lubrication is very effective in preventing and overcoming shield jamming. Therefore it is recommended that a special emphasis should be given to incorporate a more efficient lubrication system on TBM shields.

The results are realistic and plausible and show the potential for use of this approach to assess the risk of machine entrapment in weak rocks for deep tunnels.

Recommendations for the future studies are numerical evaluation of overcut and over excavation that have great influence on stability of tunnels mined by TBM. Furthermore, incorporation of over excavation could not be represented in the present model. It is highly recommended that this phenomenon should be included to numerical modeling by integration of PFC3D code with FLAC3D.

Shield length and shield thickness are two significant machine parameters that play an important role in the analysis for investigation applicability of double shield TBM in potentially squeezing ground. Numerical analysis for evaluation impact of shield length and shield thickness can be carried out to study TBM entrapment in squeezing rocks.

Other ground improvement methods may be applied around a tunnel excavation with a DS-TBM. Numerical simulations of such methods can be essential for selecting an effective method for preventing shield and machine jamming in different ground conditions.

Lubrication mechanism can be studied by numerical analysis when there is a contact between shield and ground. Mechanism of applying lubricant such as bentonit in order to reduce frictional forces between shield and ground can be analyzed as interaction between two solid materials with a fluid.

REFERENCES

- [1] Ramoni, M., Anagnostou, G., Tunnel boring machines under squeezing conditions, *Tunnelling and Underground Space Technology*, 25(2), 139-157, **2010**.
- [2] Kovari, K., Tunnelling in squeezing rock, *Tunnel*, 5(98), 12–31, **1998**.
- [3] Billig, B., Ebsen, B., Gipperich, C., Schaab, A., Wulff, M., Grouting to cope with rock deformations in TBM tunneling and underground space, *ITA World Tunnel Congress, Taylor & Francis Group London*, 2, 1487-1492, Prague, **2007**.
- [4] Schneider, E., Spiegl, M., Convergency compatible support systems, *Tunnels & Tunnelling International*, 40(6), 40-43, **2008**.
- [5] Hisatake, M., Iai, Y., A method to determine necessary thrust force for TBM, *Developments in geotechnical engineering, Options for tunneling*, 74, 519-528, **1993**.
- [6] Moulton, B., Cass, T., Nowak, D., Tunnel boring machine concept for converging ground, *Rapid excavation and tunnelling conference, SME Inc. Littleton*, San Francisco, 509-523, **1995**.
- [7] Feknous, N., Ambrosii, G., Henneberg, I., Simard, R., Design and performance of tunnel support in squeezing rock at Yacambu, *Rock Mechanics: tools and techniques, 2nd North American Rock Mechanics Symposium*, Montreal, A.A.Balkema, Rotterdam, 1, 803–810, **1996**.
- [8] Vigl, L., Jager, M., Double shield TBM and open TBM in squeezing rock - a comparison, *Tunnels for people, ITA World Tunnel Congress 97*, Vienna, A.A.Balkema Rotterdam Brookfield, 2, 639-643, **1997**.
- [9] Garber, R., Design of deep galleries in low permeable saturated porous media, *The report No 2721*, EPFL Lausanne, **2003**.
- [10] Schubert, W., TBM excavation of tunnels in squeezing rock, *Lo scavo meccanizzato delle gallerie, mir2000-VIII ciclo di conferenze di meccanica e ingegneria delle rocce*, Torino, Pàtron Editore Bologna, 355–364, **2000**.
- [11] Sulem, J., Panet, M., Guenot, A., Closure analysis in deep tunnels, *International Journal of Rock Mechanics and Mining Science*, 24(3), 145-154, **1987**.
- [12] Farrokh, E., Mortazavi, A., Shamsi, G., Evaluation of ground convergence and squeezing potential in the TBM driven Ghomroud Tunnel Project, *Tunnelling and Underground Space Technology*, 21(5), 504-510, **2006**.
- [13] Jafari, A., Mollaei, M., Shamsi, H., Investigation into ground convergence effect on TBM performance in squeezing ground, *The second half century of rock mechanics, 11th Congress of the International Society for Rock Mechanics (ISRM)*, Lisbon, Taylor & Francis Group, London, 2, 939-942, **2007**.

- [14] Khademi Hamidi, J., Bejari, H., Shahriar, K., Rezai, B., Assessment of ground squeezing and ground pressure imposed on TBM shield, *12th International conference of the International Association for Computer Methods and Advances in Geomechanics (IACMAG)*, 3907-3914, **2008**.
- [15] Kawatani, T., Tezuka, H., Morita, R., Shimaya, S., Tunnel construction with a large-scale TBM in a collapse-prone poor rock, *Challenges for the 21st century, ITA World tunnel congress 99*, Oslo, A.A. Balkema, Rotterdam, 2, 895-901, **1999**.
- [16] Farrokh, E., Rostami, J., Correlation of tunnel convergence with TBM operational parameters and chip size in the Ghomroud Tunnel, Iran, *Tunnelling and Underground Space Technology*, 23(6), 700-710, **2008**.
- [17] Farrokh, E., Rostami, J., Effect of adverse geological condition on TBM operation in Ghomroud Tunnel Conveyance Project, *Tunnelling and Underground Space Technology*, 24(4), 436-446, **2009**.
- [18] Cantieni, L., Anagnostou, G., The effect of the stress path on squeezing behaviour in tunneling, *Rock Mechanics and Rock Engineering*, 42(2), 289-318, **2009**.
- [19] Lombardi, G., Panciera, A., Problems with TBM & linings in squeezing ground, *Tunnels & Tunnelling International*, 29(6), 54-56, **1997**.
- [20] Graziani, A., Capata, A., Romualdi, P., Analysis of rock-TBM-lining interaction in squeezing rock, *Felsbau magazine*, 25(6), 23-31, **2007**.
- [21] Wittke, W., Wittke-Gattermann, P., Wittke-Schmitt, B., TBM-heading in rock, design of the shield mantle, *ECCOMAS Thematic conference on computational methods in tunnelling, EURO:TUN 2007*, Vienna, Vienna University of Technology, **2007**.
- [22] Shalabi, FI., FE analysis of time-dependent behaviour of tunnelling in squeezing ground using two different creep models, *Tunnelling and Underground Space Technology*, 20, 271-279, **2005**.
- [23] Amberg, F., Numerical simulations of tunnelling in soft rock under water pressure, *ECCOMAS Thematic conference on computational methods in tunnelling, EURO:TUN 2009*, Bochum, Aedificatio Publishers Freiburg, 353-360, **2009**.
- [24] Lombardi, G., Neuenschwander, M., Panciera, A., Gibraltar Tunnel Project update- the geomechanical challenges, *Geo-mech Tunnel*, 2(5), 578-590, **2009**.
- [25] Ramoni, M., Anagnostou, G., On the feasibility of TBM drives in squeezing ground, *Tunnelling and Underground Space Technology*, 21(3-4), 262, **2006**.
- [26] Ramoni M., Anagnostou, G., Numerical analysis of the development of squeezing pressure during TBM standstills, *The second half century of rock mechanics, 11th Congress of the International Society for Rock Mechanics (ISRM)*, Lisbon, Taylor & Francis Group, London, 2, 963-966, **2007**.

- [27] Ramoni, M., Anagnostou, G., TBM drives in squeezing rock-shield-rock interaction, *Building underground for the future, AFTES International Congress Monaco*, Montecarlo, Edition spécifique Limonest, 163–172, **2008**.
- [28] Cantieni, L., Anagnostou, G., The effect of the stress path on squeezing behaviour in tunneling, *Rock Mechanics and Rock Engineering*, 42(2), 289-318, **2009**.
- [29] Ramoni, M., Anagnostou, G., Thrust force requirements for TBMs in squeezing ground, *Tunnelling and Underground Space Technology*, 25(4), 433-455, **2010**.
- [30] Sterpi, D., Gioda, G., Ground pressure and convergence for TBM driven tunnels in visco-plastic rocks, *ECCOMAS Thematic conference on computational methods in tunnelling, EURO:TUN 2007*, Vienna. University of Technology, 89-95, **2007**.
- [31] Einstein, HH., Bobet, A., Mechanized tunnelling in squeezing rock-from basic thoughts to continuous tunneling, *Tunnels for people, ITA World Tunnel Congress 97*, Vienna, 2, **1997**.
- [32] Ramoni, M., Anagnostou, G., The effect of advance rate on shield loading in squeezing ground, *Underground space-the 4th dimension of metropolises, ITA World Tunnel Congress 2007*, Prague, Taylor & Francis Group, London, 1, 673-677, **2007**.
- [33] Maidl, B., Schmid, L., Ritz, W., Herrenknecht, M., *Hardrock Tunnel Boring Machines*, **2008**.
- [34] Zhao, K., Janutolo, M., Barla, G., A completely 3D model for the simulation of mechanized tunnel excavation, *Rock Mechanics and Rock Engineering*, 45, 475-497, **2012**.
- [35] Barla, G., Tunnelling under squeezing rock conditions, *Kolymbas D (ed) Tunnelling Mechanics*, Eurosummer School, Logos Verlag, Innsbruck, 169-268, **2001**.
- [36] Singh, B., Jethwa, J.L., Dube, A.K., Singh, B., Correlation between observed support pressure and rock mass quality, *Tunnelling and Underground Space Technology*, 7, 59-74, **1992**.
- [37] Goel, R.K., Jethwa, J.L., and Paithakan, A.G., Tunnelling through the young Himalayas-a case history of the Maneri-Uttarkashi power tunnel, *Engineering. Geology*, 39, 31-44, **1995**.
- [38] Aydan, Ö., Akagi, T., Kawamoto, T., The Squeezing Potential of Rocks Around Tunnels; Theory and Prediction, *Rock Mechanics and Rock Engineering*, 26(2), 137-163, **1993**.
- [39] Hoek, E., Marinos, P., Predicting tunnel squeezing, *Tunnels and Tunnelling International*, Part 1 and 2, **2000**.
- [40] Barton, N., Lien, R. Lunde, J., Engineering classification of rock masses for the design of tunnel support, *Rock Mechanics*, 6(4), 189-236, **1974**.

- [41] Hoek, E., Reliability of Hoek-Brown estimates of rock mass properties and their impact on design, *International Journal of Rock Mechanics and Mining Science*, 35, 63-68, **1998**.
- [42] Hoek, E., Big tunnels in bad rock, *ASCE Journal of Geotechnical and Geoenvironmental Engineering*, Terzaghi Lecture, Seattle, **2000**.
- [43] Brown, E.T., Bray, J.W., Ladanyi, B., Hoek, E., Characteristic line calculations for rock tunnels, *Journal of Geotechnical Engineering Division, Proceedings of the American Society of Civil Engineers*, 109, 15-39, **1983**.
- [44] Ramoni, M., Anagnostou, G., The interaction between shield, ground and tunnel support in TBM tunnelling through squeezing conditions, *Rock Mechanics and Rock Engineering*, 44, 37-61, **2011**.
- [45] Barla, G., Zhao, K., Janutolo, M., 3D advanced modelling of TBM excavation in squeezing rock condition, *1st Asian and 9th Iranian Tunnel Symposium, Tehran, Iran*, **2011**.
- [46] Vlachopoulos, N., Diederichs, MS., Improved longitudinal displacements profiles for convergence confinement analysis of deep tunnel, *Rock Mechanics and Rock Engineering*, 42, 131-146, **2009**.
- [47] Barla, G., Bonini, M., Debernardi, D., Time Dependent Deformations in Squeezing Tunnels, *International Journal of Geoenvironment and Case Histories*, 2(1), 40-65, **2010**.
- [48] Fjaer, E., Holt, R.M., Horsrud, P., Raaen, A.M., Risnes, R., *Petroleum Related Rock Mechanics*, 2nd Edition, **2008**.
- [49] Farmer, T., *Engineering Behaviour of Rocks*, Chapman and Hall, London, **1983**.
- [50] Ladanyi, B., Time-dependent response of rock around tunnels, *Comprehensive Rock Engineering*, Pergamon Press J.A.Hudson editorial, 2, 78-112, **1993**.
- [51] Cristescu, N., Rock rheology, *Comprehensive Rock Engineering*, Pergamon Press, J.A. Hudson editorial, 1, 523-544, **1993**.
- [52] Sulem, J., Panet, M., Guenot, A., An analytical solution for time-dependent displacements in a circular tunnel, *International Journal of Rock Mechanics and Mining Science and Geomechanics Abstract*, 24(3), 155-164, **1987**.
- [53] Sulem, J., Analytical methods for the study of tunnel deformation during excavation, *Gallerie in condizioni difficili, MIR'94*, Torino, G. Barla editorial, 301-317, **1994**.
- [54] Itasca, FLAC3D, *Fast Lagrangian analysis of continua in 3D dimensions, User's guide*, **2006**.
- [55] ITA, Long traffic tunnels at great depth, *ITA Working group N°17, Long tunnels at great depth*, ITA Lausanne, **2003**.

- [56] Anagnostou, G., Cantieni, L., Design and analysis of yielding support in squeezing ground, *The second half century of rock mechanics, 11th Congress of the International Society for Rock Mechanics (ISRM)*, Lisbon, 2, 829-832, Taylor & Francis Group London, **2007**.
- [57] Gutter, W., Romualdi, P., New design for a 10 m universal Double Shield TBM for long railway tunnels in critical and varying rock conditions, RETC 2003, **2003**.
- [58] Chapman, D., Metje, N., Stark, A., *Introduction to Tunnel Construction*, Spon, London and New York, **2010**.
- [59] NFF, Rock mass grouting in Norwegian tunneling, *Norwegian tunnelling society*, Publication no. 20, **2011**.
- [60] Woodward, J., An Introduction to geotechnical processes, Spon Press, London, **2005**.
- [61] Baker, W.H., Planning and performing structural chemical grouting, *Grouting in Geotechnical Engineering*, American Society of Civil Engineers, Reston, VA, 515-539, **1982**.
- [62] Whittaker, B.N., Frith, R.C., *Tunnelling: Design Stability and Construction*, Institution of Mining and Metallurgy, London, **1990**.
- [63] ITA/AITES, Settlements induced by tunnelling in soft ground, *Tunnelling and Underground Space Technology*, 22(2), 119-49, **2007**.

APPENDIX A

Chapter 6: Time Dependent Analysis, CPOW Model Results

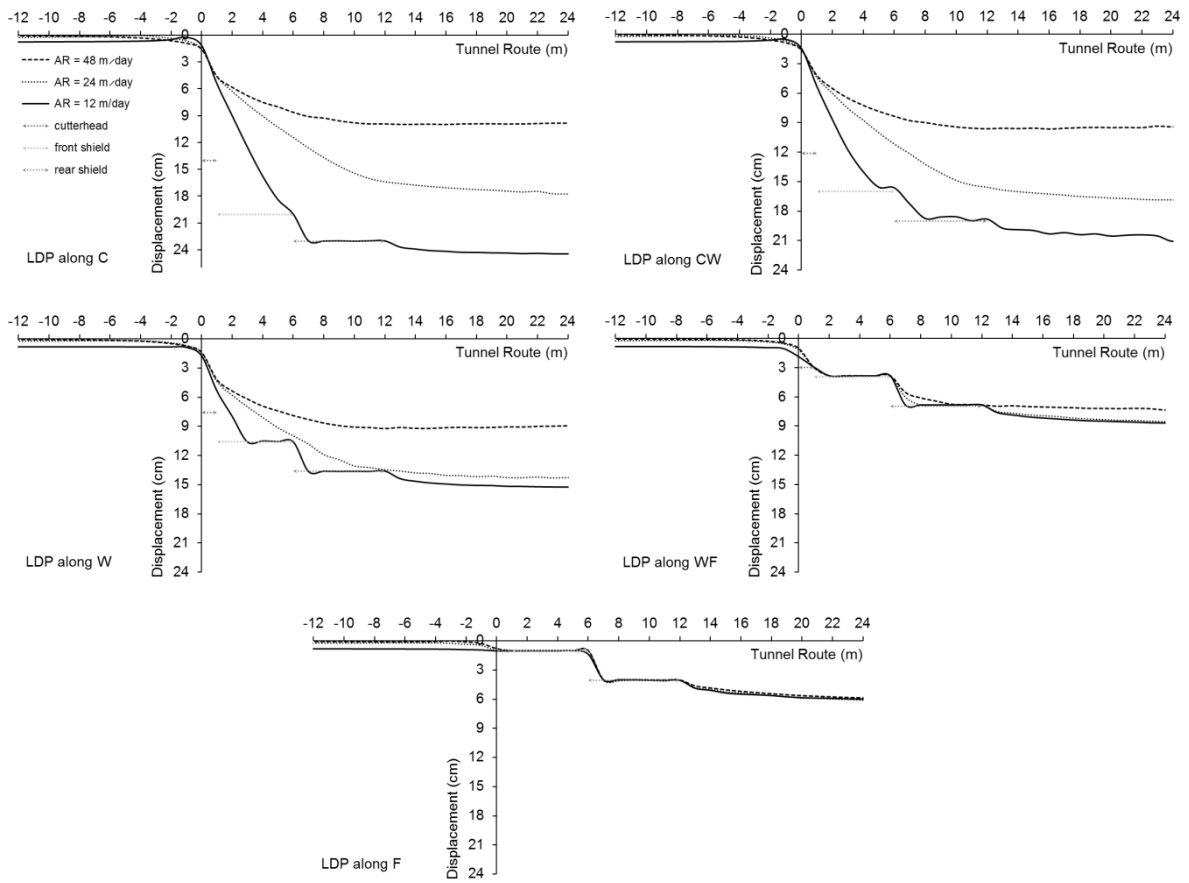
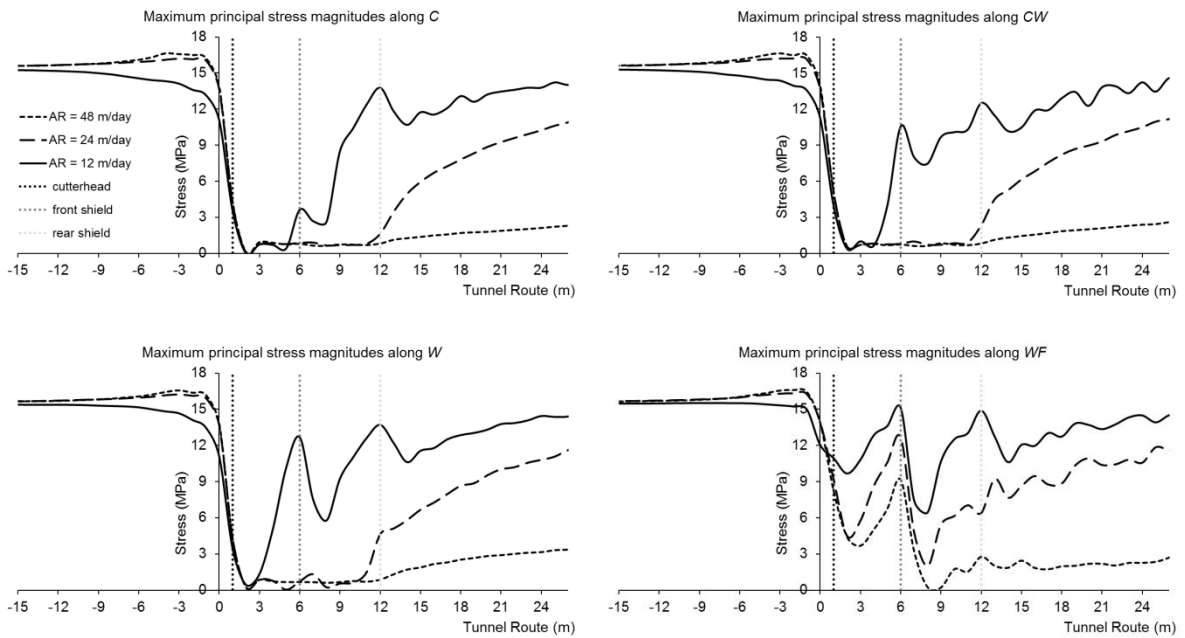


Figure 6.a. LDP for different advance rates at five reference points



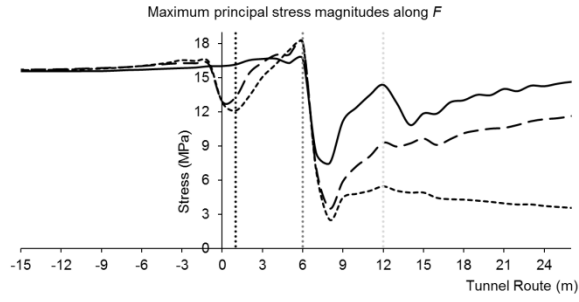


Figure 6.b. LSP for different advance rates at five reference points

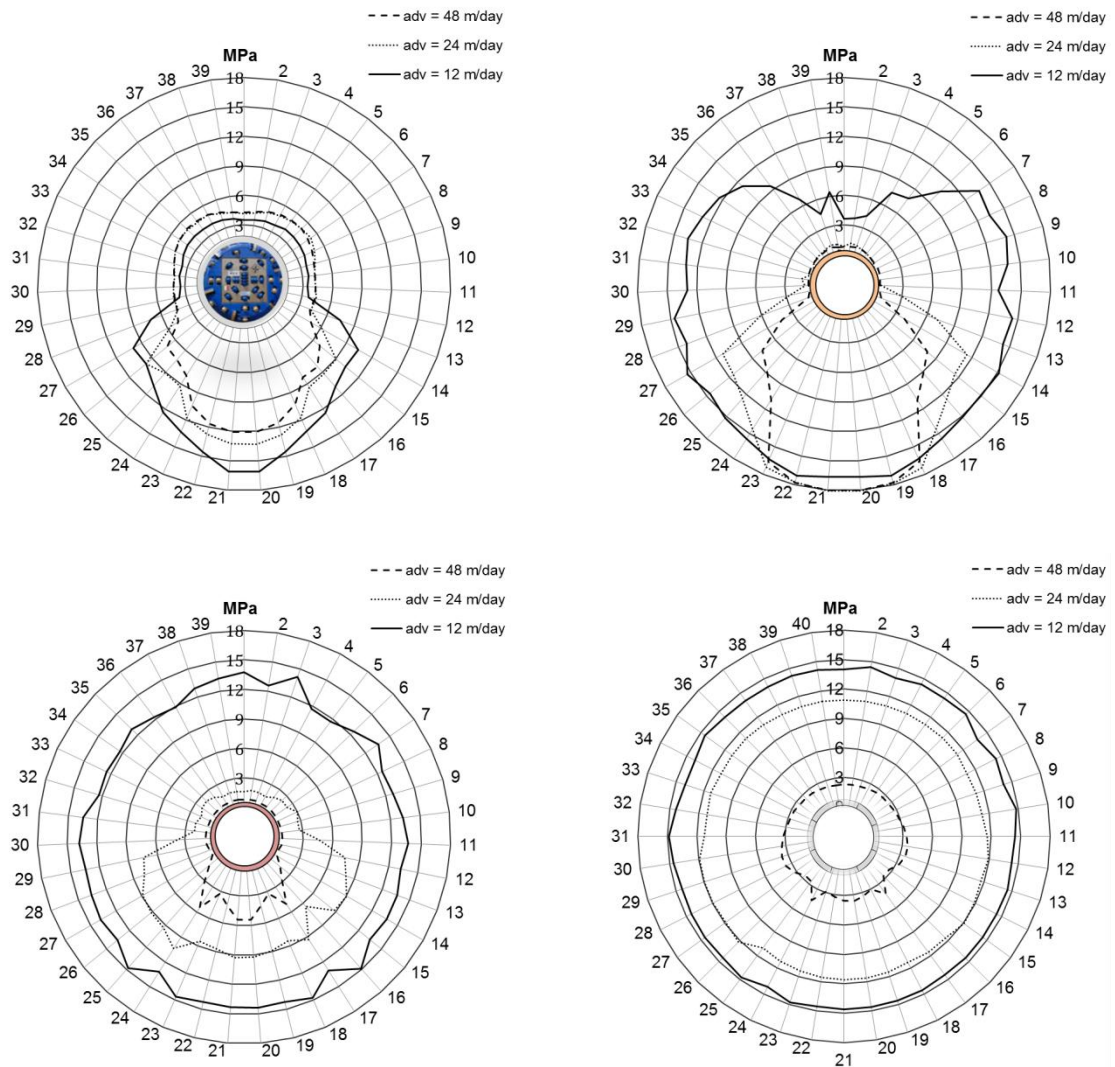


Figure 6.c. Sectional contact pressures profile between ground and shields and between ground and lining

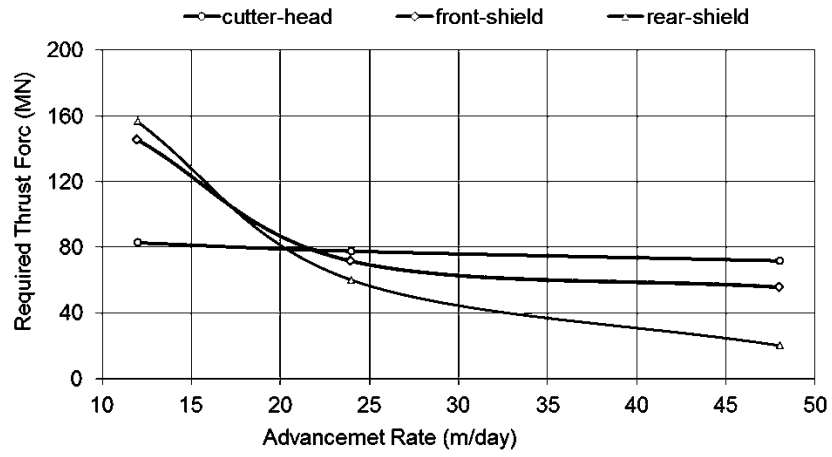


Figure 6.d. Required thrust force diagram versus different advance rates

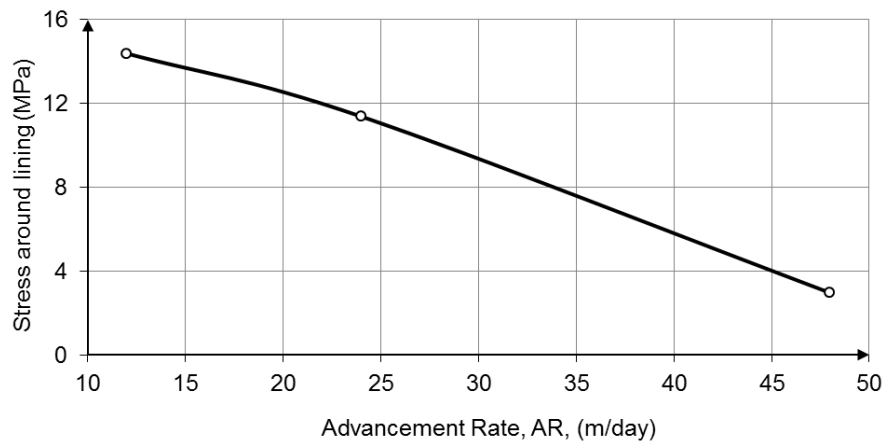


Figure 6.e. Average stress-advance rate diagram for lining

APPENDIX B

Chapter 7: Impact of Overcut on Interaction between Shield, Ground and Support

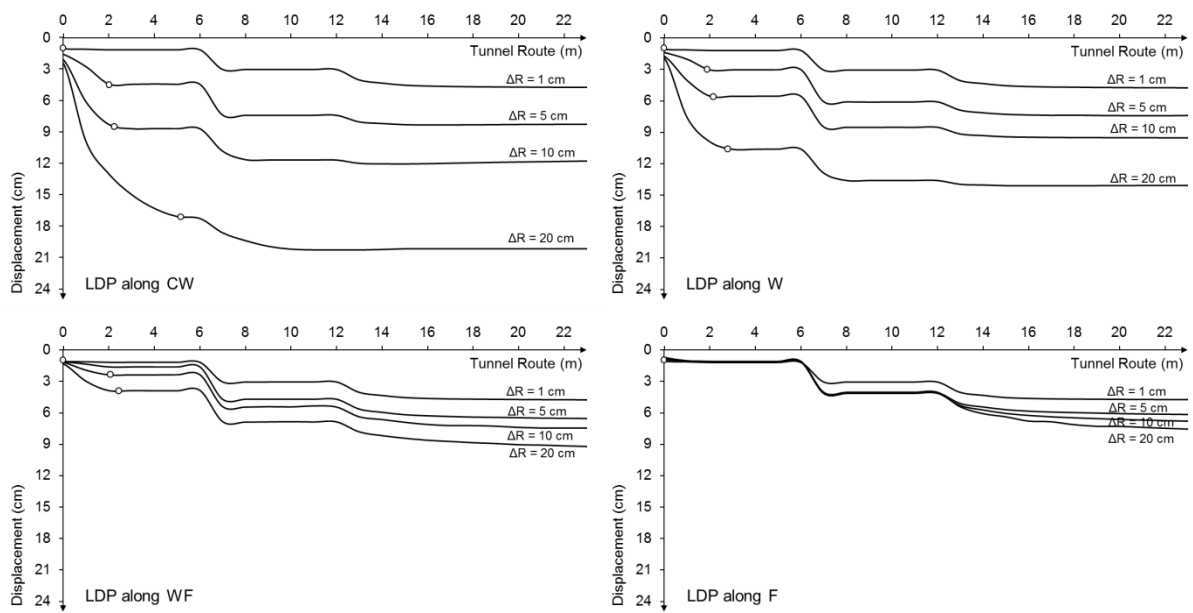


Figure 7.a Radial displacement of the ground at the tunnel circumference for different overcut, ΔR , of 1, 5, 10 or 20 cm at reference points

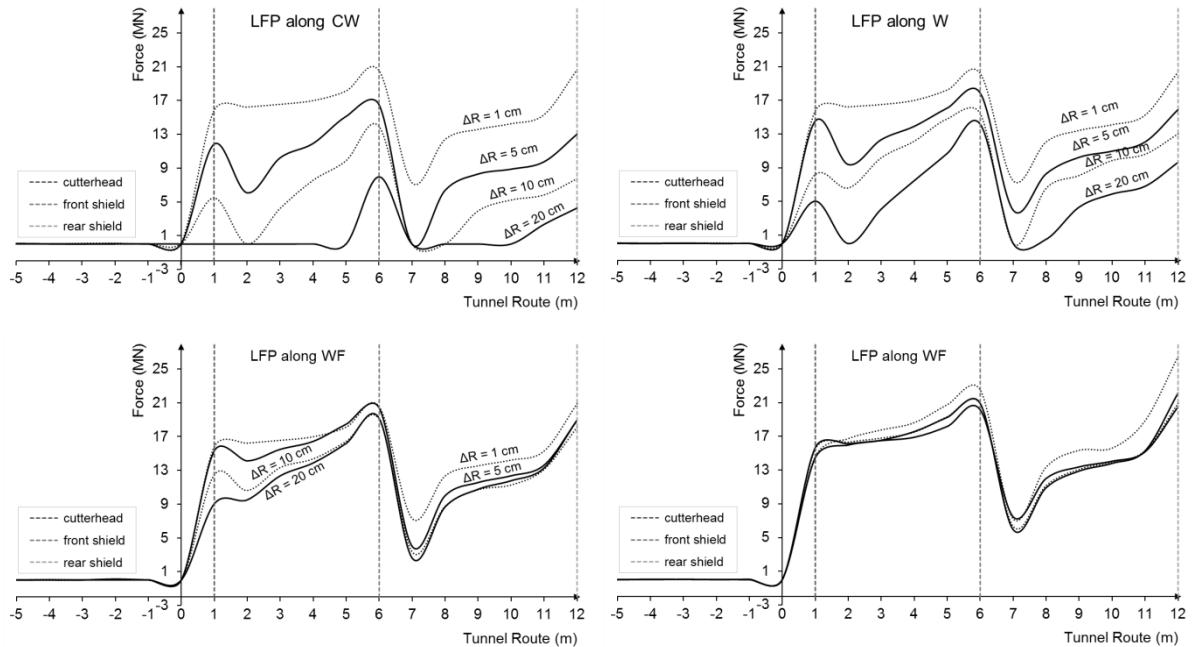


Figure 7.b contact forces for a 1 m cutter-head, 5 m front shield and 6 m rear shield at different overcut ΔR of 1, 5, 10 or 20 cm at reference points

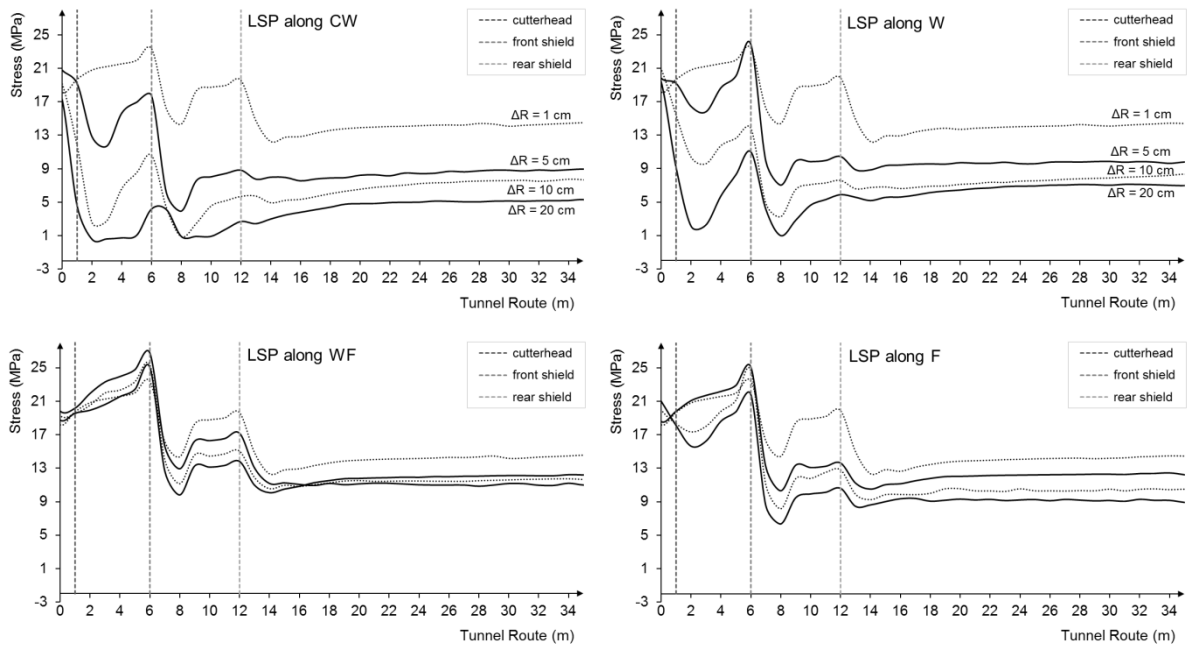


Figure 7.c Maximum principal stress of the ground around machine components for different overcut, ΔR , of 1, 5, 10 or 20 cm at reference points

CURRICULUM VITAE

Personal Information

Name : Rohola
Surname : Hasanpour
Nickname : Ayma
Place of Birth : Khoy, West Azerbaijan, Iran
Date of Birth : 25/05/1982
Marital status : Married
Nationality : Iranian
E-mail : roha93@gmail.com

Education

High School (1997-2001): Mathematics and Physics Diploma, Ghaem & Jihad High Schools, Chaypare, West Azerbaijan, Iran

BS.C (2001-2005): Mining Engineering, Department of Mining Engineering, Imam Khomeini International University, Qazvin, Iran

BSc Thesis Title: Methods of excavation tunnels in soft soil, under supervision of Dr. Masud Monjezi

MSc (2005-2008): Rock Mechanics Engineering, Mining Engineering Department, Sahand University of Technology, Tabriz, Iran

MS Thesis Title: Measurement of rock fracture characterization under mixed-mode loading by using the numerical and experimental methods, under supervision of both Dr. Naghdali Choupani and Dr. Hamid Aghababaei

PhD (2009-2013): Mining Engineering Department, Hacettepe University, Ankara, Turkey.

PhD Thesis Title: Evaluation of Applicability of Double Shield Tunnel Boring Machines in Potentially Squeezing Grounds”, under supervision of both Prof. Dr. Bahtiyar Unver and Dr. Jamal Rostami

Foreign Languages

Azerbaijani (Mother Tongue), Turkish (Native), Persian (Native), English (Advanced)

Publications from Thesis

- [1] Rohola Hasanpour, Bahtiyar Ünver, Jamal Rostami, Time Dependent Numerical Analysis for Investigation of Entrapment Risks in DS-TBM Tunnelling in Squeezing Grounds, Euro TUN 2013.
- [2] Rohola Hasanpour, Jamal Rostami, Bahtiyar Ünver, 3D Finite Difference Model for Simulation of Double Shield TBM Tunneling in Squeezing Grounds' Under review in International Journal of Tunnelling and Underground Space Technology.
- [3] Rohola Hasanpour, Bahtiyar Ünver, Jamal Rostami, Numerical Simulation for Evaluation of Ground Improvement Methods to Prevent the Machine Seizure in DS-TBM Tunneling in Squeezing Grounds, EUROCK 2013.
- [4] Rohola Hasanpour, Bahtiyar Ünver, Jamal Rostami, Comments on the article "A completely 3D model for the simulation of mechanized tunnel excavation" by J Kai Zhao et al. [Rock mechanics and rock engineering (2012) DOI 10.1007/s00603-012-0224-3]

Other Publications

- [5] Rohola Hasanpour, Hamid Chakeri, Yilmaz Ozcelik, Hasan Denek, "Comparisons of the results of analytical, numerical and direct measurements of surface settlements in Istanbul metro" Bulletin of Engineering Geology and Environment, 2011.
- [6] R. Hasanpour, N. Choupani, "Rock Fracture Characterizations by Using the Modified Arcan Test Specimen: Numerical and Experimental Results" Published in International Journal of Rock Mechanics & Mining Sciences, 2008.
- [7] B. Ünver, R. Hasanpour, H. Chakeri, M. A. Hindistan, "Preliminary 3D numerical modeling of a hypothetical LNG storage cavern having an irregular geometry", EUROCK 2010.
- [8] R. Hasanpour, N. Choupani, "Mixed-Mode Study of Rock Fracture Mechanics by using the Modified Arcan Specimen Test", Published in International Journal of Mathematical, Physical and Engineering Sciences, 3:1 2009.
- [9] R. Hasanpour, N. Choupani, "Prediction of crack propagation angle in rock by using the numerical and experimental methods". Accepted in Amirkabir Journal of Science and Technology, Amirkabir University of Technology, Iran-2007.
- [10] R. Hasanpour, N. Choupani, "Measurement of rock fracture characterization for Rocks by Using the Numerical and Experimental Methods", Accepted and presented in the 3rd Iranian Rock Mechanics Engineering Conference, Amirkabir University of Technology, Iran-2007.
- [11] Hamid Chakeri, Rohola Hasanpour, Mehmet Ali Hindistan, Bahtiyar Ünver, (2011), "Interaction analysis between tunnels in soft ground by 3D numerical modeling", Bulletin of Engineering Geology and the Environment journal.

- [12] Rohola Hasanpour, Naghd Ali Choupani, Mehmet Ali Hindistan, Bahtiyar Ünver, Numerical study of dimensions effects on measurement of rock fracture characterizations by using the modified Arcan test specimen, EUROCK 2010.